UNIVERSIDADE D
COIMBRA

João Guilherme de Almeida Nascimento

BUILDING A TONSIL-ON-CHIP

VOLUME 1

Dissertação no âmbito do Mestrado em Biotecnologia Farmacêutica orientada pelo Professor Doutor Luís Pereira de Almeida e pela Professora Doutora Helena Soares e apresentada à Faculdade de Farmácia da Universidade de Coimbra

Setembro de 2023

Agradecimentos

Esta tese é o culminar de um ano intenso, onde tive a oportunidade perceber o que é trabalhar em ciência. Chega, assim, ao fim mais uma etapa da minha vida, que me permitiu crescer, tanto a nível pessoal como a nível profissional. Deste modo, gostaria de agradecer a todos os que, de uma forma ou de outra, me apoiaram e ajudaram.

Agradeço à Professora Doutora Helena Soares por me ter recebido no seu laboratório e por me ter dado a oportunidade de perceber o que é ser investigador e trabalhar em ciência.

Agradeço à Doutora Juliana Gonçalves por todo o apoio e ajuda que me deu durante este ano. Por me dar espaço para aprender e crescer como investigador.

Aos restantes membros do grupo de Imunobiologia e Patogénese Humana, agradeço todos os momentos de amizade, de apoio, de motivação e entreajuda.

Aos meus pais, Cristina e Carlos, agradeço-vos por tudo. Sem vocês teria sido impossível ter chegado onde cheguei

Aos meus amigos, agradeço pelos momentos de descontração, pelos desabafos e pelos conselhos. Sei que para onde quer que vá, posso contar com vocês.

Abstract

The production of high-affinity antibodies is crucial for the development of protective immunity. It is a complex and highly dynamic process involving several cells, chemical signals and where the spatial organization is key. These reactions occur in germinal centers, a specialized microstructure that appears inside lymphoid follicles once an immune response is initiated.

The adaptative immune response is initiated in secondary lymphoid organs (SLOs), such as the palatine tonsils. Due to their placement at the front of the digestive and respiratory systems, palatine tonsils can effectively screen ingested and inhaled pathogens, being key players in the protection of the host. Additionally, these structures are easily accessible and are commonly extracted as treatment for obstructive sleep apnea (OSA) or recurrent tonsillitis, which makes them ideal to study human SLOs.

This work focuses on the study of human palatine tonsils as models for SLOs and the development of tonsil organoid cultures. To do so, mononuclear cells (MNCs) were isolate form human tonsils and immunophenotyped, to understand their immune landscape. The presence of germinal centers was observed by performing an H&E staining on tonsil tissue samples. Additionally, tonsil MNCs were stimulated with Staphylococcal Enterotoxin B (SEB) and cultured in a transwell system up to 15 days, to induce cell reaggregation and organoid formation.

Results of these study showed that the immune landscape of human palatine tonsils is in accordance with what is expected for SLOs. Both T and B lymphocytes were detected, including the specialized follicular helper T cells, that are crucial for antibody production, showing that these organs are immunocompetent. Tonsil organoids were established, and cell viability was maintained for 10 days.

With this work, the first steps have been taken towards the development of an organ-on-chip system for human tonsils, that will accurately recapitulate the structure and function of human SLOs *in vitro*.

Keywords: human palatine tonsils, SLOs, organoids, organ-on-chip

Resumo

A produção de anticorpos com elevada afinidade é crucial para o desenvolvimento da imunidade protetora. Este é um processo complexo e altamente dinâmico que envolve várias células, sinais químicos e onde a organização espacial é fundamental. Estas reações ocorrem nos centros germinativos, uma microestrutura especializada que surge no interior dos folículos linfoides quando se inicia uma resposta imunitária.

A resposta imune adaptativa é iniciada nos órgãos linfoides secundários (OLSs), como as amígdalas palatinas. Devido à sua localização na entrada dos sistemas digestivo e respiratório, as amígdalas palatinas conseguem fazer um rastreio eficaz dos agentes patogénicos que são ingeridos e inalados, o que faz destas intervenientes fundamentais na proteção do hospedeiro. Além disso, estas estruturas são facilmente acessíveis e são normalmente extraídas para tratamento da apneia obstrutiva do sono ou de amigdalites de repetição, o que as torna ideais para o estudo de OLSs humanos.

Este trabalho centra-se no estudo das amígdalas palatinas humanas como modelos de OLSs e no desenvolvimento de culturas de organoides de amígdalas. Para tal, células mononucleares (CMNs) das amígdalas foram isoladas e o seu fenótipo foi caracterizado, para compreender o panorama imunológico destes órgãos. A presença de centros germinativos foi observada através da realização de uma *staining* H&E em amostras de tecido das amígdalas. Adicionalmente, as CMNs das amígdalas foram estimuladas com Enterotoxina B Estafilocócica e cultivadas num sistema *transwell* até 15 dias, para induzir a reagregarão celular e a formação de organoides.

Os resultados deste estudo mostraram que a panorama imunológico das amígdalas palatinas humanas está de acordo com o que é esperado para os OLSs. Foram detetados linfócitos T e B, incluindo as células T auxiliares foliculares, que são cruciais para a produção de anticorpos, mostrando que estes órgãos são imunocompetentes. Foi, ainda, possível estabelecer organoides de amígdalas onde viabilidade celular foi mantida durante 10 dias a

Com este trabalho, foram dados os primeiros passos para o desenvolvimento de um sistema de órgãos-em-chip para amígdalas humanas, que recapitulará com precisão a estrutura e a função dos OLSs humanos *in vitro*.

Palavras-chave: amígdalas palatinas humanas, OLSs, organoides, órgãos-em-chip

Contents

List of Figures

List of Tables

List of Abbreviatures and Symbols

°C	Degrees Celsius
APC	Antigen presenting cells
Bcl6	B-cell lymphoma 6
BFA	Brefeldin A
CD	Cluster of differentiation
CXCR	C-X-C chemokine receptor
CXCRL	C-X-C chemokine ligand
DAMP	Damage-associated molecular patterns
DC	Dendritic cell
DZ	Dark zone
FACS	Fluorescence-activated cell sorting
FBS	Fetal bovine serum
FoxP3	Forkhead box P3
g	g force
GC	Germinal center
GrB	Granzyme B
GrK	Granzyme K
ICOS	Inducible co-stimulator
IFNγ	Interferon γ
Ig	Immunoglobulin
IL	Interleukin
LZ	Light zone
mg	Milligram
MHC	Major histocompatibility complex
min	Minutes
mL	Milliliter
mm	Millimeter
MNCs	Mononuclear cells
MyD88	Myeloid differentiation primary-response protein 88
MZ	Marginal zone
ng	Nanogram
NK	Natural killer
PAMP	Pathogen-associated molecular pattern

PBS	Phosphate Buffered Saline
PD-1	Programmed cell death protein
PFA	Paraformaldehyde
PMA	Phorbol 12-myristate 13-acetate
PRR	Pattern recognition receptor
RPMI	Roscow Park Memorial Institute
RT	Room temperature
SLO	Secondary lymphoid organ
SMH	Somatic hypermutation
T-bet	T-box TBX21
TCR	T cell receptor
T_{FH}	T-follicular helper cell
TGF-β	Transforming growth factor β
T_H	T-helper cell
TLR	Toll-like receptors
T_{reg}	T-regulatory cell
TRIF	TIR-domain containing adaptor inducing IFN-β
µg	Microgram
µm	Micrometer

1.Introduction

1.1 Overview of the immune system

The immune system is the tool by which an organism defends itself against pathogens or other foreign bodies, that may cause harm to the host. It is comprised of a complex network of lymphoid organs, cells and humoral factors (Parkin e Cohen, 2001). Two types of immune responses can be identified depending on their speed and specificity: the innate response and the adaptive response.

1.1.1Innate immunity

Innate immunity is the first to be activated, providing an immediate protection. This first line of defense against infection encompasses physical and chemical barriers, such as the skin or mucosal surfaces, that are followed by a cellular response, which includes neutrophils, monocytes, macrophages, eosinophils, basophils, mast cells, natural killer cells and dendritic cells (DCs) (Stephen e Hajjar, 2017). Some of these cells, such as DCs and macrophages, have the capacity to present antigens to other immune cells. These antigen-presenting cells (APCs) are specialized cells that bind, internalize and process foreign antigens, making them available to be presented to immune cells, particularity T lymphocytes, eliciting a broader immune response (Gaudino e Kumar, 2019).

These cellular components act in an antigen-unspecific manner, but still have the capacity to sense non-self signals, by expressing pattern recognition receptors (PPRs) that recognize molecular patterns that are unique to foreign microorganism. This “non-self” signals produced by microorganisms are called pathogen-associated molecular patterns (PAMPs) (Kennedy, 2010). PRRs can be divided into four major families, that include C-type lectin receptors, NOD-like receptors, RIG-I-like receptors and Toll-like receptors (TLRs) (Amarante-Mendes *et al.*, 2018), the latter being one of the most studied. TLRs are expressed by all innate immune cells (Refat El-Zayat, Sibaii e Mannaa, 2019) but can, also, be found in other cell populations (Takeda, Kaisho e Akira, 2003). So far, ten distinct types of TLRs have been identified in humans, named TLR1 to TLR10 (Imler e Hoffmann, 2001). These receptors exist as membrane-bound receptors – TLR1, TLR2, TLR5 and TLR6 – or can be found in the cytoplasm, in endosomal compartments – TLR3, TLR7, TLR8 and TLR9 (Coico e Sunshine, 2015).

TLR4 is primarily expressed on the cell membrane, but following ligand recognition, this receptor is internalized and expressed in endosomes (Husebye *et al.*, 2006). As for TLR10, the biology and function of this receptor remains unclear, being regarded as an “orphan receptor” of the innate immune system (Balachandran *et al.*, 2022; Fore *et al.*, 2020; Sameer e Nissar, 2021)

TLRs can recognize a wide range of PAMPs (Fig.1.1) from viral, bacterial, fungal or parasitic origins, but also have the capacity to interact with host-derived damage-associated molecular patterns (DAMPs) (Refat El-Zayat, Sibaii e Mannaa, 2019). The activation of TLRs can induce immune responses through different signaling pathways. The cytoplasmatic Toll/IL-1 domain of the receptor can interact with two possible adaptor proteins: the myeloid differentiation primary-response protein 88 (MyD88) or the TIR-domain containing adaptor inducing IFN-β (TRIF) (Coico e Sunshine, 2015; Sameer e Nissar, 2021). MyD88 induces a proinflammatory cytokine response, while TRIF will enhance the expression of type 1 IFN genes (Sameer e Nissar, 2021).

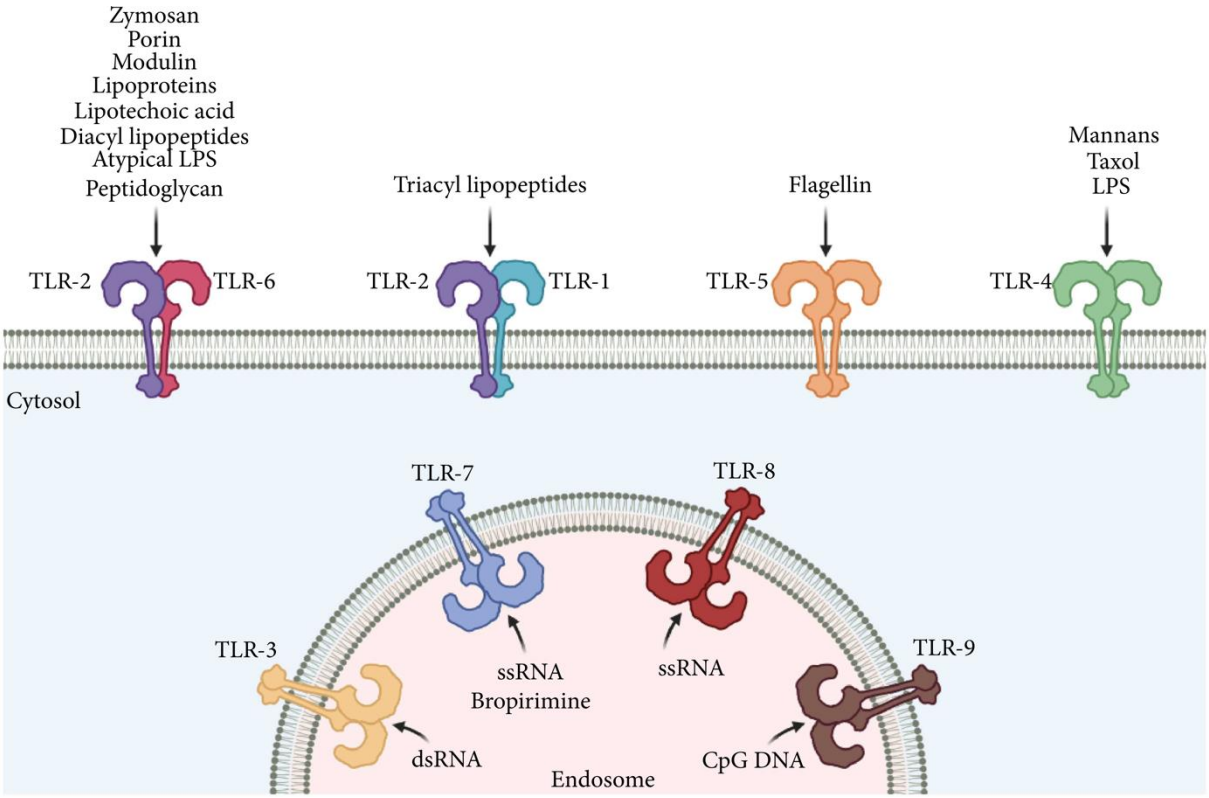

Figure 1.1 – PAMP recognition by various TLRs. TLRs can recognize PAMPS from viral, bacterial, fungal and parasitic origins. Adapted from reference (REFF)

1.1.2 Adaptive immunity

Adaptive immunity is the antigen-specific response of the immune system and evolves as the host encounters different pathogens and antigens, during its life. An adaptive response can be classified as being humoral or cellular-mediated, depending on its mode of action. Humoral immunity is carried out by B lymphocytes that produce antibodies against specific antigens. Cellular immunity depends on the action of T lymphocytes that orchestrate the immune response and eliminate infected cells. This type of immunity can lead to the development of memory cells that, in the case of future exposures, will initiate a specific response more rapidly. Nonetheless, the adaptive response takes longer to fully develop, even with the presence of memory cells, as it takes some time for the adaptive immune system to recognize and respond to pathogens. That is why the two counterparts of the immune system work in close coordination to ensure powerful and effective protection of the host (Parkin e Cohen, 2001).

Both T and B lymphocytes develop from the common lymphoid progenitor, a specialized type of stem cell that originates from pluripotent hematopoietic stem cells in the bone marrow (Murphy e Weaver, 2017). After, T lymphocytes leave to the thymus to mature while B lymphocytes development continues in the bone marrow. After maturing in the thymus, two major types of T cells can be identified, depending on which co-receptor they express: CD4 or CD8. $CD4^+$ T cells are referred to as T helper lymphocytes (T_H) while $CD8^+$ cells are called T cytotoxic (T_C) lymphocytes. Both T_H and T_C lymphocytes express a T cell receptor (TCR) on its surface, that recognize fragments of specific antigens that are presented by molecules of the major histocompatibility complex (MHC). There are two major classes of MHC protein molecules: MHC class 1 is expressed by all nucleated cells and presents endogenous peptides, while MHC class II is expressed on professional APC and presents extracellular antigens that have been phagocytosed (Marshall *et al.*, 2018). T_H lymphocytes recognize antigens presented by MHC class II and T_C lymphocytes recognize antigens presented by MHC class I.

T_H and T_C lymphocytes have intrinsically different functions. T_C lymphocytes can directly kill other cells that have been infected, as they secrete cytotoxic mediators, such as granzymes and perforin that induce the apoptosis of target cells. T_H lymphocytes, traditionally, have no cytotoxic function and cannot directly kill cells (Marshall *et al.*, 2018). Instead, they mediate and optimize the immune response, by

secreting cytokines and recruiting other cellular subsets capable of preforming these tasks, while regulating the type of immune response that will form (Marshall *et al.*, 2018). T_H lymphocytes can differentiate into different subsets, that are associated with a specific cytokine profile. These include the T_H1, T_H2, T_H17, T-regulatory (T_{reg}) and T-follicular helper (T_{FH}) cells (Fig. 1.2), that have distinct immune functions.

T_H1 cells secrete interferon (IFN)-γ, tumor necrosis factor (TNF)-α and interleukin (IL)-2 (Raphael *et al.*, 2015) and are involved in cell-mediated immunity, protecting against intracellular pathogens (Raphael *et al.*, 2015; Zhu e Zhu, 2020). They promote the differentiation of CD8 T cells and the enhancement of macrophages' antimicrobial defenses (Murphy e Weaver, 2017; Zhu e Zhu, 2020). T_H2 cells secrete IL-4, IL-5, and IL-13 (Berger, 2000) and defend the host against large, multicellular parasites (Raphael *et al.*, 2015). T_H17 cells protect against the invasion of extracellular bacteria, fungi and other eukaryotic pathogens and secrete IL-17 and IL-22 (Raphael *et al.*, 2015). T_{reg} cells have their major role in maintaining immune self-tolerance and avoiding immunopathology by regulating the response of effector T cells (Luckheeram *et al.*, 2012). Several regulatory mechanisms for T_{reg} cells have been identified: the secretion of IL-10, transforming growth factor (TGF) -β and IL-35; the sequestering of IL-2 and expression of inhibitory receptors (Murphy e Weaver, 2017; Zhu e Zhu, 2020). T_{FH} cells are essential for providing help to B cells during antibody production, through the expression CD40L, IL-4 and IL-21(Crotty, 2019). This specialized CD4 T cell subset is characterized by the expression of C-X-C chemokine receptor 5 (CXCR5) (Schaerli *et al.*, 2000), that enables the localization of T_{FH} cells to the follicles, and the programmed cell death protein 1(PD-1) (Haynes *et al.*, 2007; Ioannidou *et al.*, 2021), that is thought to have an inhibitory role by preventing excess CD4 T cell proliferation (Crotty, 2011). Additionally, they are also characterized by the expression of the inducible co-stimulator (ICOS)

Another subset of T cells arising from the thymus are the $\gamma\delta$ T cells. These are a minor CD3-positive T cell subpopulation that are rarely found in secondary lymphoid organs (SLOs) (Ribot, Lopes e Silva-Santos, 2021) but have increased frequencies in mucosal tissues (Kabelitz, 2020), such as the skin, intestines and lungs (Ribot, Lopes e Silva-Santos, 2021). Same as other T cells, $\gamma\delta$ T cells develop in the thymus, but express a different TCR, consisting of $\gamma\delta$ chains (Prinz, Silva-Santos e Pennington, 2013), instead of the more common $\alpha\beta$ chains expressed on CD4 and CD8 T cells. Additionally, $\gamma\delta$ T cells do not recognize antigens presented in a MHC-dependent

manner and are able to recognize nonpeptidic phosphoantigens produced by bacteria (Kabelitz, 2020).

B cells are crucial players of humoral immunity since their major role is to produce antibodies. These cells can recognize antigens directly, without the need for APCs and can act as such to other cell subsets, including T cells, as they express MHC class II molecules. Once a B cell encounters an antigen and becomes activated, it can differentiate into plasma cells, that are short-lived and secrete the first wave of antibodies (Stebegg *et al.*, 2018) or memory B cells, that are long-lived and provide protection in case of future exposures by ensuring a faster response.

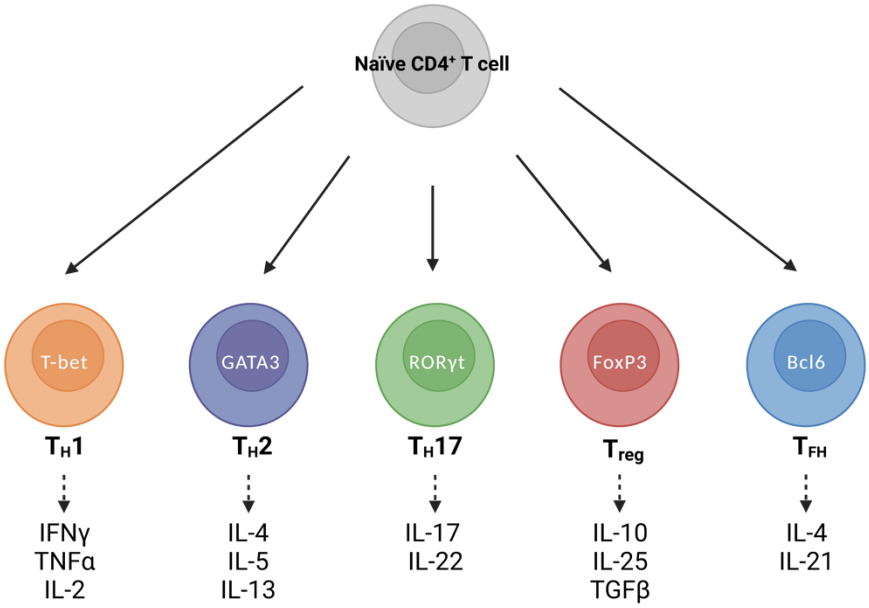

Figure 1.2 – Functional subsets of CD4 T cells. Naïve CD4 T cells can differentiate into T_H1, T_H2, T_H17, T_{reg} and T_{FH} cells. Each subset produces a different type of cytokines.

1.2 Lymphatic System and Immunity

The lymphatic system is crucial for the proper functioning of the immune system. It is made up of a network of vessels, tissues and organs, the latter being divided into two categories: the primary lymphoid organs, where T and B cells mature, and the secondary lymphoid organs (SLO), where mature lymphocytes are maintained, ready to be activated. These include the lymph nodes, palatine tonsils, Peyer´s patches and the spleen. Additionally, it is through the lymphatic vessels that immune cells and

antigens travel and are able to arrive to the SLOs so that an adaptative immune response can be initiated.

Palatine tonsils are located at the transition of the mouth to the oropharynx (Nave, Gebert e Pabst, 2001) and belong to a group of oropharyngeal lymphoid tissues known as Waldeyer´s ring. Their positioning at the front of both the respiratory and digestive tracts is strategic for immune protection against ingested and inhaled pathogens, making tonsils front runners in initiating immune responses.

Due to being easily accessible, palatine tonsils are often used as a model to study the structure and function of human lymphoid organs, helping to further the knowledge on follicle formation and antibody production. Tonsils are oval-shaped structures lined by a stratified squamous non-keratinizing epithelium that encapsulates the lymphoid tissue. The epithelial surface of human tonsils is characterized by the formation of tubular crypts (Nave 2001). Usually, each tonsil contains 10-20 crypts, increasing the surface area up to 300 cm^2(Howie, 1980). While the surface epithelium is a continuous tissue, the epithelium of the crypts is disrupted and is populated with non-epithelial cells (Nave, Gebert e Pabst, 2001). This reticulated nature of the crypt epithelium allows for an increased efficiency in presenting antigens to the underlying lymphoid tissue.

Regarding the structure of the lymphoid component, similarly to all SLOs, two distinct zones can be identified where T cells and B cells concentrate - T-cell zones and B-cell zones, respectively (Murphy e Weaver, 2017). Normally, B cells are organized into round-shape structures, called follicles, that evolve into GCs, when an immune response is initiated. These follicles are located below the surface epithelium and are sites for B cell maturation and differentiation (Nave, Gebert e Pabst, 2001). Tonsillar lymphoid follicles are also populated by a network of follicular DCs and by T_C lymphocytes. Follicular DCs organize the structure of the GC (Crotty, 2019) and can retain antigens for extended periods, making them available to be presented to B cells (Crotty, 2019; Nave, Gebert e Pabst, 2001).

1.2.1Germinal center reaction

GCs are distinct microanatomical structures that host a set of complex and highly dynamic reactions that lead to the development of high-affinity antibody-producing B cells (Fig.1.2). Mature GCs can be divided into two distinct zones: the light zone (LZ) and the dark zone (DZ), each one associated with a specific function of the

GC reaction. LZ is generally turned towards the source of foreign antigens. On tonsils this translates to the LZ being positioned towards the mucosal surface (Allen, Okada e Cyster, 2007).

The GC reaction (Fig. 1.3) starts when B cells encounter antigens and became activated. These antigen-bound B cells migrate to the T cell zone, where they present their antigen to T_{FH} cells, which in turn provide them with survival and co-stimulatory factors (Gatto e Brink, 2010; Stebegg *et al.*, 2018). Additionally, interaction between CD40, that is constitutively expressed by B cells, with its ligand, CD40L, that is expressed on the surface of T_{FH} cells, is crucial for the initiation and maintenance of GC responses (Gatto e Brink, 2010; Papa e Vinuesa, 2018). After this, B cells enter the GC, becoming GC B cells, and start to divide. Proliferating GC B cells in the DZ, also called centroblasts, accumulate mutations through somatic hypermutation (SMH), producing a population of cells that express receptors with different affinities for antigens. These cells then leave the DZ to the LZ, becoming centrocytes, where the antigen-binding affinity of the newly formed receptors will be tested, through interactions with follicular DCs and T_{FH} cells. GC B cells capture antigens presented by follicular DCs, internalize, process and present them to T_{FH} cells, that positively select GC B cells that express receptors with higher affinities for antigens. The selected B cells move again to the DZ, and the cycle repeats until a population of mature high-affinity antibody secreting B cells is generated. Cells with disadvantaged mutations that impair antigen-biding affinity are eliminated by apoptosis (Gatto e Brink, 2010).

The migrating dynamics of B cells take advantage of the differential expression of the chemokines CXCL12 and CXCL13 between the DZ and LZ. Centroblasts express higher levels of CXCR4 on their surface making them more responsive to CXCL12. As this molecule is more expressed on the DZ, centroblasts migrate to this zone in a CXCR4-dependent manner. Centrocytes express more CXCR5 and the ligand of this receptor, CXCL13, is abundant on the LZ, orientating theses B cells to this area of the GC (Allen *et al.*, 2004).

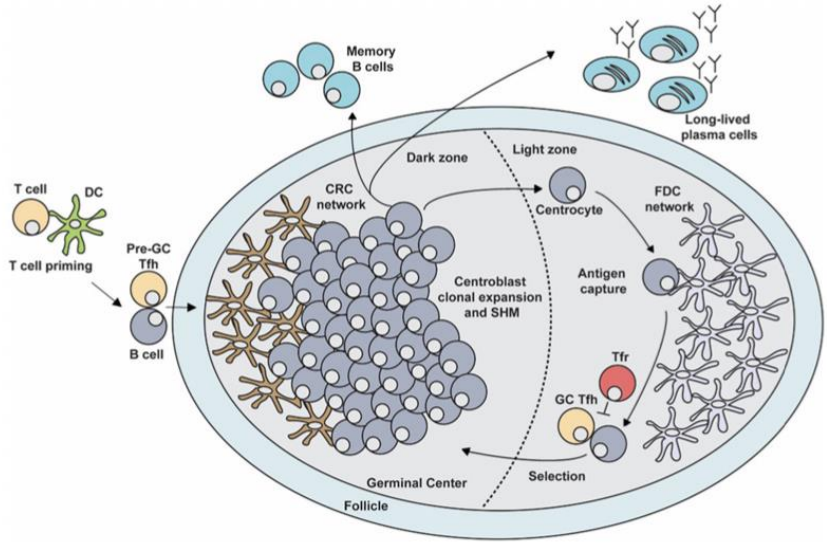

Figure 1.3– The germinal center (GC) reaction. The GC is a microanatomical structure that forms on secondary lymphoid organs when an adaptive immune response is initiated. The GC has two distinct zones: the dark zone (DZ) and light zone (LZ). DZ is where GC B cells proliferate and undergo somatic hypermutation (SHM). The LZ is where GC B cells are positively selected by interacting with follicular dendritic cells and T-follicular helper cells. The selected B cells return to the DZ for further rounds of proliferation and SHM. After, B cells can exit the GC as memory B cells or as high-affinity antibody-secreting plasma cells. Adapted from reference (Stebegg *et al.*, 2018).

1.3 Tridimensional cell cultures

Two-dimensional (2D) cell cultures and animal models are the standard practice in biomedical research and new drug development and have contributed greatly to the scientific knowledge we possess today. However, some limitations are associated to these models, as animal physiology is not totally comparable to that of humans, which translates into different responses to pathogens or drugs (AKHTAR, 2015; Norman, Van, 2019; Watkins *et al.*, 2008). Additionally, ethical issues related to using animals for research purposes are also an impediment for the usage of animal models. As for 2D cell cultures, these allow for easy and fast replication of cells, that can be maintained for long periods of time, but fail to replicate the real three-dimensional (3D) microenvironment of tissues and organs. Comparing 2D cultures to *in vivo* tissues, cell morphology is altered as well as the gene expression, and cell-cell interactions are reduced (Kapałczyńska *et al.*, 2016; Sakalem *et al.*, 2021). All this together ends up limiting advancements in research and wasting resources.

In recent years, the need for the development of organotypic platforms that better represent the human biology has grown and the trend is moving to the development of 3D cell cultures. Comparing to 2D cultures, the 3D approach allows for a better representation of the tissue/organ *in vivo* structure and are a step in the direction of overcoming the abovementioned limitations. Several approaches can be taken to develop 3D culture system, using one or more cellular types that self-organize to form a 3D structure that mimic tissues or organs *in vitro* (ThermoFisher Scientific, 2020).

Despite already being a great improvement from 2D cell cultures, 3D systems still fail to replicate same key features of living organs, mainly the physiological gradients that are crucial for tissues and organs to function normally. If the goal is to accurately replicate human physiology *in vitro*, these features must be considered when developing more reliable systems. The next step in 3D cell culture research is to implement the knowledge gathered until now to develop systems that integrate crucial mechanical and chemical signals in the development of a culture system. These new systems are referred to as Organ-on-a-chip (OoC) (Huh, Hamilton e Ingber, 2011).

OoC is an emerging technology that combines the advancements in microsystems with biology and tissue engineering(Leung *et al.*, 2022)to create a platform that better mimics human physiology. OoC consists of a hollow chamber, where the desired cells are cultured, and a network of very fine microfluidic channels

that transport fluids in and out of the cell chamber. This way, it is possible to control the microenvironment that is established, introducing stimulating factors or removing metabolites and debris (Zoio e Oliva, 2022). These platforms can be developed using primary tissues (e.g. organ slice from biopsy) or engineered tissues (e.g. organoids), in a top-down approach, or using isolated cells obtained from primary, immortalized or stem cell-derived sources, in a bottom-up approach (Leung *et al.*, 2022) It is also possible to combine two or more chips, establishing multi-organ systems allowing to evaluate interactions between different organs or tissues (Ingber, 2022; Leung *et al.*, 2022; Picollet-D'hahan *et al.*, 2021).

Over the years, OoC technology has been applied to several research fields and used to model a wide range of human tissues and organs, such as the skin (Zoio, Lopes-Ventura e Oliva, 2022), liver (Liu *et al.*, 2022), adipose tissue (Rogal *et al.*, 2022), among others. Regarding the immunology field, OoC can prove helpful to better understand the mechanisms that underlay the interactions between immune cells and drug or vaccine candidates and assess their efficiency and safety more accurately. To establish a lymphoid OoC the following aspects must be taken into account: the development of a biomimetic scaffold where immune cells can be seeded and grow, the generation of an appropriate microenvironment, the establishment of dynamic flow conditions and the replication of key functional features of the lymphoid organ (Shanti *et al.*, 2021). A successful example of a lymphoid OoC are the lymphoid follicles on chip developed by Goyal *et al*. This group reported the first *in vitro* model that supports the formation of human lymphoid follicles, using primary human cells obtained from peripheral blood. The group also demonstrated that this platform can be used to test immunization responses to vaccines and adjuvants *in vitro* (Goyal *et al.*, 2022).

1.4 Aim of the study

The aim of this study is to characterize human tonsils, regarding the MNCs phenotype and the presence of GCs, and to establish a tonsil organoid. Therefore, this work stands on three objectives. The first, is to isolate MNCs and evaluate their phenotype. The second objective is to document the functional architecture of secondary lymphoid organs. The final objective is to establish a tonsil organoid, using a transwell system.

2. Materials and Methods

2.1 Patient samples and informed consent

Tonsils were collected from individuals undergoing tonsillectomy due to medical indication at Hospital Dona Estefânia – Centro Hospitalar Lisboa Central. The parents or legal tutor of all children signed the informed consent. All experiments were conducted with the approval of hospital Dona Estefânia and NOVA Medical School ethics committee (nº127/2020/CEFCM), in accordance with the provisions of the Declaration of Helsinki and the Good Clinical Practice guidelines of the International Conference on Harmonization.

After collection, whole tonsils were kept at 4 °C in Roswell Park Memorial (RPMI) 1640 medium supplemented with 10% fetal bovine serum (FBS) and 1% antibiotic/antimycotic until processed.

2.2 Immunophenotyping human palatine tonsils

2.2.1 Isolation of tonsillar mononuclear cells

Whole tonsils were put on a 60-mm dish containing Phosphate Buffered Saline (PBS) 1x and the cauterized parts, fibroid tissue and bloody/inflamed tissue were removed to ensure a more efficient isolation of the cells. After, the tonsils were cut into small pieces and filtered through a 70 µm cell strainer into a 50 mL tube containing 1mL of PBS 1x. To avoid wasting cells, the PBS from the dish that contained the tonsils was also filtered through the cell strainer. The resulting cell suspension was homogenized and diluted with PBS 1x, if necessary. To prepare for the density gradient centrifugation, Ficoll medium was added to a 50 mL tube, in 1:2 proportion of Ficoll:cell suspension. The suspension was then carefully layered over Ficoll medium, with the caution not to mix the two layers. The tube was centrifuged at 700 x g for 30 min, without brake. After density gradient centrifugation, the mononuclear cell (MNC) layer was collected and transferred to a 15 mL tube and PBS 1x was added up to 10 mL. The tube was centrifuged at 700 x g for 15 min (1st wash). After centrifugation, instead of discarding it, the supernatant was decanted into another 15mL tube to minimize cell waste. The two tubes were centrifuged again, at 700 x g for 15 min (2nd wash). After the second centrifugation, the supernatant of the two tubes was discarded, and the cells were counted and resuspended in RPMI medium.

2.2.2 Immunophenotyping tonsillar mononuclear cells

For phenotyping tonsillar immune cells, previously isolated MNCs were incubated overnight at 37 °C with complete RPMI 1640 medium. When assessing cytokines and cytotoxic molecules, cells were stimulated overnight (~15 hours) with 50 ng/mL of PMA, 500ng/mL of Ionomycin and 2µg/mL of the protein transport inhibitor, BFA. On day 1, MNCs were washed once with PBS 1x and transferred to 96-well round-bottom plates, where the staining protocol was performed. For viability, cells were incubated for 20 min at 4 °C in the dark with Fixable Viability Dye eFluor 506. After, cells were washed once with FACS buffer (2% FBS in PBS 1x). Surface staining was performed with the antibodies listed on Table 2.1 for 1 hour at 4 °C in the dark. After surface staining, cells were washed twice with FACS buffer, fixed with 1% PFA for 20 min at RT in the dark, and permeabilized with 0.1% Saponin for 20 min at RT in the dark. Intracellular staining was performed with the antibodies listed on Table 2.2, for 1 hour at RT in the dark. After, cells were washed once with FACS+Saponin (0.1% Saponin in FACS buffer) followed by a second wash with FACS buffer. When assessing transcription factors, cells were instead fixed and permeabilized with Foxp3/Transcription Factor Staining Buffer Set for 1 hour at RT in the dark and washed once with permeabilization buffer 1x (1:10 Foxp3 Fixation/Permeabilization diluent in H_2OMQ). The intracellular staining followed as mentioned previously and, after, cells were washed twice with permeabilization buffer 1x. Finally, to prepare for flow cytometry analysis, cells were resuspended in FACS buffer and transferred to FACS tubes. Acquisition was performed in a BD FACSAria III instrument (BD Biosciences) and analyzed with FlowJo v.10.8.1.

Table 2.1 - List of antibodies and respective clone, fluorochrome supplier and catalog number used for surface staining on tonsil immunophenotyping.

Antibody	Clone	Fluorochrome	Source/Catalog#
Anti-CD3	UCHT1	A700	Biolegend/300424
Anti-CD4	SK3	PE-Fire 700	Biolegend/344665
Anti-CD8	HIT8a	Pacific Blue	Biolegend/300927
Anti-CD19	SJ25C1	BV650	Biolegend/363025
Anti-CD27	O323	APC	Biolegend/302809
Anti-CD38	HIT2	APC-Cy7	Biolegend/303525
Anti-CD40L	24-31	BV711	Biolegend/310837
Anti-CD40L	24-31	PerCP-Cy5.5	Biolegend/310833
Anti-CXCR3	G025H7	APC	Biolegend/353707
Anti-CXCR5	J25D4	APC-Cy7	Biolegend/356925
Anti-PD-1	EH12.2H7	PE-Cy7	Biolegend/329918
Anti-TLR4	HTA125	Unconjugated	Biolegend/312804)
Streptadivin	-	PE-Cy5	Biolegend/405205

Table 2.2 - List of antibodies and respective clone, fluorochrome supplier and catalog number used for intracellular staining on tonsil immunophenotyping.

Antibody	Clone	Fluorochrome	Source/Catalog#
Anti-CD40L	24-31	PE	Biolegend/310805
Anti-CD40L	24-31	A488	Biolegend/310815
Anti-CD40L	24-31	PerCP-Cy5.5	Biolegend/310833
Anti-CD40L	24-31	PE-Cy7	Biolegend/310831
Anti-Ki-67	Ki-67	PE	Biolegend/350503
Anti-Ki-67	Ki-67	A647	Biolegend/350509
Anti-TLR7	4G6	PE	Novus/NBP2-27251
Anti-TLR7	S18024F	PE	Biolegend/376903
Anti-TLR9	S16013D	BV421	Biolegend/394806
Anti-FoxP3	206D	BV421	Biolegend/320124
Anti-CXCR5	J25D4	APC-Cy7	Biolegend/356925
Anti-CXCR5	J252D4	A488	Biolegend/356911
Anti-IL-4	8D4-8	PE	Biolegend/500703
Anti-IL-10	JES3-19F1	PE-Dazzle	Biolegend/506811
Anti-IL-17	BL168	APC-Cy7	Biolegend/512320
Anti-TNFα	MAb11	PerCP-Cy5.5	Biolegend/502925
Anti-IFNγ	4S.B3	A647	BD Pharmingen/563495
Anti-Granzyme B	REA226	PE	MACS Miltenyi/130-116-486
Anti-Granzyme K	GM26E7	FITC	Biolegend/370507
Anti-Perforin BD48	B-D48	PE-Cy7	Biolegend/353316
Perforin	dG9	BV510	Biolegend/308119

2.3 Quantitation of germinal center area

For hematoxylin and eosin (H&E) stain, a section of the tonsil was cut and left in PFA 4% for, at least, 48 hours to fixate. After, the section was delivered to the NMSResearch Histology Facility, where the H&E staining protocol was performed. Images were taken using a Zeiss Imager Z2 microscope equipped with a Zeiss Axiocam 105 color using a 5x objective in a ZEN Blue 2012 software. GC area was determined on Fiji/ImageJ v.2.9.0/1.53t, as exemplified on Figure 2.1

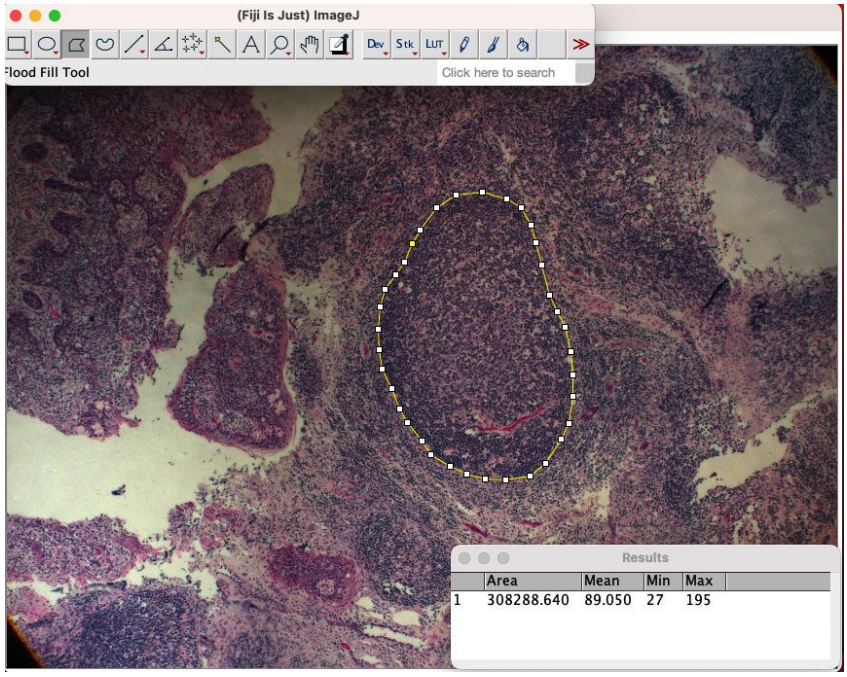

Figure 2.1 – Example of GC delimitation a respective area measurement using Fiji/ImageJ software, in μm^2.

2.4 Establishment of tonsil organoid cultures

2.4.1 Isolation of tonsillar mononuclear cells

Isolation of tonsillar mononuclear cells was performed as section 2.2.1, with the exception that, when mentioned, Ficoll density centrifugation was skipped.

2.4.2 Organoid preparation

For the development of tonsillar organoids, previously isolated MNCs were adjusted for $60x10^6$ cells/mL in RPMI. Cells were plated into 0.4 µm pore size cell culture inserts with polycarbonate membranes (Merck Millipore), 100 µL per insert, with the lower chamber consisting of 1ml of RPMI. To stimulate the cells, Staphylococcal Enterotoxin B (SEB) (1µg/mL) was added to the cell-containing insert. Cultures were incubated for at 37 °C, 5% CO2 with humidity and supplemented with additional medium to the lower chamber, as necessary.

2.4.3 Immunophenotyping tonsil organoid immune cells

Flow cytometry analysis was performed on day 0, 5, 10 and 15. On the day of each staining, cells were harvested by rinsing the cell insert membranes with PBS 1x. Cell were, then, centrifuged at 300 x g for 5 min, washed once with PBS 1x and transferred to 96-well round-bottom plates where the staining protocol was performed. Cells were surface stained and fixed according to what is mentioned on section 2.2.2. The antibodies used for the staining are listed on table 2.3. Finally, to prepare for flow cytometry analysis, cells were resuspended in FACS buffer and transferred to FACS tubes. Acquisition was performed in a BD FACSAria III instrument (BD Biosciences) and analyzed with FlowJo v10.8.1.

Table 2.3 - List of antibodies and respective clone, fluorochrome supplier and catalog number used for surface staining on tonsil organoid immunophenotyping.

Antibody	Clone	Fluorochrome	Source/Catalog#
Anti-CD3	HIT3a	APC-Cy7	Biolegend/300424
Anti-CD3	UCHT1	A700	Biolegend/344665
Anti-CD4	SK3	PE-Fire 700	Biolegend/344665
Anti-CXCR5	J252D4	PE	Biolegend/356904
Anti-PD-1	EH12.2H7	PE-Cy7	Biolegend/329918
Anti-ICOS	C398.4A	Pacific Blue	Biolegend/313521
Anti-CD69	FN50	PE-Cy5	Biolegend/310908
Anti-CD19	SJ25C1	BV650	Biolegend/363025
Anti-CD27	O323	APC	Biolegend/302809
Anti-CD38	HIT2	APC-Cy7	Biolegend/303525

2.5 Statistical analysis

Statistical analysis was performed using GraphPad Prism v.9.0.0. First, normality of the data was tested using Shapiro-Wilk normality test ($n \leq 6$). If samples followed a normal distribution, the appropriate parametric tests were applied, if not, non-parametric tests were chosen.

Overall, a p value ≤ 0.05 was considered statistically significant. The p values were calculated using the true distribution (exact p values). Results were considered significant at $*p \leq 0.05$, $**p \leq 0.01$, $***p \leq 0.001$, $****p \leq 0.0001$. For multiple comparisons adjusted p values were used.

For paired data comparisons between two groups Paired *t*-test and Wilcoxon matched-pairs signed rank tests were used.

For paired data comparisons between three or more groups Repeated measures one-way ANOVA with Tukey's multiple comparisons test and Friedman test were used.

All data is shown as mean ± standard deviation (SD).

The number of biological replicates (n) is specified in the legends of the figure as well as the statistical tests that were applied.

3. Results

3.1 Cohort description

The demographic and clinical data for the tonsil donors enrolled in this study are shown in table 3.2. Tonsils samples (*n*=7) were obtained mainly from female donors (*n*=4). The mean age of the cohort was 5.43 ± 1.8 years. All samples were collected from patients undergoing tonsillectomy due to obstructive sleep apnea (OSA).

Table 3.1 – Demographic data and experiments performed with tonsil samples.

Subject ID	Age (years)	Gender	Cause of extraction	MNC Phenotyping	Tonsil Organoid	Histology
HD_1	6	F	OSA	+		
HD_2	5	F	OSA	+		
HD_3	6	F	OSA			+
HD_4	4	F	OSA			+
HD_5	4	M	OSA	+		
HD_6	4	M	OSA	+	+	+
HD_7	9	M	OSA	+	+	+

HD – Human donor
F – Female
M – Male
OSA – Obstructive sleep apnea

3.2 Lymphocytes subpopulations in human tonsils

The first step to characterize human tonsils was to determine the frequency of the major lymphocyte populations. MNCs obtained from five tonsil samples (n=5) were stained for CD3, CD4, CD8 and CD19 markers. T-helper (T_H) lymphocytes appear as $CD3^+CD4^+$ cells, T-cytotoxic (T_C) lymphocytes appear as $CD3^+CD8^+$ and B lymphocytes appear as $CD3^-CD19^+$ cells. The gating strategy for selecting these lymphocyte populations is present on figure 3.1-A It was possible to infer that T_H cells represent 15.0 ± 5.5%, T_C cells represent 3.8 ± 3.5 5% and B cells represent 57.34 + 9.3% of the total tonsillar lymphocytes (Fig. 3.1-B).

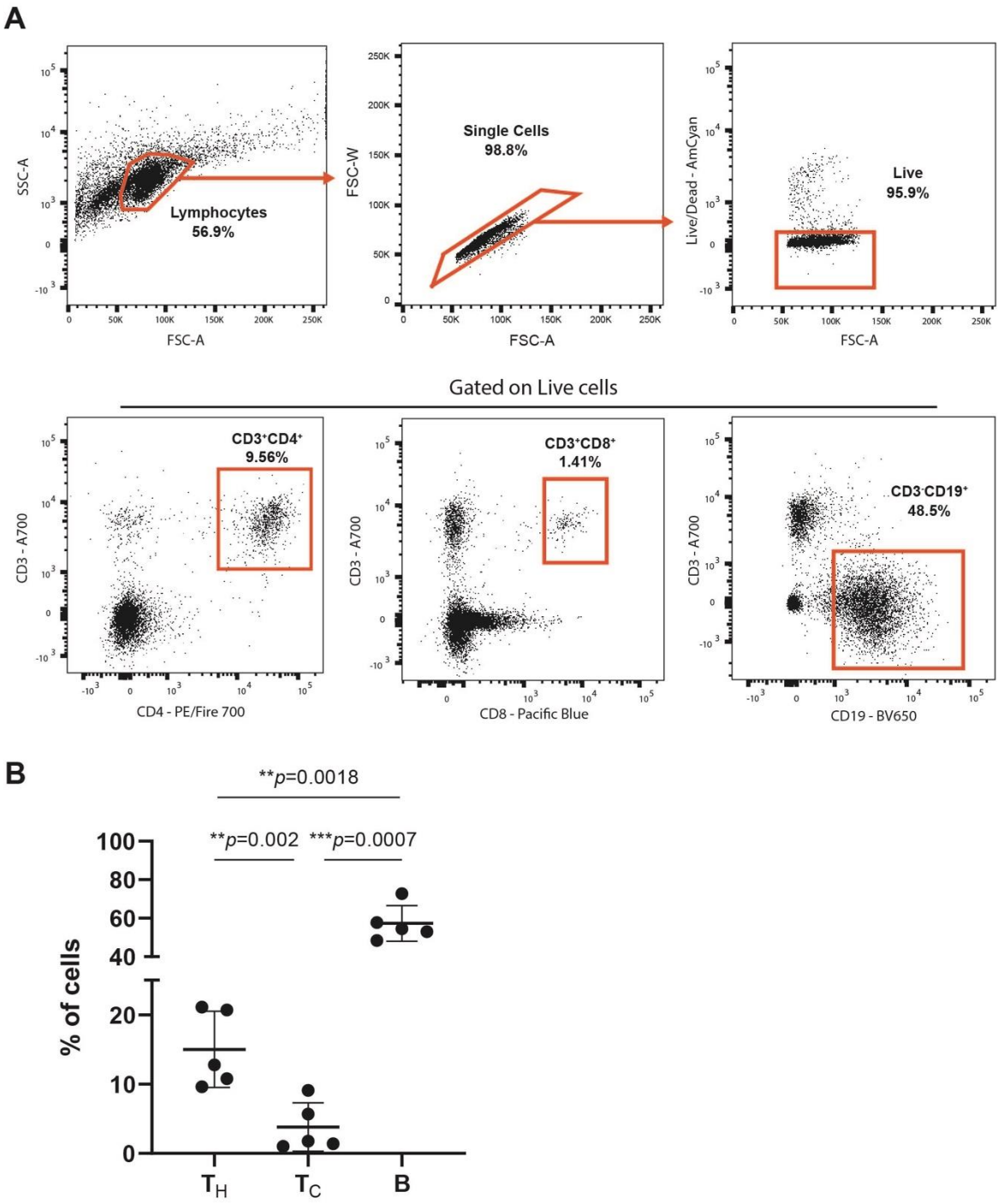

Figure 3.1 – T_H, T_C and B lymphocytes in MNCs of human tonsils. A – Gating strategy of $CD3^+CD4^+$ (T_H), $CD3^+CD8^+$ (T_C) and $CD3^-CD19^+$ (B) lymphocytes in human tonsil mononuclear cells. **B** – cumulative frequency of T_H, T_C and B lymphocytes in MNCs form human tonsils (n=5). Data presented as mean ± SD; sample normality distribution was tested by Shapiro-Wilk normality test; P value **p≤0.01 and ***p≤0.001 were determined by Repeated measures one-way ANOVA with Tukey's multiple comparisons.

3.3 Expression of CXCR5 and PD-1 markers on T lymphocytes

To characterize T_H and T_C lymphocytes regarding the presence of follicular helper phenotype, cells were stained for CXCR5 and PD-1 markers (n=5) (Fig. 3.2-A). It was observable that these markers where present on T_H cells (21.02 ± 7.61%) while on T_C cells their expression was much lower (1.11 ± 1.33%), indicating that follicular helper phenotype is not common on T_C cells (Fig. 3.2-B)

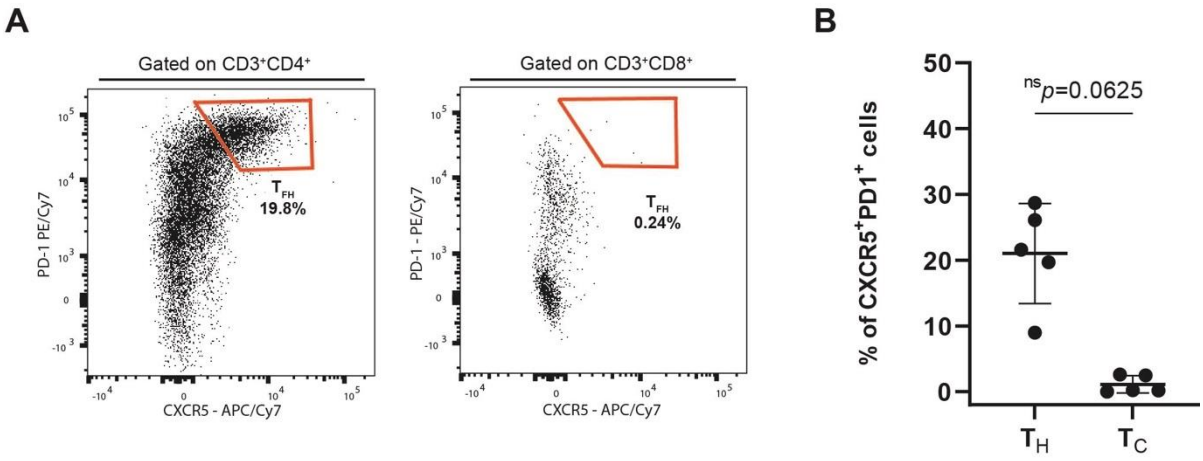

Figure 3.2 – Follicular helper phenotype of T_H and T_C lymphocytes. A – Representative plot for $CXCR5^+PD\text{-}1^+$ cells, gated on $CD3^+CD4^+(T_H)$ and $CD3^+CD8^+$ (T_C). **B** – Cumulative frequencies of $CXCR5^+PD\text{-}1^+$ cells in T_H and T_C lymphocytes (n=5). Data presented as mean ± SD; sample normality distribution was tested by Shapiro-Wilk normality test; P value ns (not significant) was determined by Wilcoxon matched pairs signed rank test.

3.4 Cytotoxic molecules expression by T_H cells and T_C cells

Granzyme B (GrB) , granzyme K (GrK) and perforin mediate the cytotoxic response, by inducing apoptosis of target cells. The study of the production of these molecules by tonsillar lymphocytes is important to better understand the type of immune response that is induced on human tonsils (Dan *et al.*, 2019). The production of GrB, GrK and perforin was analyzed on $CD4^+$ T_H cells (n=5) and on CD8+ T_C cells (n=3) on day 1 after stimulation with PMA+Iono.

3.4.1 Granzyme B, Granzyme K and Perforin in T_H cells

$CD4^+$ T_H cells produced GrB in low concentrations, on both stimulated (0.73 ± 0.46%) and unstimulated conditions (0.53 ± 0.19%) (Fig. 3.3-A). Stimulation seemed to induce a slight increase in the production of GrB, but this increase does not have statistical significance. MFI GrB seemed to counter this tendency (Fig. 3.3-B). The mean fluorescence of unstimulated conditions was higher and more dispersed, with MFI values raging from 777 to 15 053, while for the stimulated conditions, MFI values were more concentrated and lower, indicating that the production of GrB is reduced on stimulated cells. The differences observed for MFI GrB do not have statistical significance and can only be taken as predictions.

Similar to what happened with GrB, GrK was produced in low concentrations by $CD4^+$ T_H cells on both the stimulated (0.56 ± 0.5%) and unstimulated conditions (0.58 ± 0.33%) (Fig. 3.4-A). Here, stimulation did not lead to any differences on the expression profile of GrK. MFI GrK supported the previous conclusion. MFI was similar for both unstimulated and stimulated conditions (Fig. 3.4-B).

Perforin was also produced in low concentrations. Unstimulated $CD4^+$ T_H cells showed a slightly higher production (0.79 ± 0.70%) than their stimulated counterpart (0.37 ± 0.52%), but the difference is not statistically significant (Fig. 3.6-A). MFI Perforin analysis was in line with the observed tendency of perforin production by $CD4^+$ T_H cells (Fig.5-B).

Overall, stimulation with PMA+Iono did not lead to significant changes in the production of GrB, GrK or Perforin by CD4+ TH cells.

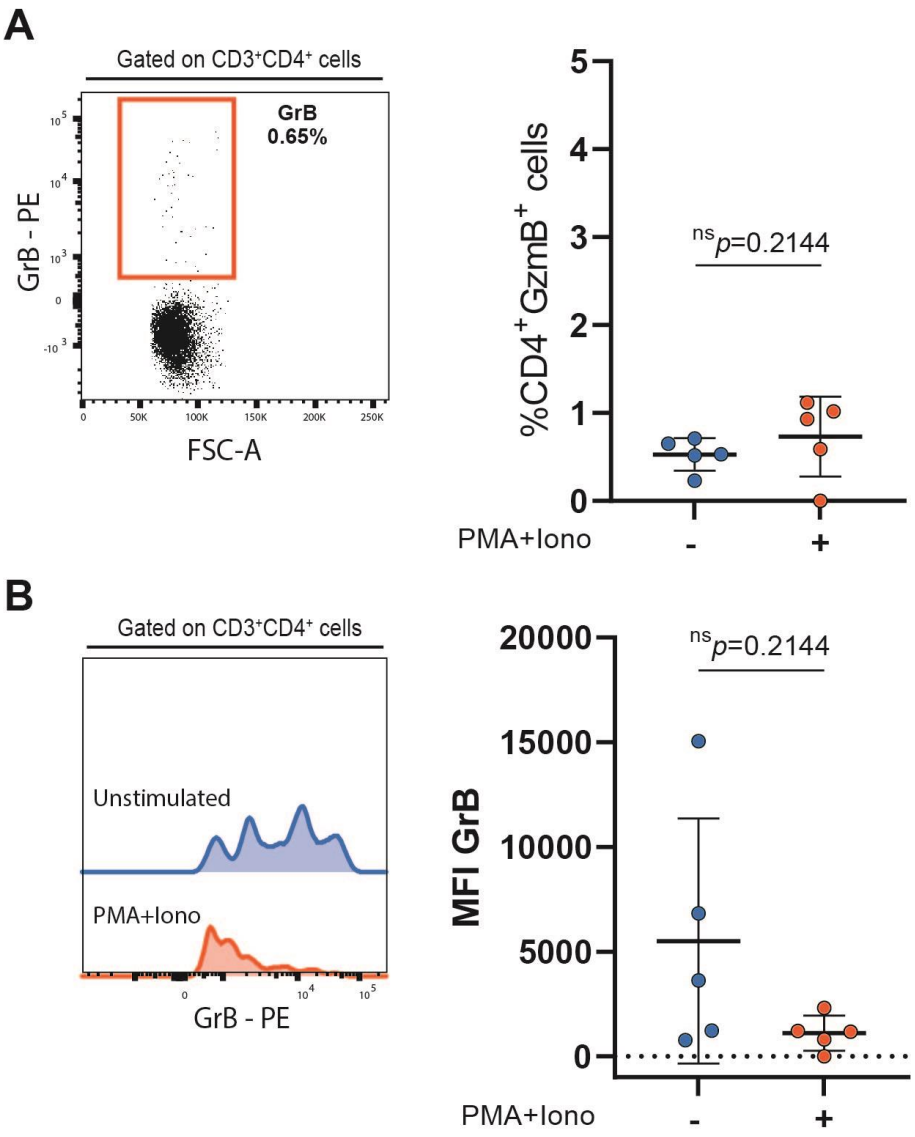

Figure 3.3 – Granzyme B (GrB) expression by T_H lymphocytes. A – Representative plot and cumulative frequencies for GrB expression by T_H lymphocytes (n=5) in unstimulated condition (blue) and stimulated with PMA+Iono (orange). **B** – Representative histogram and cumulative frequency of GrB MFI in unstimulated condition (blue) and stimulated with PMA+Iono (orange). Data presented as mean ± SD; sample normality distribution was tested by Shapiro-Wilk normality test; P value ns (not significant) was determined by (**A**, **B**) paired t-test.

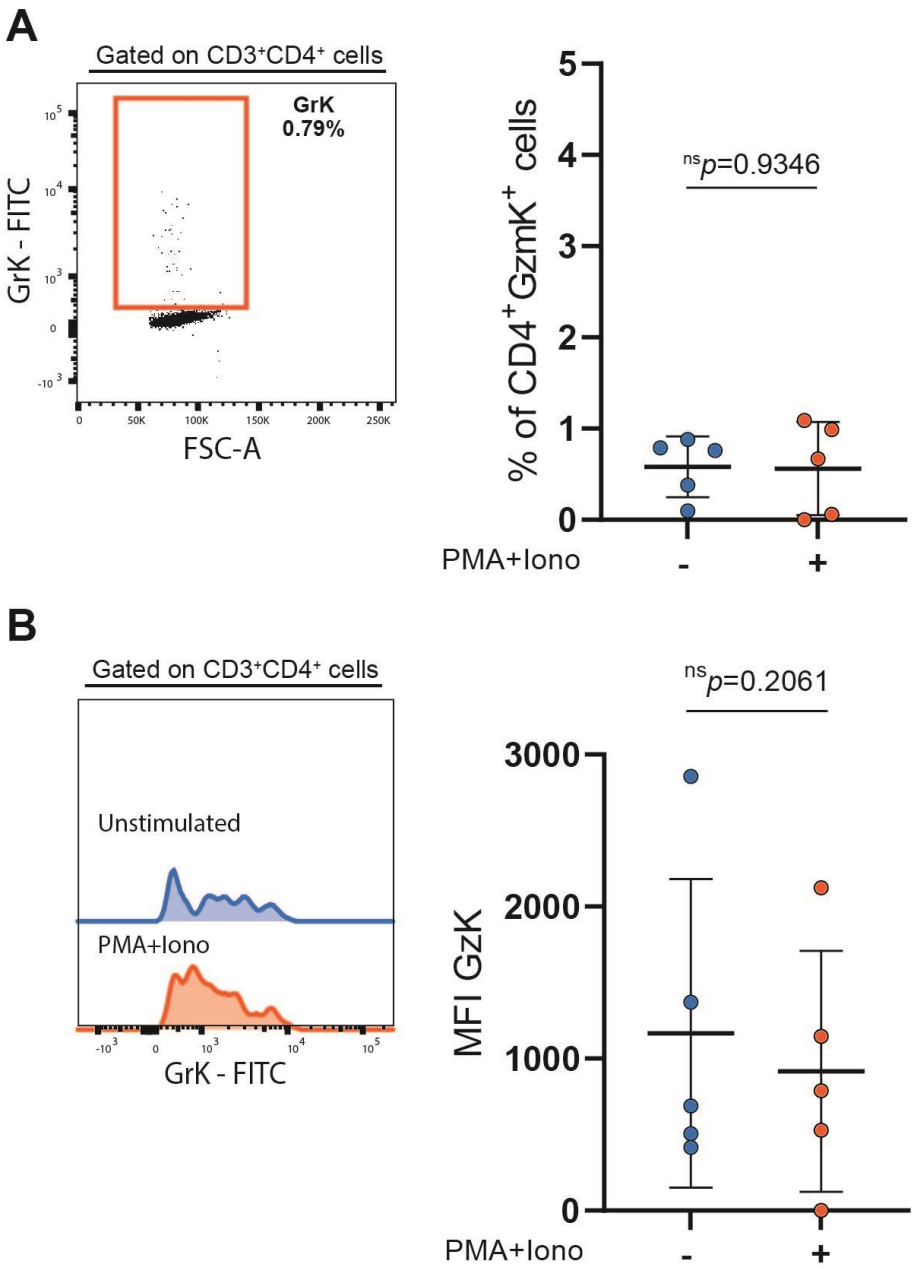

Figure 3.4 – Granzyme K (GrK) expression by T_H lymphocytes. A – Representative plot and cumulative frequencies for GrK expression by T_H lymphocytes (n=5) in unstimulated condition (blue) and stimulated with PMA+Iono (orange). **B** – Representative histogram and cumulative frequency of GrK MFI in unstimulated condition (blue) and stimulated with PMA+Iono (orange). Data presented as mean ± SD; sample normality distribution was tested by Shapiro-Wilk normality test; P value ns (not significant) was determined by (**A**, **B**) paired t-test.

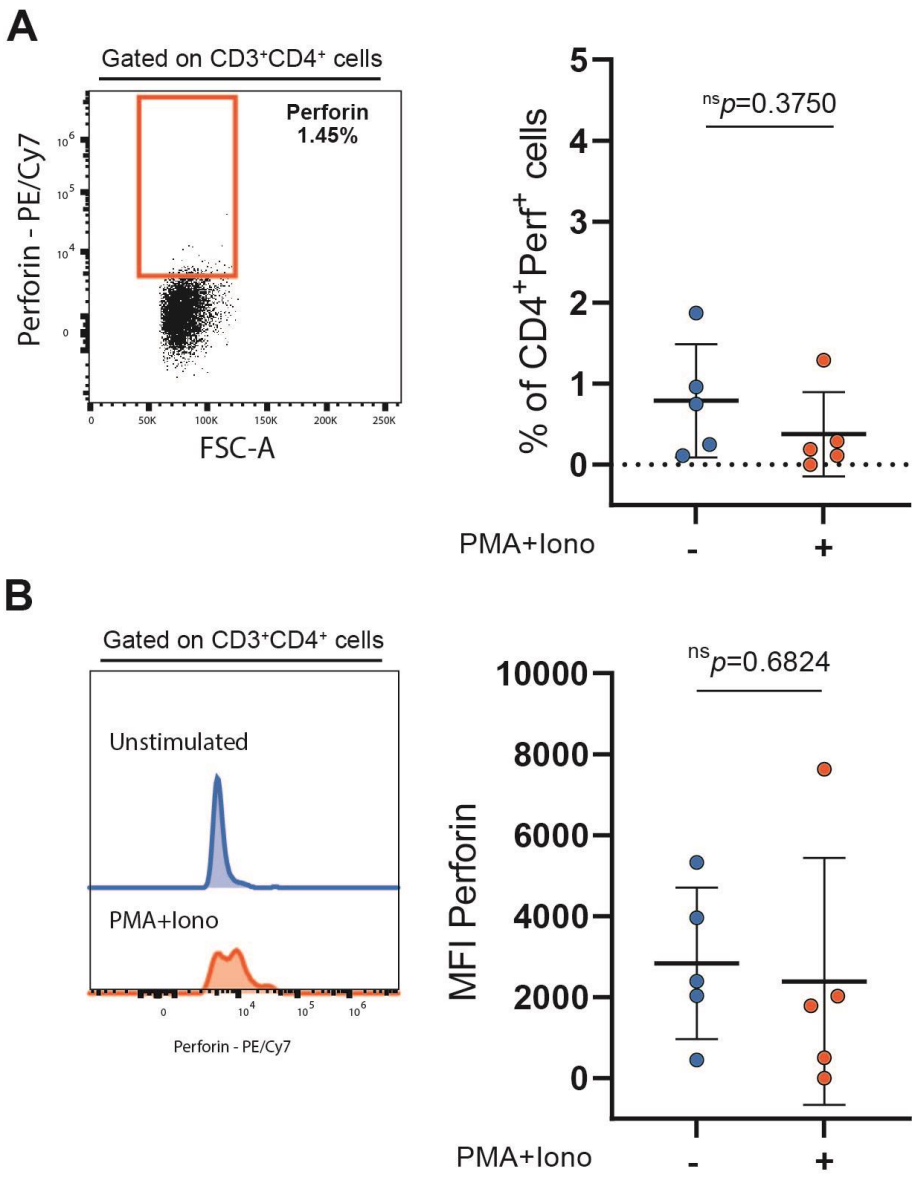

Figure 3.5 – Perforin expression by T_H lymphocytes. A – Representative plot and cumulative frequencies for Perforin expression by T_H lymphocytes (n=5) in unstimulated condition (blue) and stimulated with PMA+Iono (orange). **B** – Representative histogram and cumulative frequency of Perforin MFI in unstimulated condition (blue) and stimulated with PMA+Iono (orange). Data presented as mean ± SD; sample normality distribution was tested by Shapiro-Wilk normality test; P value ns (not significant) was determined by (**A**) Wilcoxon matched pairs signed rank test and. (**B**) paired t-test.

3.4.2Granzyme B, Granzyme K and Perforin in T_C cells

GrB, GrK and perforin production was observable in higher concentrations for $CD8^+$ T_C cells. GrB, GrK and perforin production by T_C cells was analyzed in three samples (*n*=3) cells. Production of GrB remained stable between unstimulated (13.36 ± 6.75%) and stimulated (13.30 ± 3.97%) conditions (Fig. 3.6-A). Regarding GrK, the mean expression for unstimulated cells (16.97 ± 19.23) was higher than for the stimulated conditions (11.70 ± 9.67), but not statistically significant (Fig. 3.7-A). Perforin expression does not differ between unstimulated (13.52 ± 13.9%),) and stimulated condition (9.74 ± 3,79%) (Fig. 3.8-A). The detection of cytotoxin production by T_C indicates that these cells retain their cytotoxic characteristic on human tonsils.

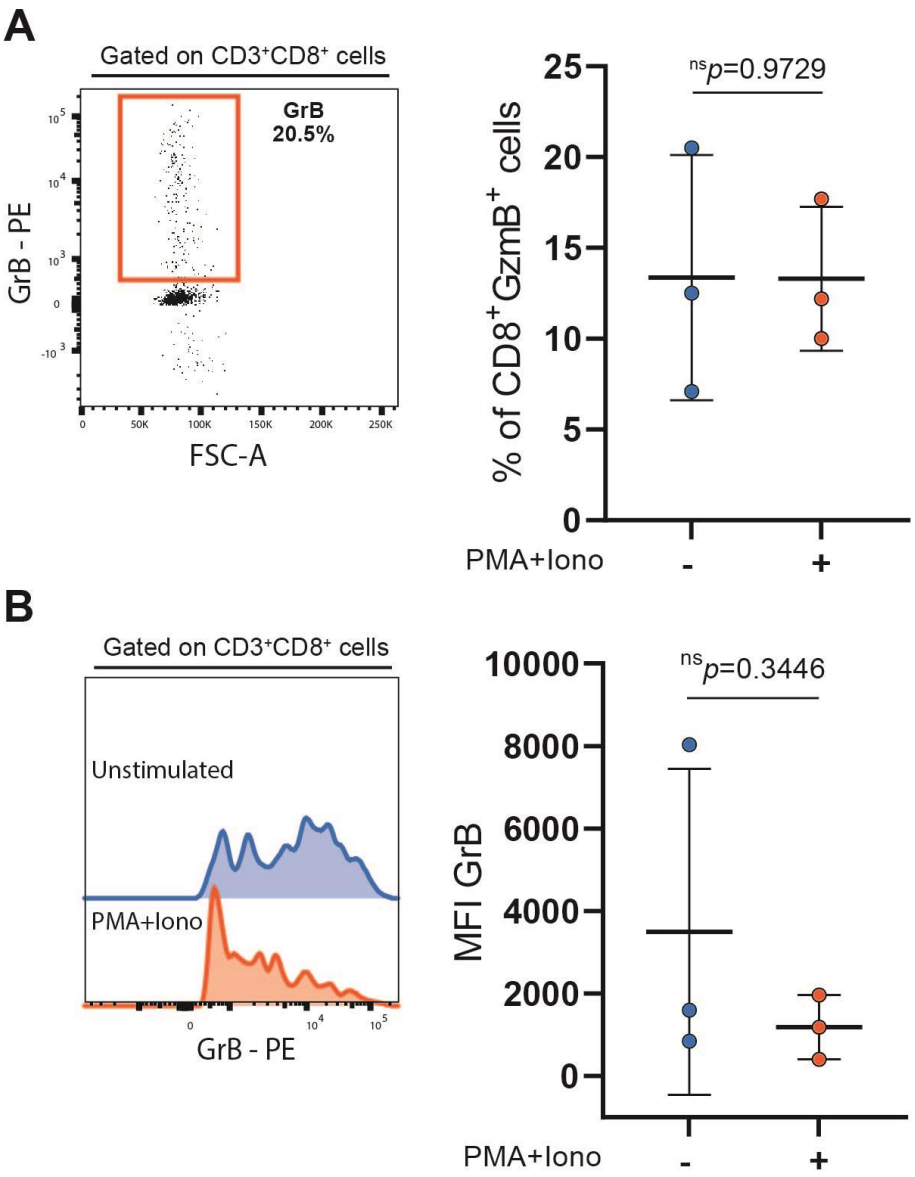

Figure 3.6 – Granzyme B (GrB) expression by T_C lymphocytes. A – Representative plot and cumulative frequencies for GrB expression by T_{FH} lymphocytes (n=3) in unstimulated condition (blue) and stimulated with PMA+Iono (orange). **B** – Representative histogram and cumulative frequency of GrB MFI in unstimulated condition (blue) and stimulated with PMA+Iono (orange). Data presented as mean ± SD; sample normality distribution was tested by Shapiro-Wilk normality test; P value ns (not significant) was determined by (**A**, **B**) paired t-test.

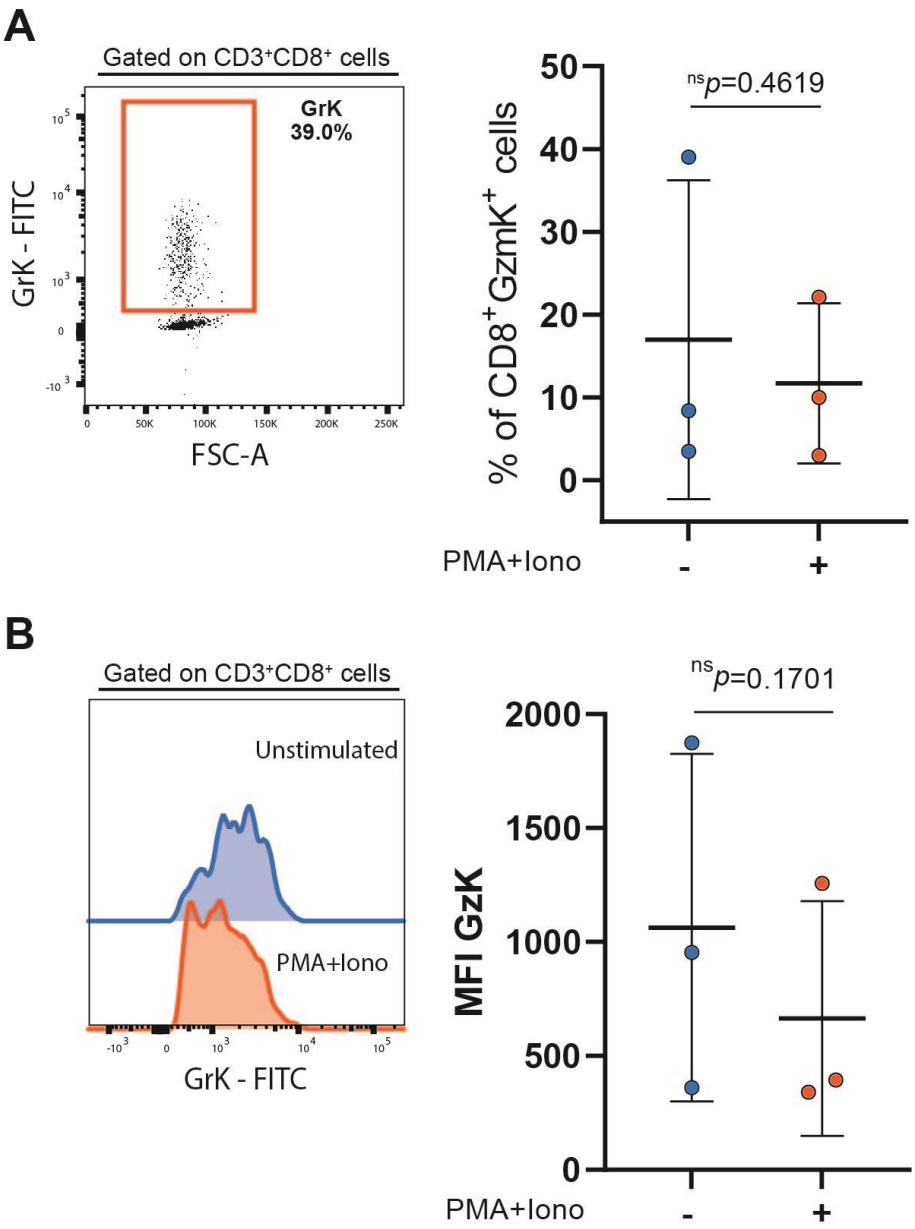

Figure 3.7 – Granzyme K (GrK) expression by T_C lymphocytes. A – Representative plot and cumulative frequencies for GrK expression by T_{FH} lymphocytes (n=3) in unstimulated condition (blue) and stimulated with PMA+Iono (orange). **B** – Representative histogram and cumulative frequency of GrK MFI in unstimulated condition (blue) and stimulated with PMA+Iono (orange). Data presented as mean ± SD; sample normality distribution was tested by Shapiro-Wilk normality test; P value ns (not significant) was determined by (**A**, **B**) paired t-test.

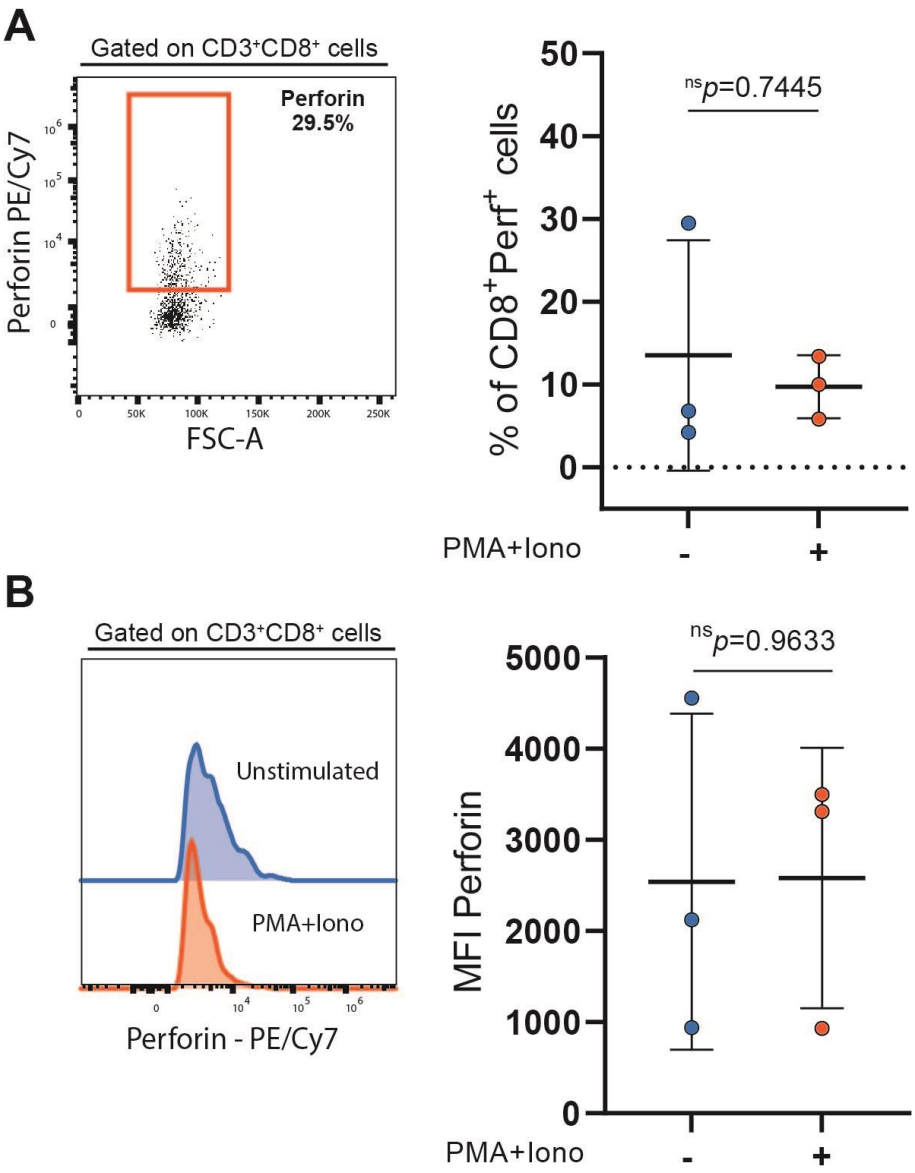

Figure 3.8 – Perforin expression by T_C lymphocytes. A – Representative plot and cumulative frequencies for Perforin expression by T_{FH} lymphocytes (n=3) in unstimulated condition (blue) and stimulated with PMA+Iono (orange). **B** – Representative histogram and cumulative frequency of Perforin MFI in unstimulated condition (blue) and stimulated with PMA+Iono (orange). Data presented as mean ± SD; sample normality distribution was tested by Shapiro-Wilk normality test; P value ns (not significant) was determined by (**A**, **B**) paired t-test.

3.5 Expression of TLR4, TLR7 and TLR9 on T_H and T_{FH} cells

TLRs have been reported to be expressed by tonsils (Claeys *et al.*, 2003; Lesmeister, Bothwell e Misfeldt, 2006; Mansson, Adner e Cardell, 2006). These receptors are fundamental for the initiation of innate responses but the activation of TLRs can also bridge the gap between the innate and adaptive immunity (Mansson, Adner e Cardell, 2006). In this study T_H (*n*=5) and T_{FH} (*n*=4) cells were characterized regarding their TLR4, TLR7 and TLR9 expression profile. TLR 7 and TLR9 were expressed on both T_H cells (39.06 ±48.22%; 3.03 ± 1,28%) (Fig. 3.9-B) and T_{FH} cells (24,76 ± 42.63%; 3.48 ± 1.32%) (Fig. 3.10-B). TLR4 was not detected neither on T_H nor on T_{FH} cells. Two donors presented a greater expression of TLR7.

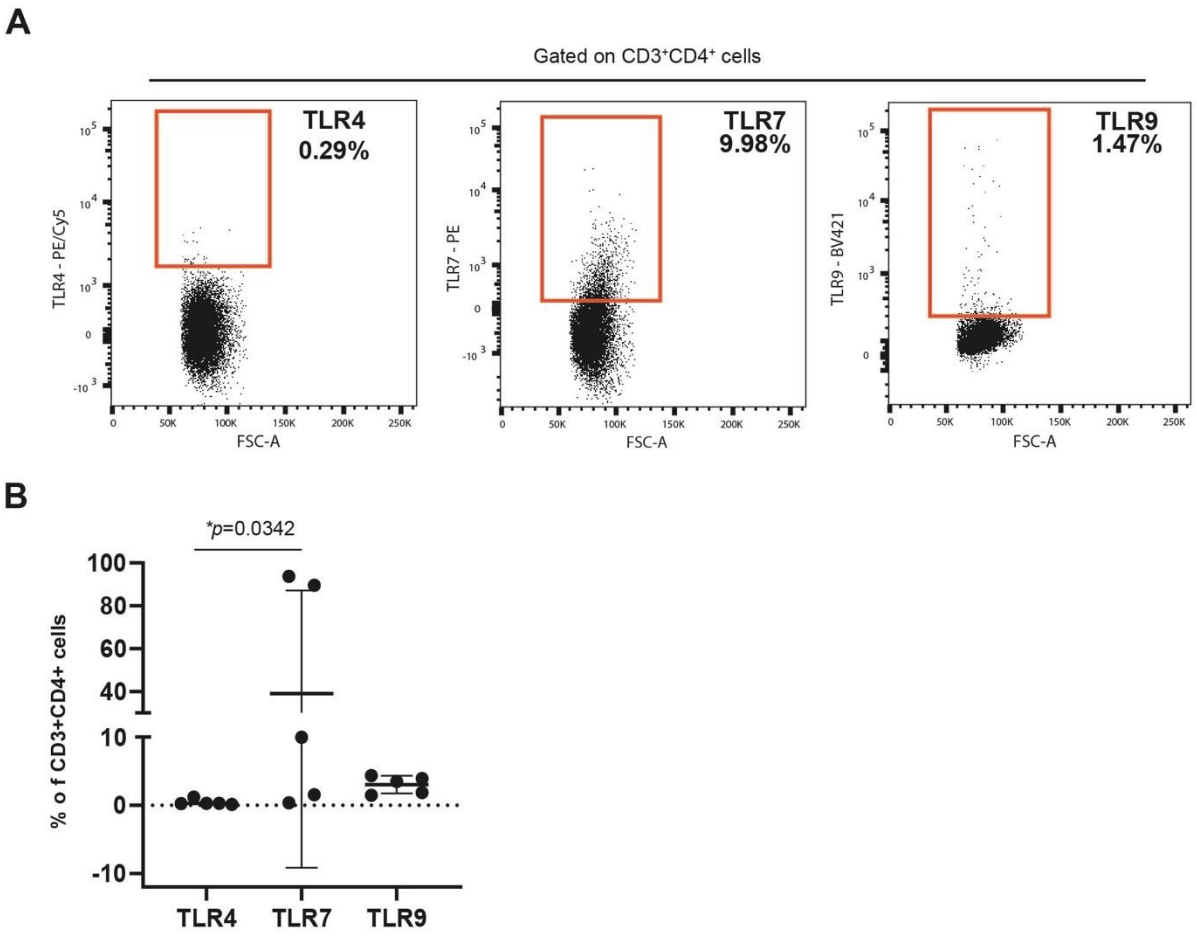

Figure 3.9 – TLR4, TLR7 and TLR9 expression on T_H lymphocytes. A – Representative plots for TLR4, TLR7 and TLR9 expression on T_H lymphocytes. **B** – Cumulative frequencies for TLR4, TLR7 and TLR9 expression on T_H lymphocytes (n=5). Data presented as mean ± SD; sample normality distribution was tested by Shapiro-Wilk normality test; P value *p≤0.05 was determined by Friedman test with Dunn's multiple comparisons.

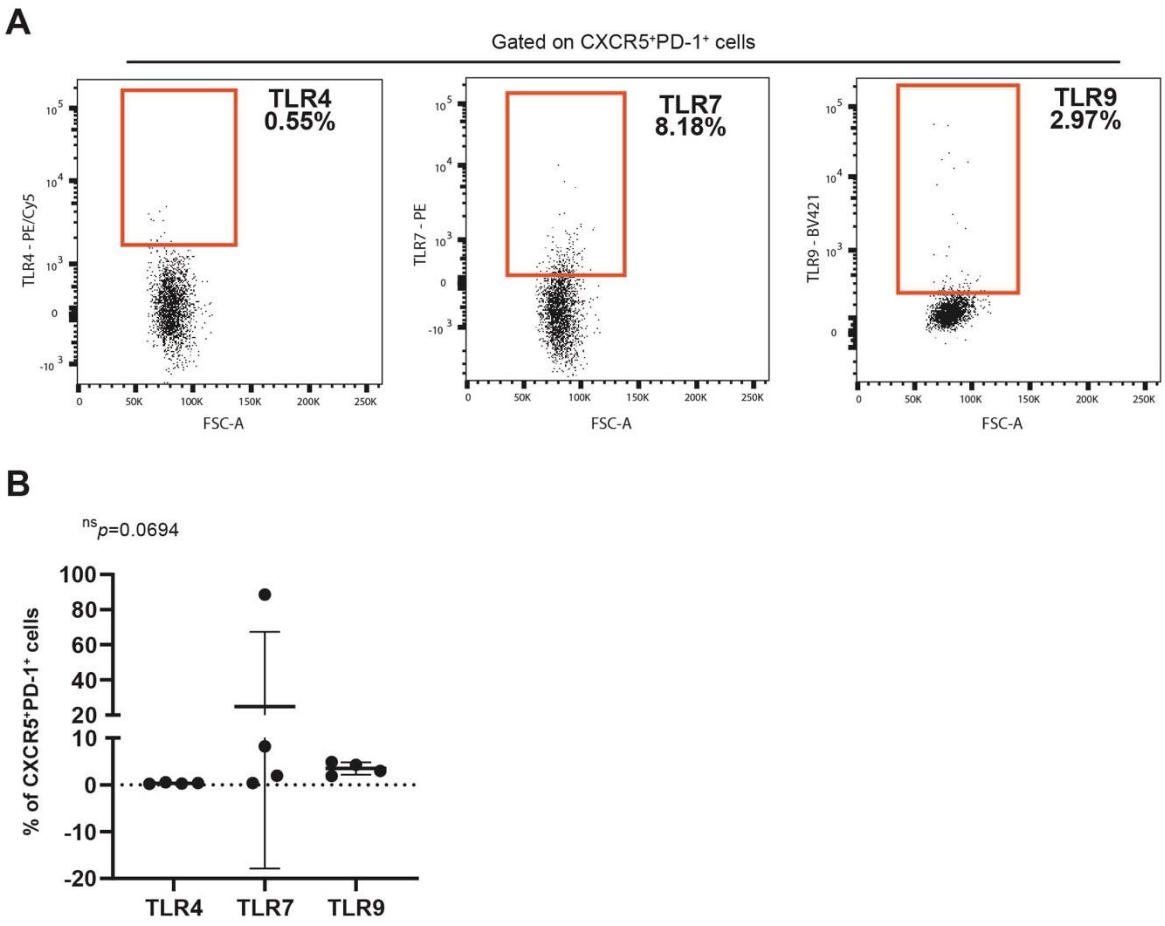

Figure 3.10 – TLR4, TLR7 and TLR9 expression on T_{FH} lymphocytes. A – Representative plots for TLR4, TLR7 and TLR9 expression on T_{FH} lymphocytes. **B** – Cumulative frequencies for TLR4, TLR7 and TLR9 expression on T_{FH} lymphocytes (n=4). Data presented as mean ± SD; sample normality distribution was tested by Shapiro-Wilk normality test; P value ns (not significant) was determined by Friedman test with Dunn's multiple comparisons.

3.6 Cytokine expression by CD4$^+$ T cells

The cytokine profile of T cells is directly related to their function. IFNγ, IL-4, IL-17 and Il-10 are the signature cytokines of the T_H1, T_H2, T_H17 and T_{reg} effector cells. These cells have distinct functions. These expression of these cytokines in the GC microenvironment can modulate the GC reaction and the class of antibodies that are produced.

TNFα is both a pro-inflammatory and anti-inflammatory cytokine that is central for the protection against infections (Mehta, Gracias e Croft, 2018). Therefore the study of cytokine production by T_H cells and T_{FH} cells is important to understand their role in the tonsil microenvironment. Cells were analyzed for cytokine production on day 1, after OVN stimulation with PMA+Iono.

3.6.1IL-4, IL-10 and IL-17 expression on CD4$^+$ T_H cells

CD4+ T_H cells expressed IL-4 in low concentrations. Although not statistically significant, IL-4 expression was slightly higher on unstimulated cells (4.39 ± 2.08%) than on the stimulated condition (3.56 ± 1.67), indicating that stimulation with PMA+Iono might reduce the expression of this cytokine (Fig. 3.11). Mean fluorescence MFI IL-4 corroborated these findings, as the values are decreased on the stimulated condition.

Similar to IL-4, CD4$^+$ T_H cells also expressed IL-10 in low concentrations, and the production pattern remained relatively the same between the unstimulated (1.41 ± 1.05%) and stimulated (1.47 ± 0.12%) conditions (Fig. 3.12).

Regarding IL-17, it was possible to observe that unstimulated cells did not express this cytokine and that, upon stimulation, IL-17 started to be produced by the cells, but in low levels (0.85 ± 5.29). This increase, however, was somewhat disperse and did not have statistical significance (Fig. 3.13).

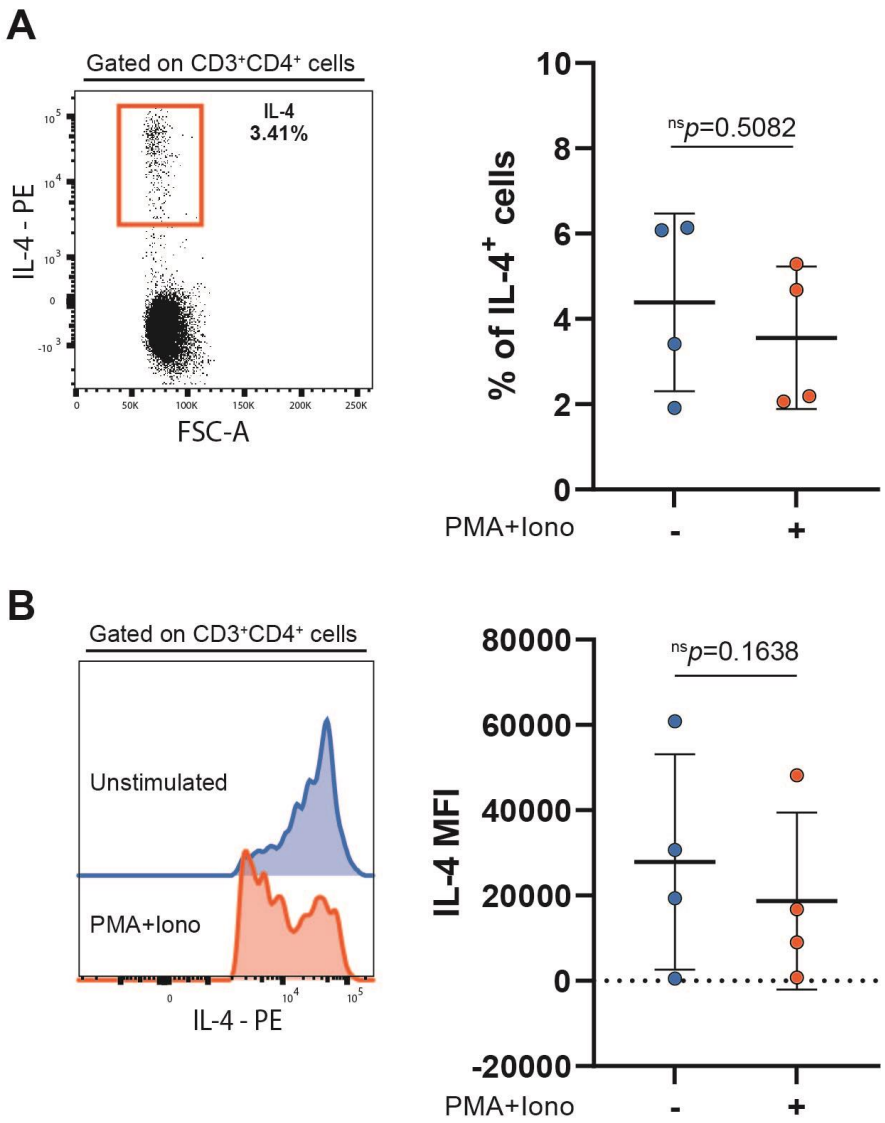

Figure 3.11 – IL-4 expression by T_H lymphocytes. A – Representative plot and cumulative frequency of IL-4 expression by T_H lymphocytes (n=4) in unstimulated condition (blue) and stimulated with PMA+Iono (orange). **B** – Representative histogram and cumulative frequency of IL-4 MFI for unstimulated condition (blue) and stimulated with PMA+Iono (orange). Data presented as mean ± SD; sample normality distribution was tested by Shapiro-Wilk normality test; P value ns (not significant) was determined by (**A**, **B**) paired t-test.

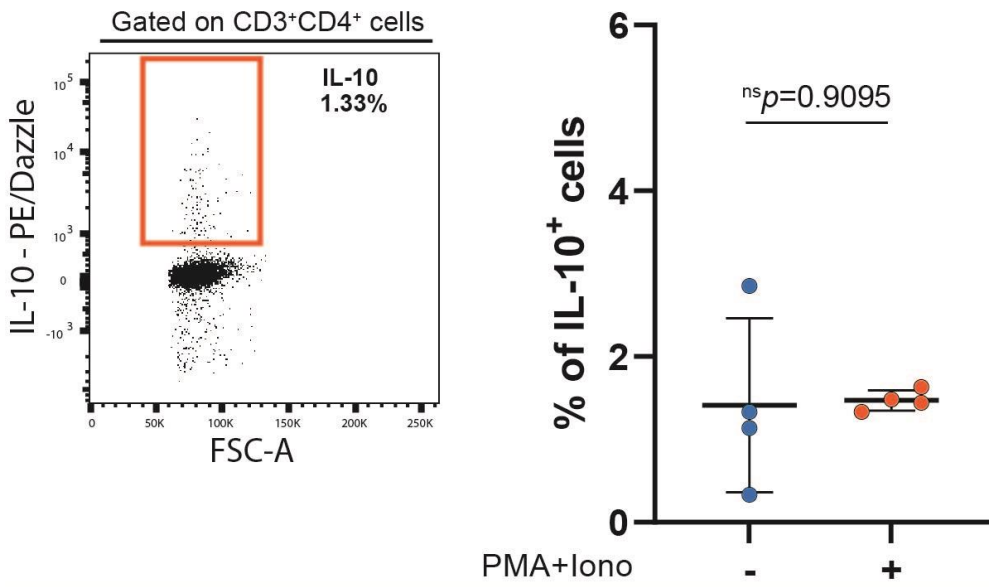

Figure 3.12– IL-10 expression by T_H lymphocytes. Representative plot and cumulative frequency of IL-10 expression by T_H lymphocytes (n=4) in unstimulated condition (blue) and stimulated with PMA+Iono (orange). Data presented as mean ± SD; sample normality distribution was tested by Shapiro-Wilk normality test; P value ns (not significant) was determined by paired t-test.

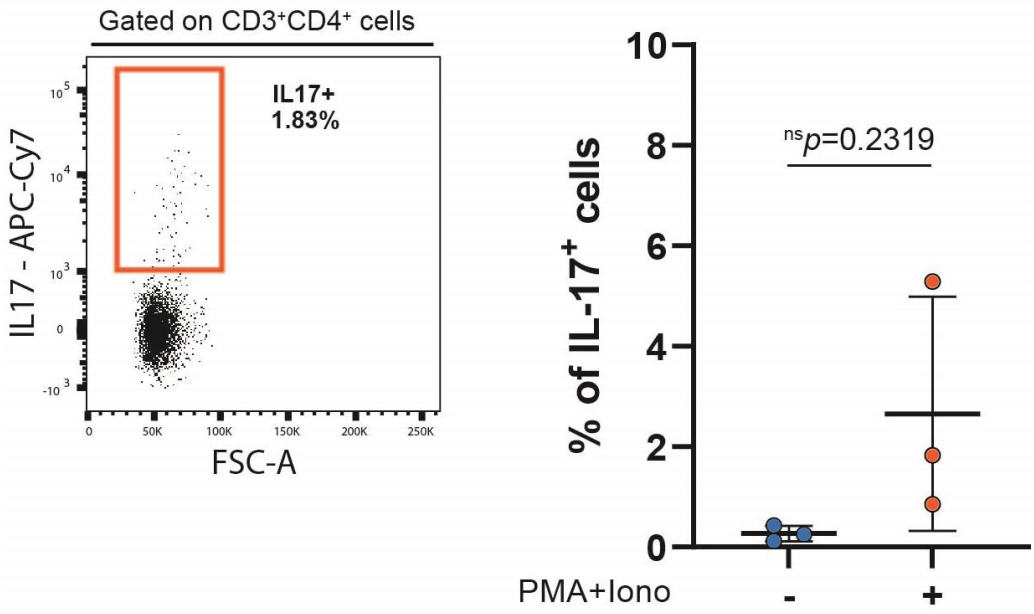

Figure 3.13 – IL-17 expression by T_H lymphocytes. Representative plot and cumulative frequency of IL-17 expression by T_H lymphocytes (*n*=3)in unstimulated condition (blue) and stimulated with PMA+Iono (orange). Data presented as mean ± SD; sample normality distribution was tested by Shapiro-Wilk normality test; P value ns (not significant) was determined by paired t-test.

3.6.2IFNγ and TNFα expression by CD4⁺ T_H cells

Naturally, CD4+ T_H cells express IFNγ in low concentrations (0.23 ± 0.30%). Upon stimulation, the expression noticeably increases (2.55 ± 1.83%). This increase is close to reaching statistical significance (*p*=0.0799), which indicates that IFNγ expression by CD4⁺ T_H is driven by stimulation (Fig. 3.14). Regarding TNFα, its expression was low in both unstimulated (0.53 ± 0.3%) and stimulated conditions (0.80 ± 0.64 %), with no effect of stimulation being observed (Fig. 3.15).

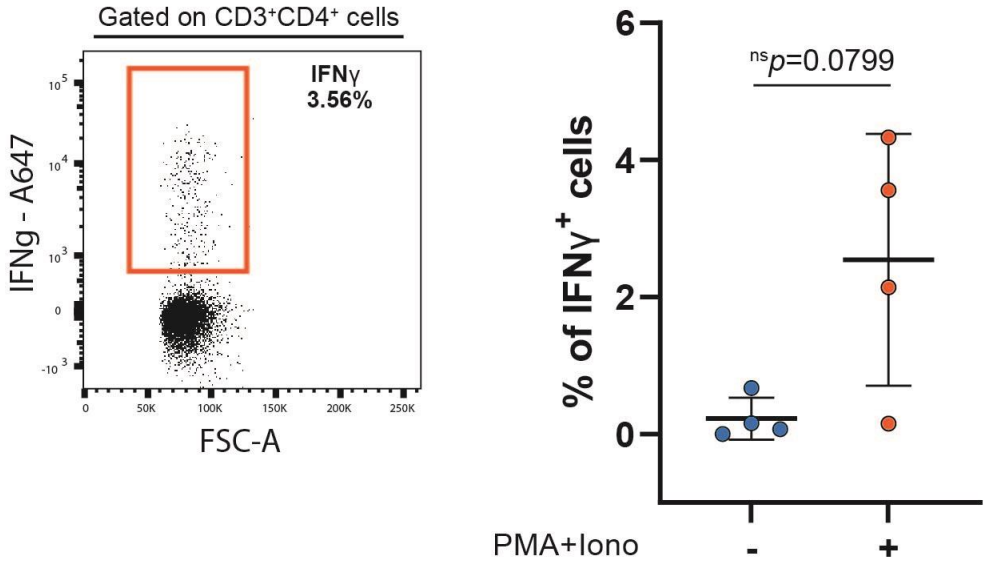

Figure 3.14 – IFNγ expression by T_H lymphocytes. Representative plot and cumulative frequency of IFNγ expression by T_H lymphocytes (n=4) in unstimulated condition (blue) and stimulated with PMA+Iono (orange). Data presented as mean ± SD; sample normality distribution was tested by Shapiro-Wilk normality test; P value ns (not significant) was determined by paired t-test.

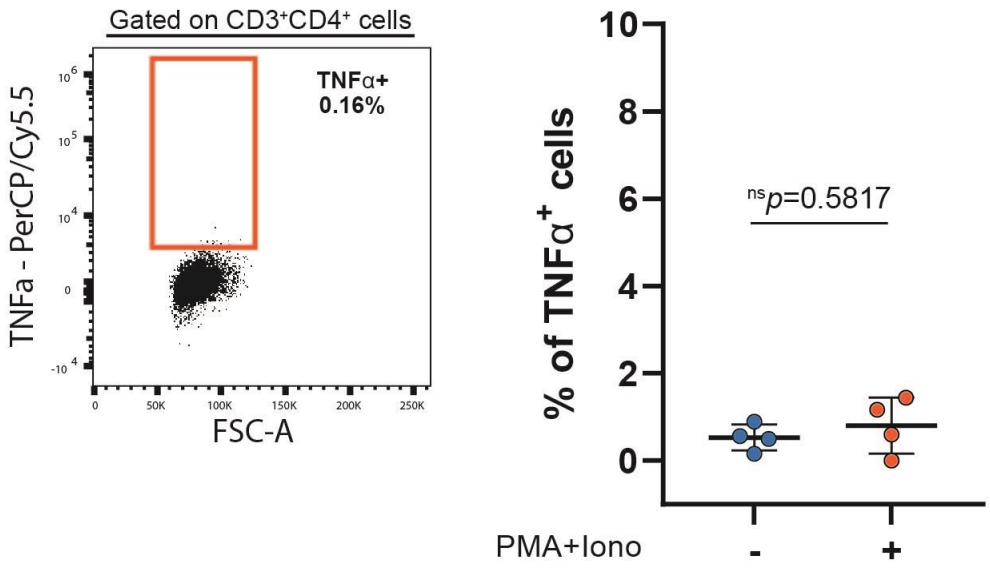

Figure 3.15 – TNFα expression by T_H lymphocytes. Representative plot and cumulative frequency of TNFα expression by T_H lymphocytes (n=4) in unstimulated condition (blue) and stimulated with PMA+Iono (orange). Data presented as mean ± SD; sample normality distribution was tested by Shapiro-Wilk normality test; P value ns (not significant) was determined by paired t-test.

After analyzing the cytokine expression on T_H cells, it is possible to understand that these cells constitutively express IL-4 and IL-10, but to a lesser degree and that the levels were not affected by PMA+Iono stimulation. IL-17 and IFNγ had low basal expression and the levels increased after stimulation. TNFα expression was not detected.

3.6.3IL-4, IL-10 and IL-17 expression on CD4+ T_{FH} cells

The pattern of IL-4 expression by CD4+ T_{FH} was very similar between unstimulated (2.95 ± 2.63%) and stimulated cells (2.91 ± 2.62%) (Fig. 3.16-A). However, when looking to MFI IL-4, it is possible to observe a slight decrease of fluorescence on the stimulated conditions (Fig. 3.16-B). IL-10 expression increases when cells are stimulated, and this difference is very close to reaching statistical significance (Fig. 3.17), which indicates that IL-10 expression by CD4+ T_{FH} cells is driven my stimulation. IL-17 expression by T_{FH} cells was only analyzed on two samples (Fig. 3.18), therefore, only predictions can be made regarding how IL-17 expression changes with stimulation. With this in mind, it seems that stimulation can increase the expression of IL-17 by T_{FH} cells, similar to what happened on T_H cells.

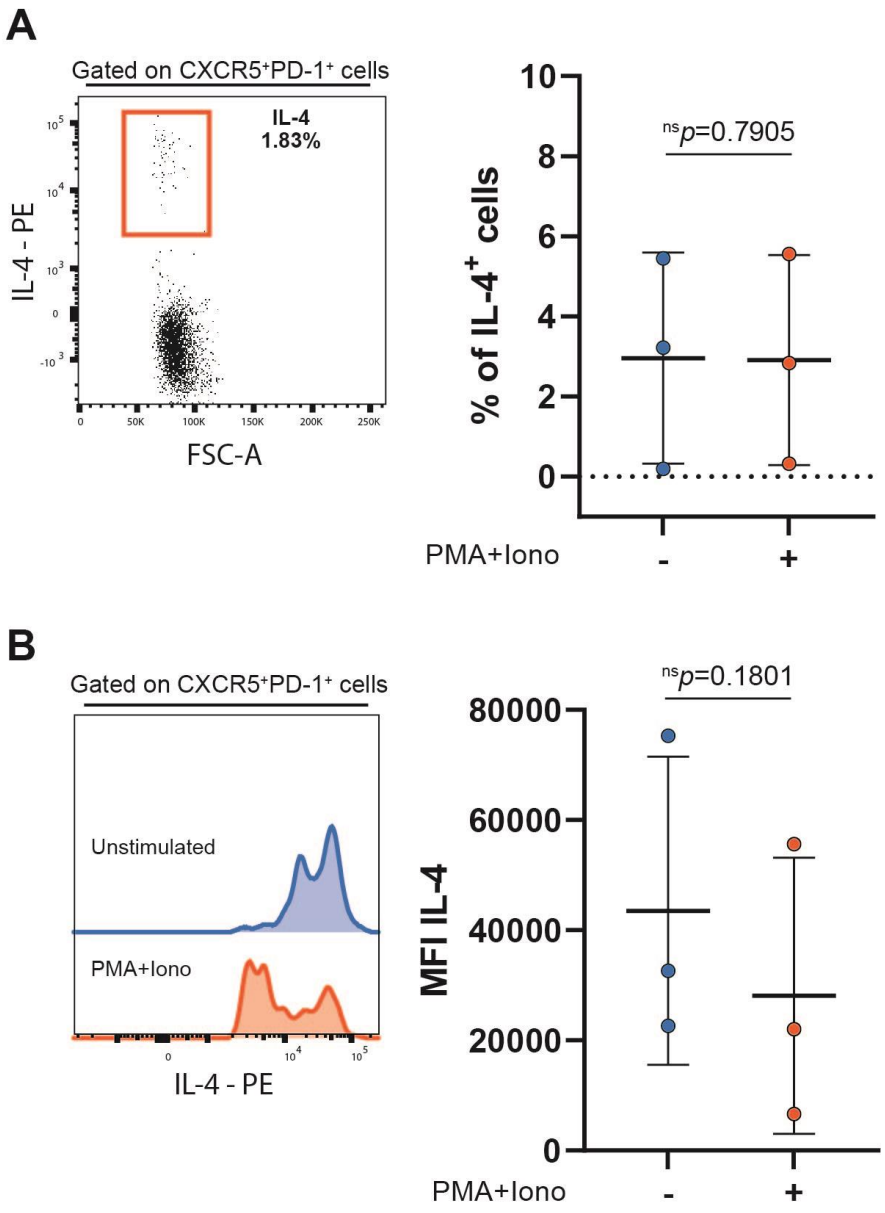

Figure 3.16 – IL-4 expression by T_{FH} lymphocytes. A – Representative plot and cumulative frequency of IL-4 expression by T_{FH} lymphocytes (n=3) in unstimulated condition (blue) and stimulated with PMA+Iono (orange). **B** – Representative histogram and cumulative frequency of IL-4 MFI for nstimulated condition (blue) and stimulated with PMA+Iono (orange). Data presented as mean ± SD; sample normality distribution was tested by Shapiro-Wilk normality test; P value ns (not significant) was determined by (**A**, **B**) paired t-test.

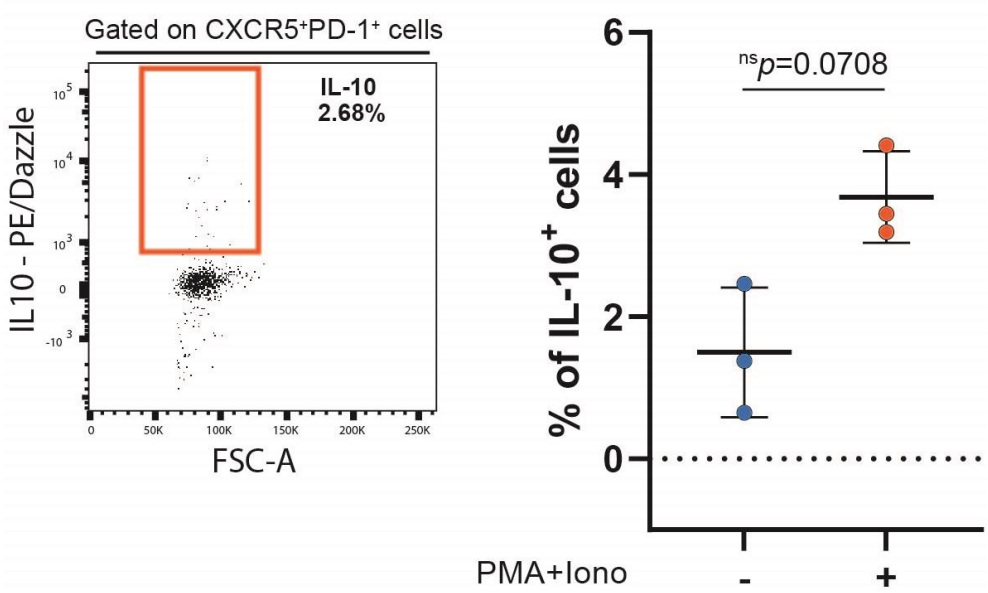

Figure 3.17 – IL-10 expression by T_{FH} lymphocytes. Representative plot and cumulative frequency of IL-10 expression by T_H lymphocytes (n=3) in unstimulated condition (blue) and stimulated with PMA+Iono (orange). Data presented as mean ± SD; sample normality distribution was tested by Shapiro-Wilk normality test; P value ns (not significant) was determined by paired t-test.

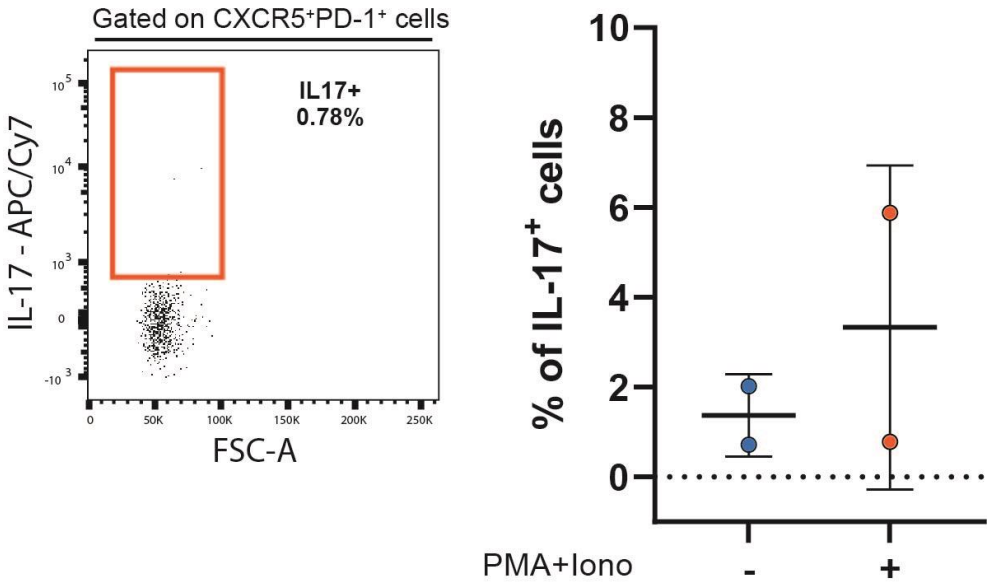

Figure 3.18 – IL-17 expression by T_{FH} lymphocytes. Representative plot and cumulative frequency of IL-17 expression by T_H lymphocytes (n=2) in unstimulated condition (blue) and stimulated with PMA+Iono (orange). Data presented as mean ± SD.

3.6.4IFNγ and TNFα expression by CD4⁺ T_{FH} cells

A slight increase in IFNγ expression by T_{FH} cells was observed on stimulated cells (1.63 ± 1.32 %) when comparing to unstimulated cell (0.71 ± 1.01%). This increase, however, was not statistically significant (Fig. 3.19). As for TNFα, its expression remained practically non-detectable on both unstimulated (0.88 ± 0.5%) and stimulated conditions (0.99 ± 0.87 %), with no effect of stimulation being observed (Fig. 3.20).

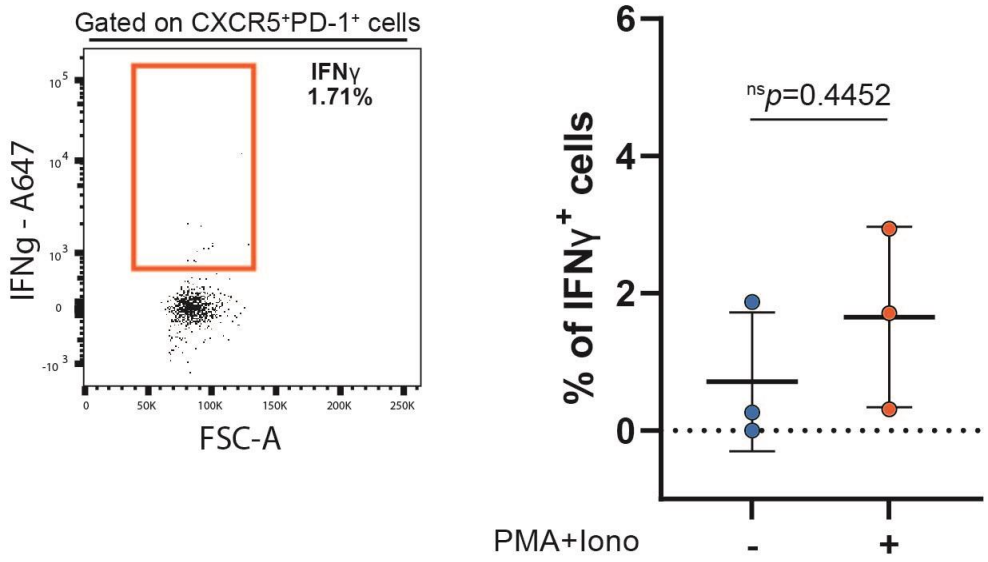

Figure 3.19 – IFNγ expression by T_{FH} lymphocytes. Representative plot and cumulative frequency of IFNγ expression by T_{FH} lymphocytes (n=3) in unstimulated condition (blue) and stimulated with PMA+Iono (orange). Data presented as mean ± SD; sample normality distribution was tested by Shapiro-Wilk normality test; P value ns (not significant) was determined by paired t-test.

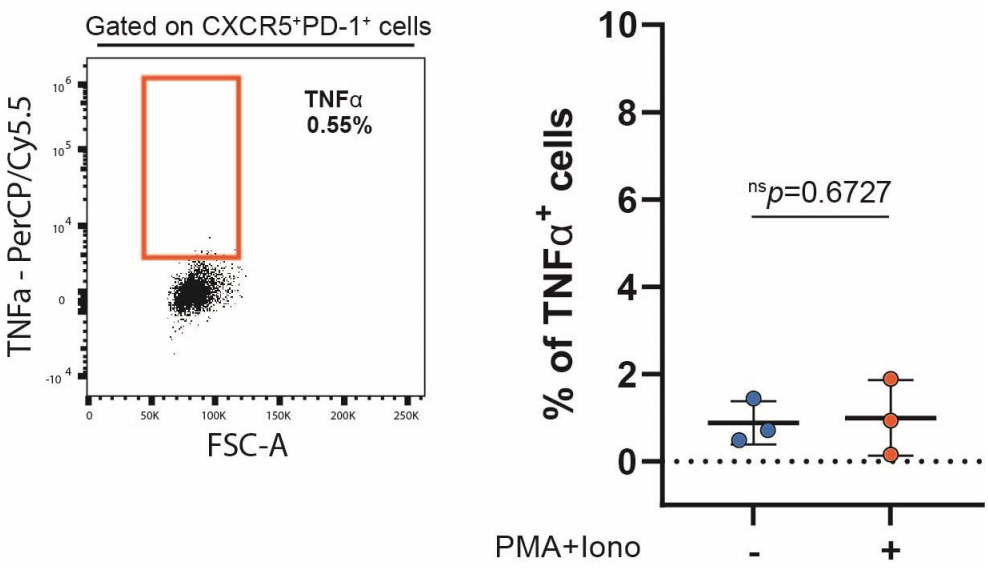

Figure 3.20 – TNFα expression by T_{FH} lymphocytes. Representative plot and cumulative frequency of TNFα expression by T_{FH} lymphocytes (n=3) in unstimulated condition (blue) and stimulated with PMA+Iono (orange). Data presented as mean ± SD; sample normality distribution was tested by Shapiro-Wilk normality test; P value ns (not significant) was determined by Paired t-test.

After analyzing the cytokine expression on T_{FH} cells, it is possible to understand that these cells constitutively express IL-4 and IL-10. Stimulation had no effect on IL-4 expression while it increased the levels of IL-10. An effect of stimulation can be observed on IL-17 and IFNγ. Expression of IL-17 seemed similar on T_{FH} and T_H cells but IFNγ expression was lower on T_{FH} cells. TNFα expression was not detected.

3.7 Expression of CXCR3 on T_H, T_{FH} and T_C cells

CXCR3 is a chemokine receptor whose expression is related with lymphocyte activation and IFNα production(Groom e Luster, 2011). The expression of this marker was analyzed on T_H, T_{FH} and T_C cells (Fig. 3.21-A), and it was possible to observe that all three cell populations expressed CXCR3. T_C cells were clearly the population CXCR3 was more expressed (31.60 ± 11.4%). Both T_H (7.99 ± 2.81%) and T_{FH} (10.51 ± 5.64 %) cells expressed CXCR3 in similar quantities but less than T_C (Fig. 3.21-B).

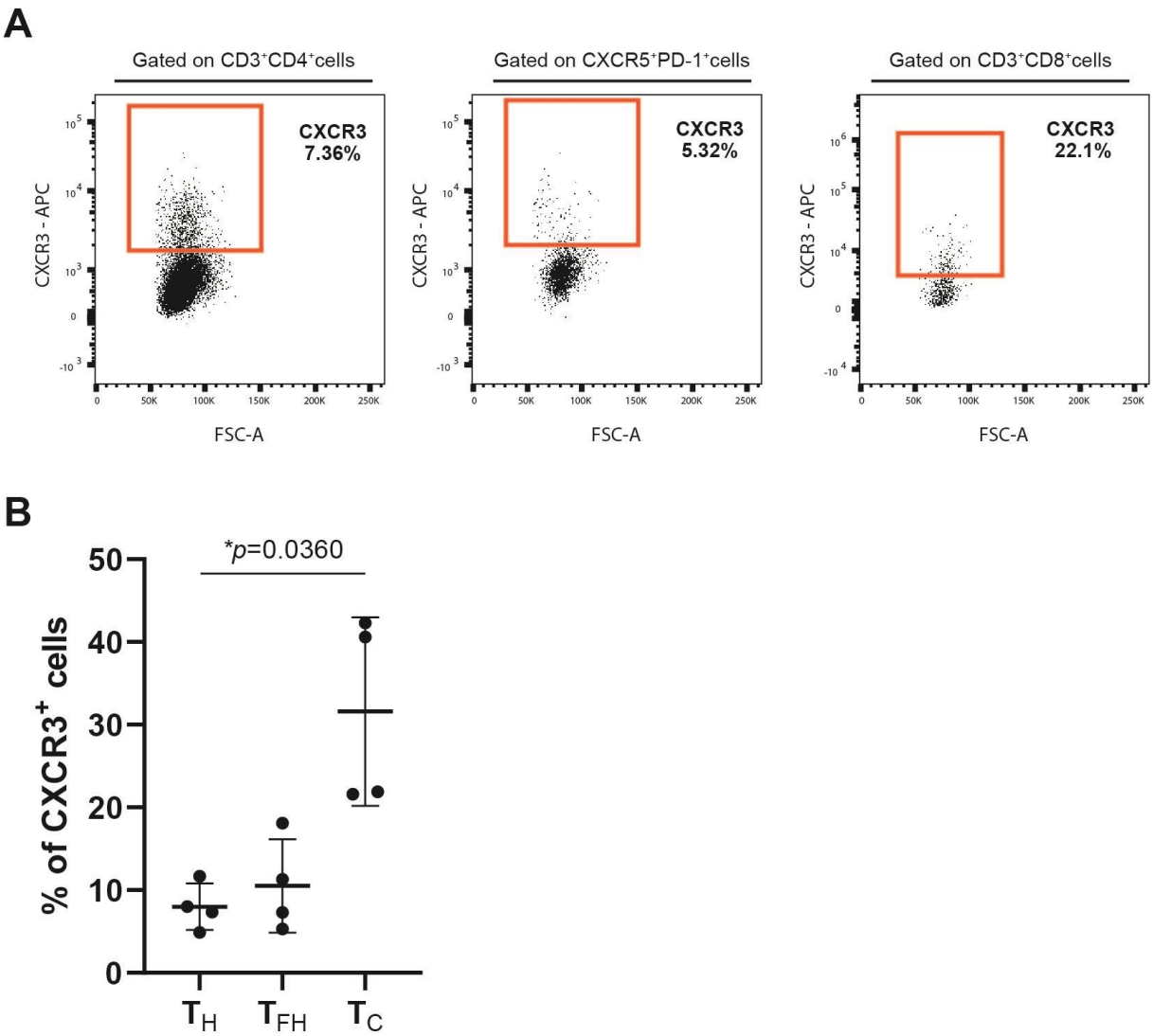

Figure 3.21 – CXCR3 expression by T_H, T_{FH} and T_C lymphocytes. A – Representative plot for CXCR3 expression by T_H, T_{FH} and T_C lymphocytes. **B** – Cumulative frequency of CXCR3 in T_H, T_{FH} and T_C lymphocytes (n=4). Data presented as mean ± SD; sample normality distribution was tested by Shapiro-Wilk normality test; P value *p≤0.05 was determined by Repeated measures one-way ANOVA with Tukey's multiple comparisons.

3.8 FoxP3 expression by T_H and T_{FH} cells

FoxP3 is a transcription factor that defines the T_{reg} lineage of CD4 T cells. In the context of GCs, T_{reg} cells can provide crucial signals for B cell development and affinity maturation (Linterman *et al.*, 2011). To investigate the presence of cells with regulatory characteristic, FoxP3 expression was analyzed within tonsillar T_H and T_{FH} cells (n=4). FoxP3 expression, was indeed detected on both cell populations, in similar quantities (T_H – 2.41 ± 1.53%; T_{FH} – 1.96 ± 0.89%) (Fig. 3.22).

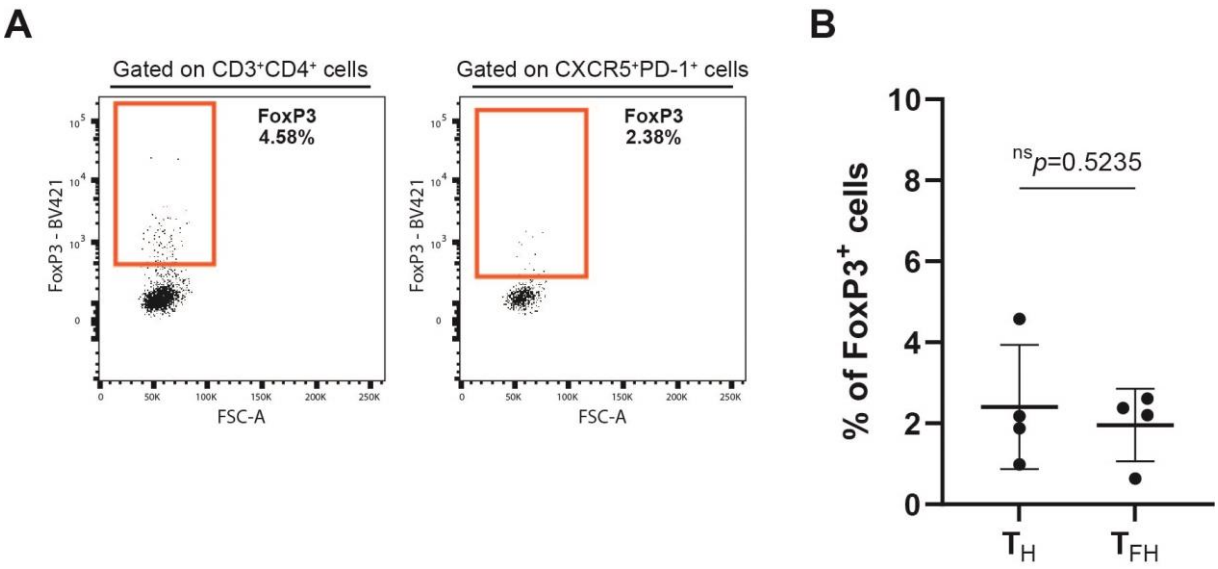

Figure 3.22 – FoxP3 expression by TH and TFH lymphocytes. A – Representative plot for FoxP3 expression by T_H and T_{FH} lymphocytes. **B** – Cumulative frequencies for FoxP3 expression by T_H and T_{FH} (n=4) lymphocytes. Data presented as mean ± SD; sample normality distribution was tested by Shapiro-Wilk normality test; P value ns (not significant) was determined by paired t-test.

3.9 B lymphocytes

3.9.1Memory and naïve B cells and plasmablasts

After being activated, B lymphocytes can differentiate form naïve cells into memory B cells or antibody-producing cells, the plasmablasts. To evaluate the frequency of these cellular populations on tonsillar lymphocytes, $CD19^+$ cells were stained for CD27 and CD38. After, naïve B cells were identified as $CD19^+CD27^-$, memory B cells as $CD19^+CD27^+$ and plasmablasts as $CD27^+CD38^+$ (Fig. 3.23-A).

A clear difference between naïve and memory B cell was visible, with naïve cells ($72.62 \pm 16.20\%$) being found in greater numbers than memory cells ($24.59 \pm 14.88\%$). CD19+ cells did not differentiate much into plasmablasts, as this cell population was found in low numbers ($1.71 \pm 1.22\%$) (Fig. 3.23-B).

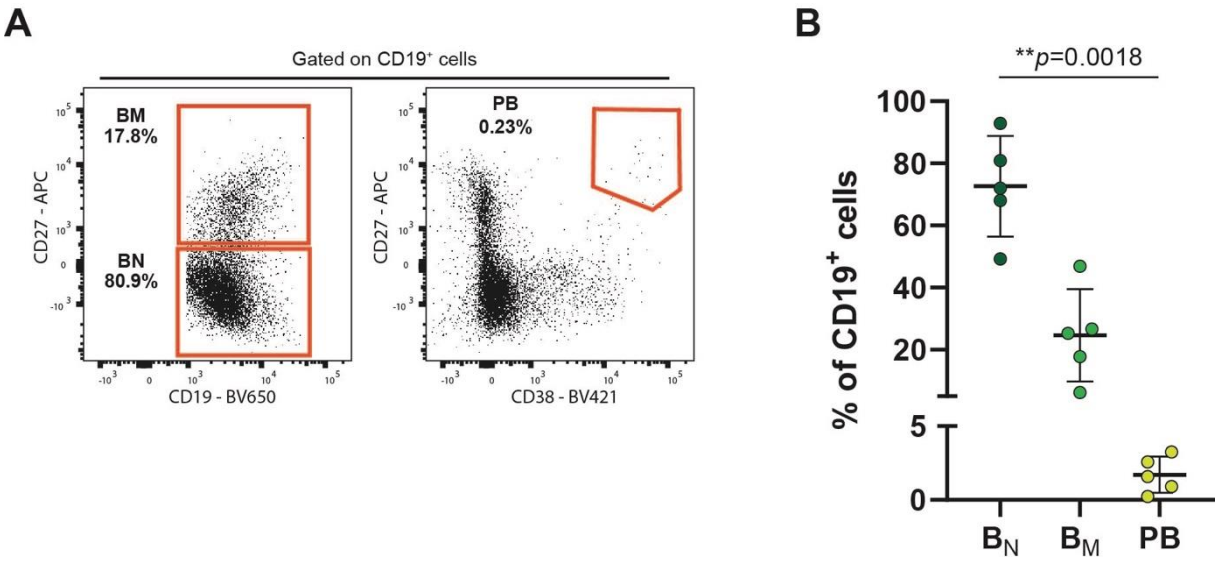

Figure 3.23 – Frequency of naïve cells (B_N), memory cells (B_M) and plasmablats (PB) among B lymphocytes. **A** – Representative plot of naïve cells (B_N), memory cells (B_M) and plasmablasts (PB), gated on $CD19^+$ cells. **B** – Cuumulative frequencies of naïve cells, memory cells and plasmablast, gated on $CD19^+$ cells (n=5). Data presented as mean ± SD; sample normality distribution was tested by Shapiro-Wilk normality test; P value **p≤0.01 was determined by Repeated measures one-way ANOVA with Sidak's multiple comparisons test.

3.9.2Ki-67 expression on B lymphocytes subpopulations

In order to assess if B lymphocyte subpopulations – naïve cells, memory cells and plasmablasts - were proliferating, cells were stained for Ki-67, as it is a cellular marker associated with cell cycle and proliferation. Among the analyzed B cell populations, plasmablasts showed higher expression of Ki-67 (Fig. 3.24-A), indicating that these cells might be proliferating more. However, this is not accompanied by an increase in fluorescence as it remained very similar on all four B cell populations (Fig. 3.24-B).

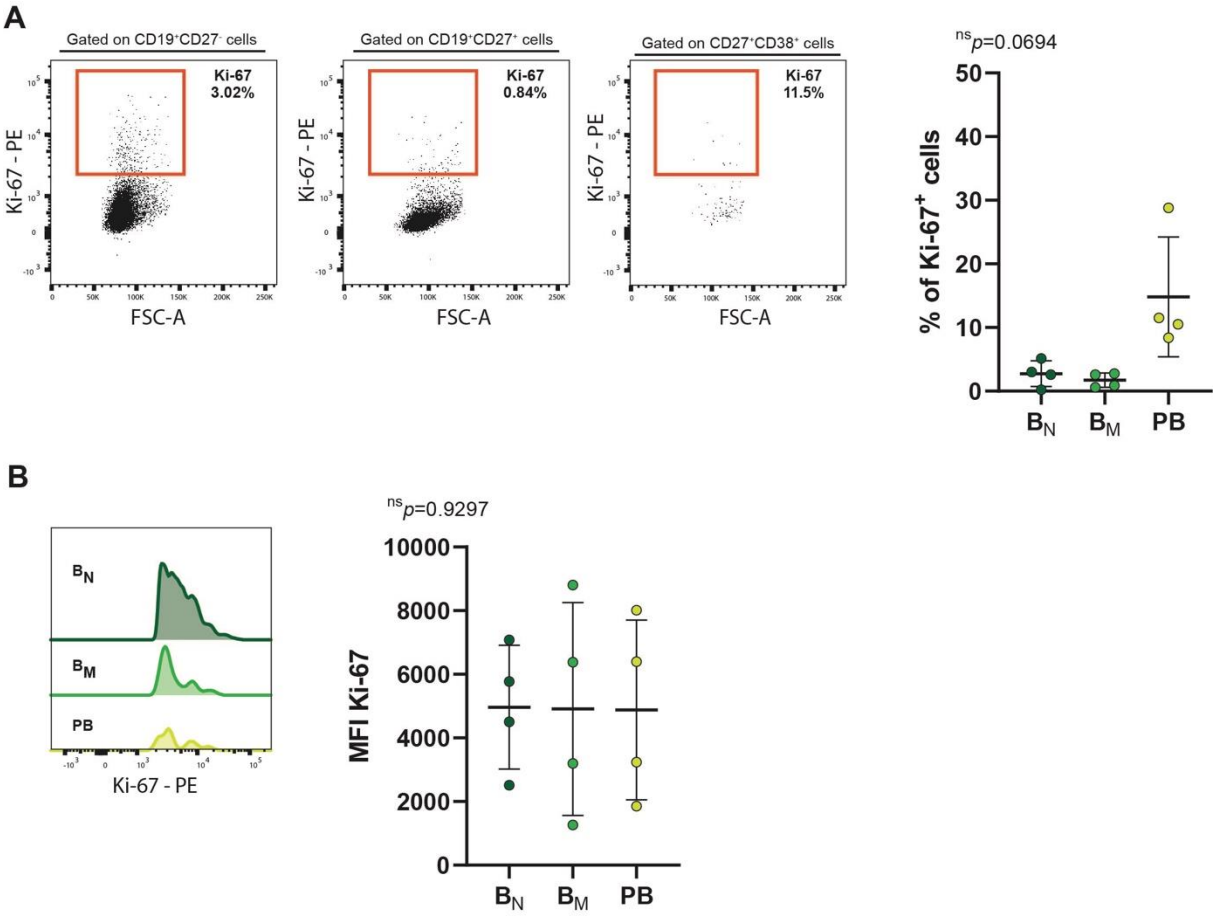

Figure 3.24 – Ki-67 expression by naïve cells, memory cells and plasmablats. A – Representative plot and cumulative frequencies of KI-67 expression by naïve cells (B_N), memory cells (B_M) and plasmablats (PB) (n=4). **B** – Representative histogram and cumulative frequencies of Ki-67 MFI in B_N, B_M and PB. Data presented as mean ± SD; sample normality distribution was tested by Shapiro-Wilk normality test; P value ns (not significant) was determined by (**A**) Friedman test with Dunn's multiple comparisons test and (**B**) Repeated measures one-way ANOVA with Tukey's multiple comparisons test.

3.10 CD40/CD40L expression on B and T lymphocytes.

CD40 and its ligand, CD40L, are crucial for the function of GCs. CD40 is constitutively expressed by B cells while CD40L is expressed on activated T cells. The interaction between CD40 and CD40L provides the costimulatory signals necessary for antibody production by B cells (Elgueta *et al.*, 2009). To investigate the CD40/CD40L signaling pathway on tonsillar lymphocytes, $CD19^+$ cells were stained for CD40 and $CD4^+$ cells were stained for CD40L. Surface and intracellular expression of CD40L was assessed on T_H and T_{FH} cells. Cells showed a disperse expression pattern, both intracellularly and on the surface (Fig. 3.25-A-B), but higher intracellular expression of CD40L was translated into higher surface expression of this marker. The expression of CD40L did not differ between T_H and T_{FH}. It was observed that B cells had high expression of CD40 (Fig. 3.24-C).

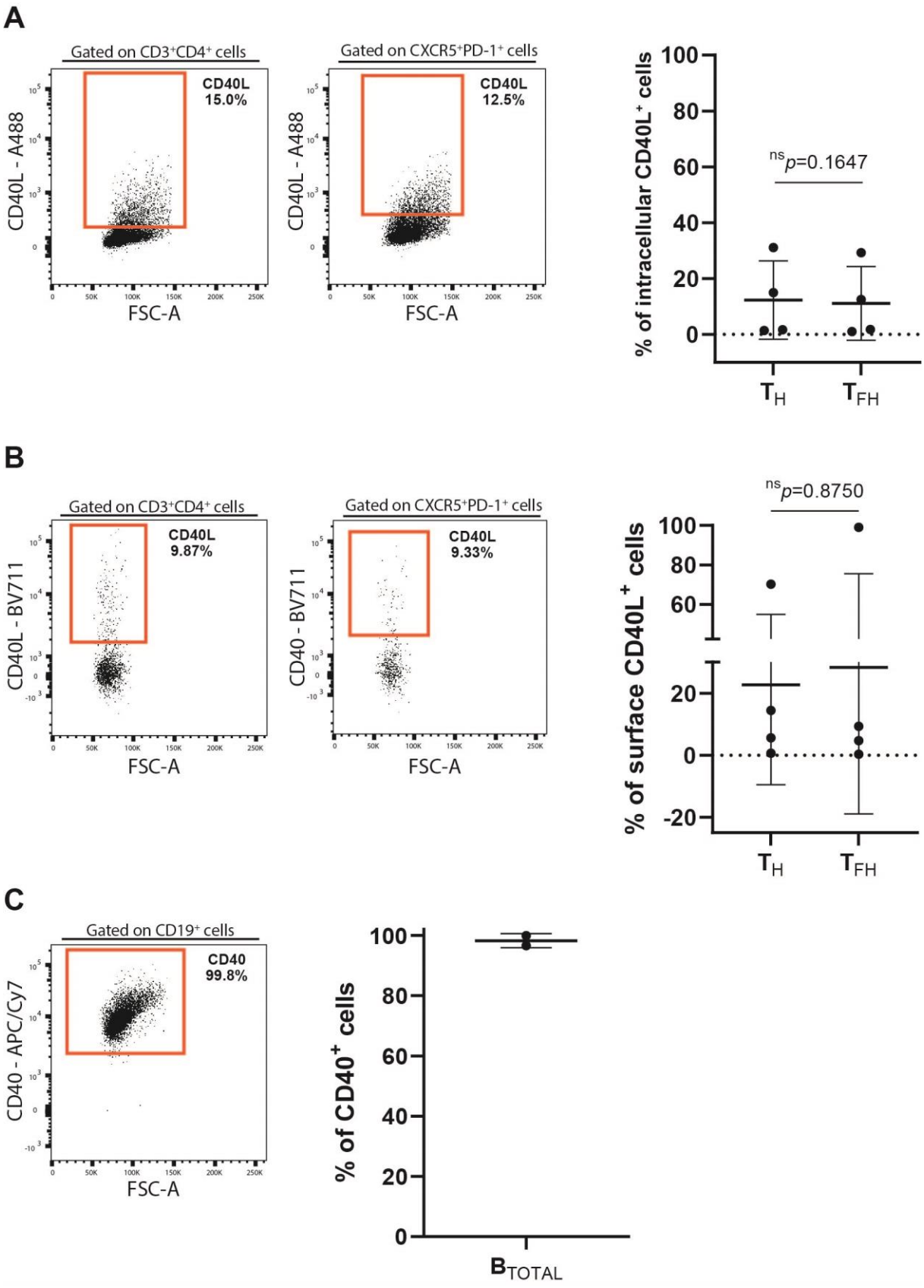
A
Gated on CD3+CD4+ cells
CD40L
15.0%
CD40L - A488
FSC-A
Gated on CXCR5+PD-1+ cells
CD40L
12.5%
CD40L - A488
FSC-A
% of intracellular CD40L+ cells
nsp=0.1647
TH
TFH
B
Gated on CD3+CD4+ cells
CD40L
9.87%
CD40L - BV711
FSC-A
Gated on CXCR5+PD-1+ cells
CD40L
9.33%
CD40 - BV711
FSC-A
% of surface CD40L+ cells
nsp=0.8750
TH
TFH
C
Gated on CD19+ cells
CD40
99.8%
CD40 - APC/Cy7
FSC-A
% of CD40+ cells
BTOTAL

Figure 3.25 – CD40 and CD40L expression on B and T lymphocytes. A – Representative plots and cumulative frequencies of CD40L intracellular expression on T_H and T_{FH} cells (*n*=4). **B** - Representative plots and cumulative frequencies of CD40L surface expression on T_H and T_{FH} cells (*n*=4). **C** - Representative plot and cumulative frequencies of CD40 expression on B cells (*n*=2). Data presented as mean ± SD; sample normality distribution was tested by Shapiro-Wilk normality test; P value ns (not significant) was determined by (**A**) Paired *t*-test and (**B**) Wilcoxon matched pairs signed rank test.

3.11 Quantitation of germinal center area

GC formation within lymphoid follicles indicates that nonimmune response is being initiated. The size and number of GCs that form in SLOs is related to the degree of immune activation. GCs were observable on tissue samples of human tonsils (Fig. 3.26-A). It was possible to identify 78 GCs among the four tonsil samples (*n*=4) analyzed by microscopy. The mean area of GCs was 0.20 ± 0.177 mm^2 (Fig.3.26-B)

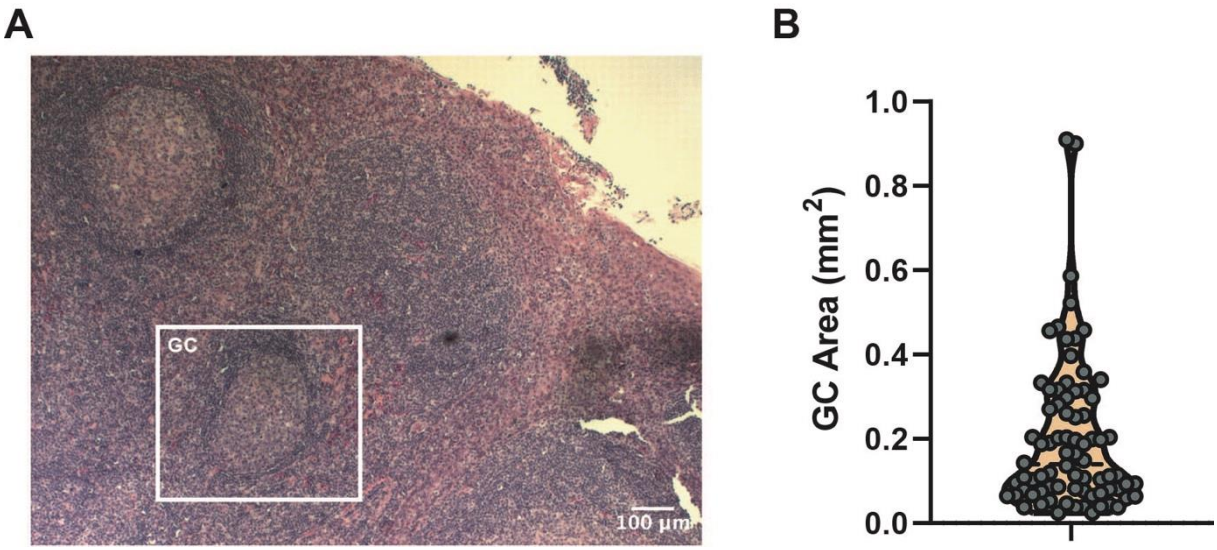

Figure 3.26 – Quantitation of GC área (in mm2). A – Representative GC, obtained from H&E stain. **B** – Cumulative graph for GC areas on human tonsils (*n*=4). Each data point represents an individual GC. Images were taken using a Zeiss Imager Z2 microscope equipped with a Zeiss Axiocam 105 color using a 5x objective in a ZEN Blue 2012 software.

3.12 Establishing organoid cultures of human tonsils

To try to establish an organoid culture of human tonsil, MNCs isolated from two donors (n=2) were cultured, independently, at high density ($60x10^6$ cell/mL per well) using a transwell system. For the first experiment MNCs were isolated without Ficoll density gradient, while for the second, this step was included. These cultures were stimulated with SEB and the evolution was monitored macroscopic and microscopically, for 10 days in the first experiment and 15 days in the second. The protocol for organoid establishment was based on the work developed by Wagar *et al* (Wagar 2021). In the first experiment, cell clusters were visible from day 3 and increased until day 10 (Fig. 3.27). For the second experiment, cluster formation was more scarce. These clusters were considered as being tonsil organoids. On figure 3.27 is shown the clsutering observed on the first organoid experiment, between day 5 and day 10.

Figure 3.27 – Cell clustering observed between day 5 and day 10 of organoid culture. Images refer to the first organoid experiment.

3.12.1 Immunophenotyping tonsil organoid immune cells

To investigate if the established organoids were able to replicate the cellular characteristics of human tonsils, the organoid cells were analyzed by flow cytometry. The frequency pf T_H, T_{FH} and B lymphocytes, as well as the differentiation of the latter population into memory cells and plasmablasts was investigated. CD69 was regarded as marker for cell activation, as expression of CD69 is induced after TCR engagement (Cibrián e Sánchez-Madrid, 2017). The expression of ICOS on TFH cells was analyzed to further understand the follicular helper phenotype. For easier understanding, results are shown grouped by experiment.

Organoid I

By looking to the position of our cells of interest on the SSC-A vs FSC-A plot, it is possible to see a shift up and to the right, indicating that the cells are bigger and more complex (Fig. 3.28). This is in line with what was observed on section 3.12, regarding cluster formation. Cell survival was maintained above 90%, up to the last day of the experiment (Fig. 3.28). Regarding

T_H cells, expression increased, in number, on day 5 and 10 but, by looking to the cell count of $CD3^+CD4^+$ cells it was clear that cells decreased during incubation (Fig. 3.29-A). T_H cells remained high expressors of CD69 during all 10 days of the experiment, indicating that these cells were activated (Fig. 3.29-B).

T_{FH} cell expression was low and decreased during culture (Fig. 3.30-A). Regardless, ICOS expression remained at high concentrations, only decreasing slightly, indicating that T_{FH} cells maintained their function. These cells also expressed CD69, in higher quantities than T_H cells (Fig. 3.30-B).

In relation to B cells, it was observed that survival was impaired, as cell numbers decreased drastically on day 5 of culture (Fig. 3.31-A). Nonetheless, it was still possible to understand that memory B cells increased relatively to naïve cells (Fig. 3.31-B). Plasmablast numbers reached a peak on day 5 of culture and drastically decreased on day 10 (Fig. 3.32 -C).

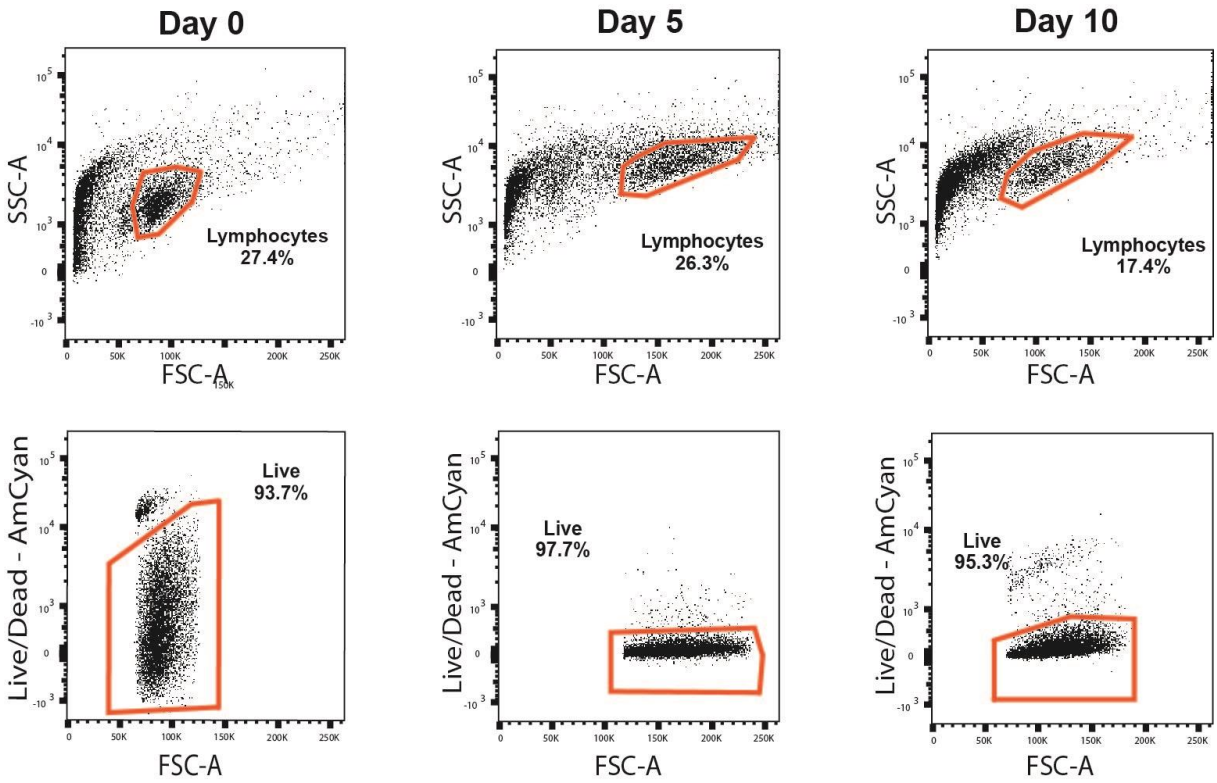

Figure 3.28 – Evolution of total lymphocyte numbers and viability on Organoid I. The cell population shifted to right on the SSC-A vs FSC-A plot indicating an increase in complexity. Cell viabilty was mantained for the duration of the experiment as cells became more complex.

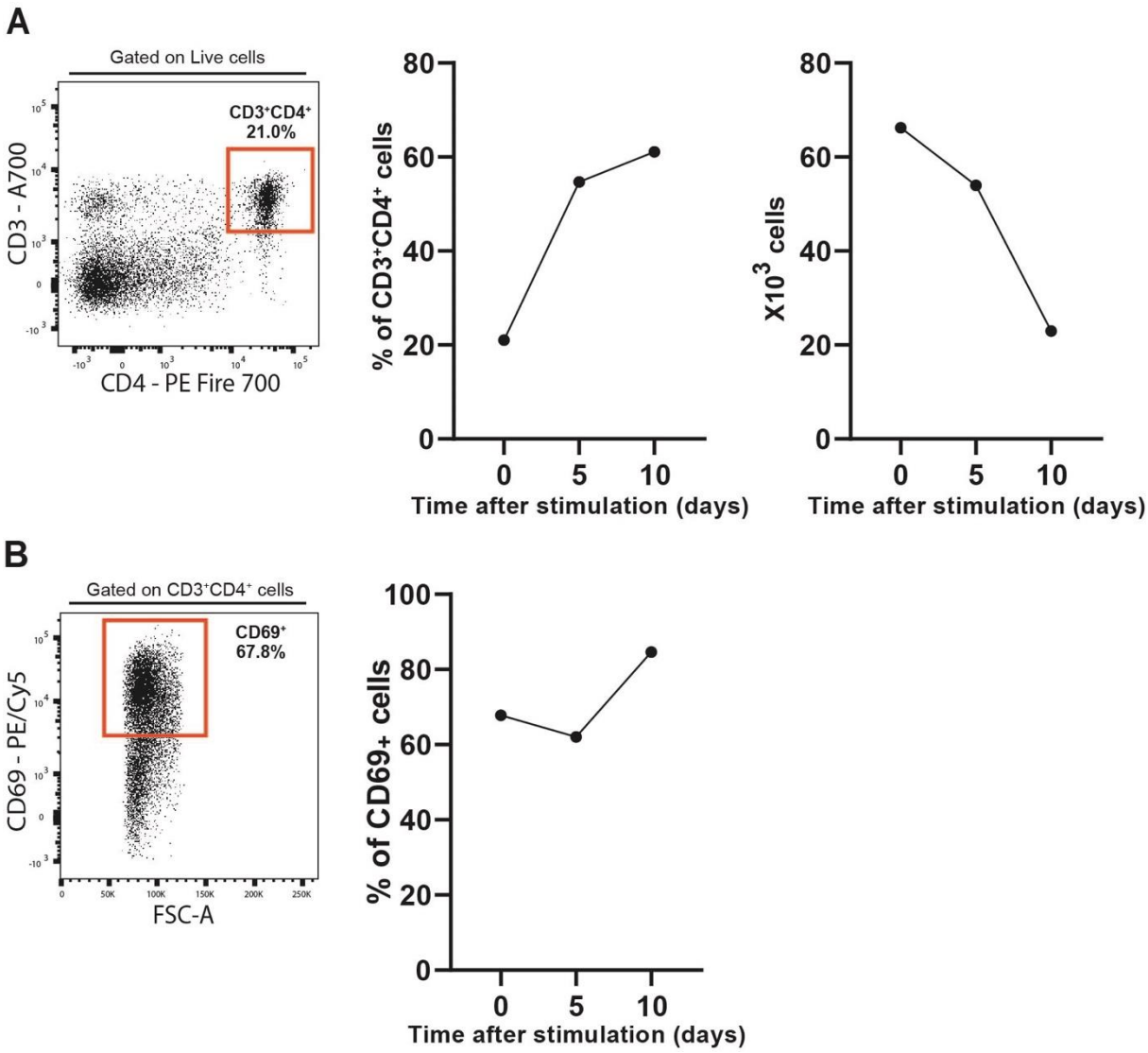

Figure 3.29 -Evolution of T_H lymphocyte frequency and activation state cell on Organoid I. A – Representative plot and evolution of T_H cell frequencies and cell numbers. **B** – representative plot and evolution of CD69 expression by T_H cells during the experiment.

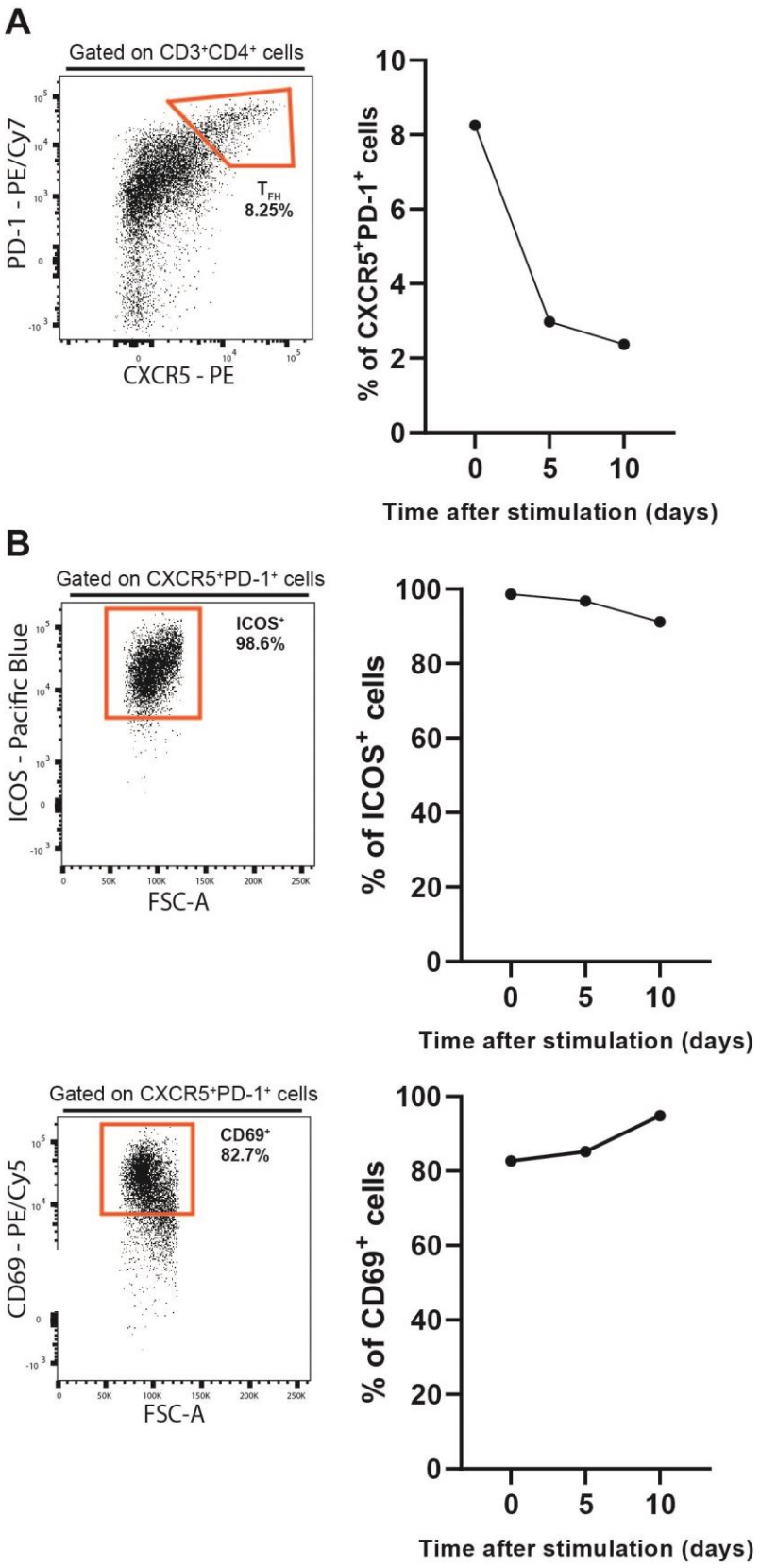

Figure 3.30 – Evolution of T_{FH} cell frequency and activation state on Organoid I. A – Representative plot and evolution of T_{FH} cell for the duration of the experiment. B - representative plot and evolution of CD69 and ICOS expression by T_H cells during the experiment.

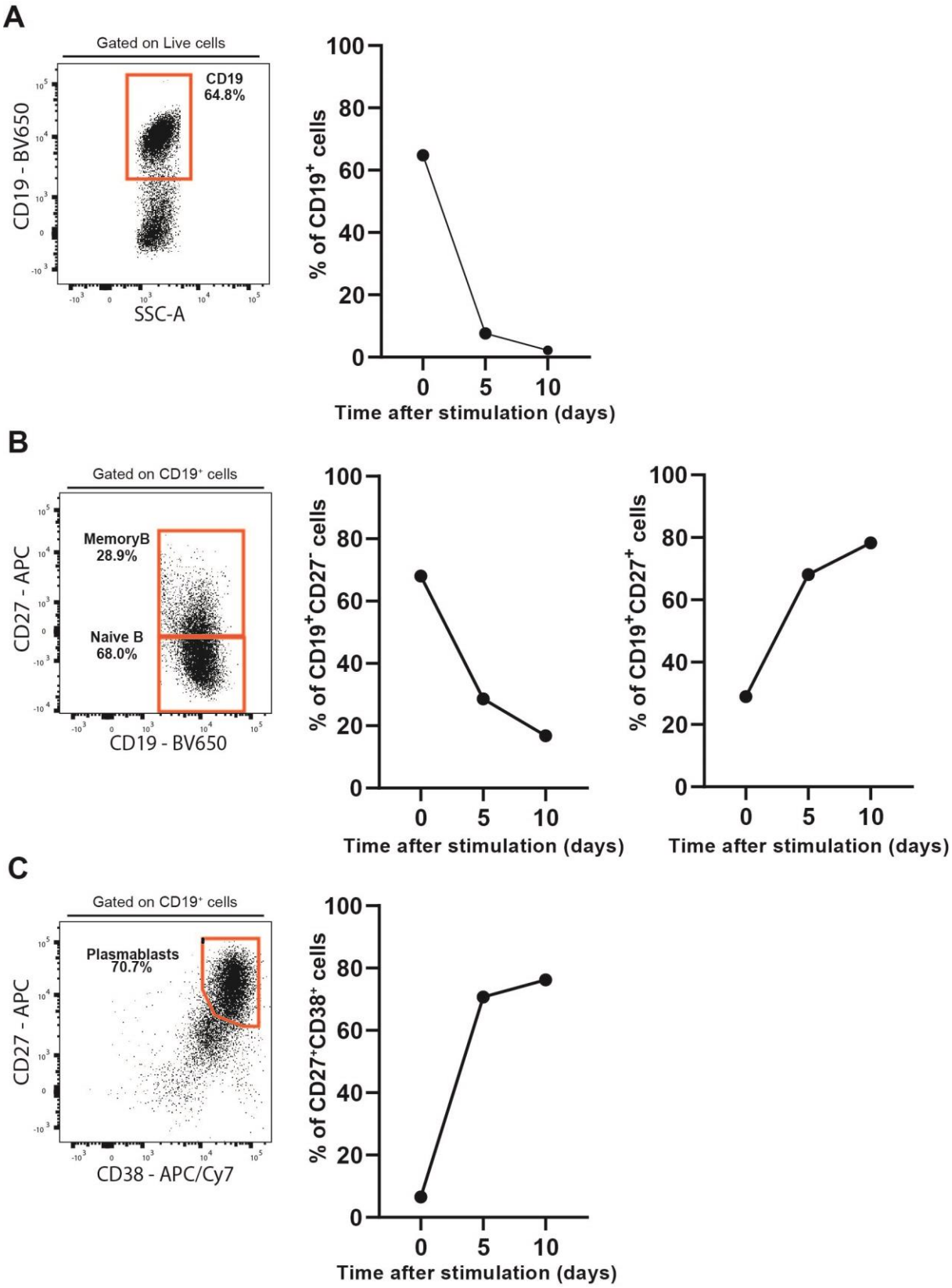

Figure 3.31 -Evolution of B lymphocyte, naïve cells (B_N), memory cells (B_M) and plasmablats (PB) on Organoid II. A – Representative plot and evolution of B cell frequency. **B** – representative plot and evolution of BN and BM frequency. **C** – Representative plot and evolution of plasmablast frequency.

Organoid II

In the 2nd organoid experiment, the shift on the SSC-A vs FSC-A was less noticeable. Cell viability on this condition good overall (88.2%), but less than the on Organoid I. On day 15 it was no longer possible to identify the total lymphocyte population on SSC-A vs FSC-A plot and, therefore, further analysis on this condition was not performed (Fig. 3.32).

Expression of T_H cells decreased on day 5 but recovered on day 10 (Fig. 3.33-A). CD69 expression on these cells decreased overtime, indicating that cells were becoming less activated (Fig. 3.33-B)

T_{FH} cells practically disappeared after day 5 (Fig. 3.34-A), and the this is accompanied by a sharp decrease of ICOS expression (Fig. 3.34-B). CD69 expression by T_{FH} cells also decreased but not so drastically (Fig. 3.34-C).

Contrary to what was observed on Organoid I, B cells viability was maintained until day 5, were a clear population was detected on the plot (Fig. 3.35-A). After this time point, it was no longer possible to detect a B cell population. Both on day 0 and day 5, the majority of B cells were naïve cells (Fig. 3.34-B) and no plasmablasts were detected (Fig. 3.35-C).

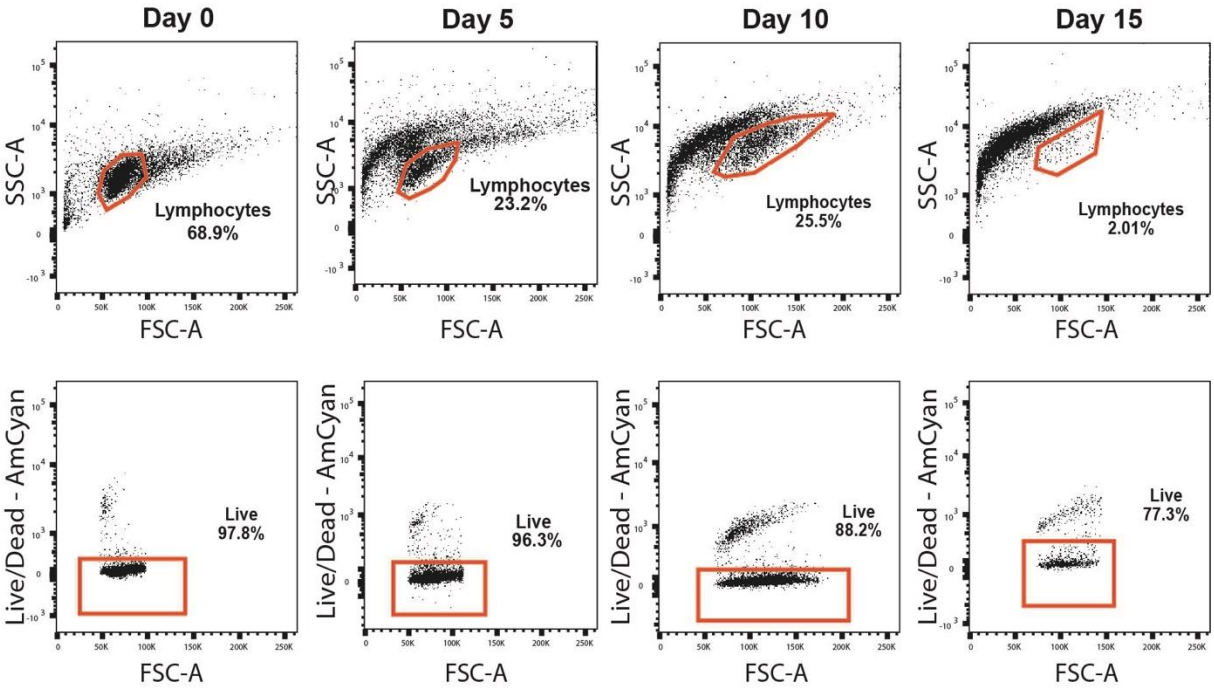

Figure 3.32 – Evolution of total lymphocyte numbers and viability on Organoid II. The cell population shifted to right on the SSC-A vs FSC-A plot indicating an increase in complexity. Cell viabilty was mantained for the duration of the experiment as cells became more complex.

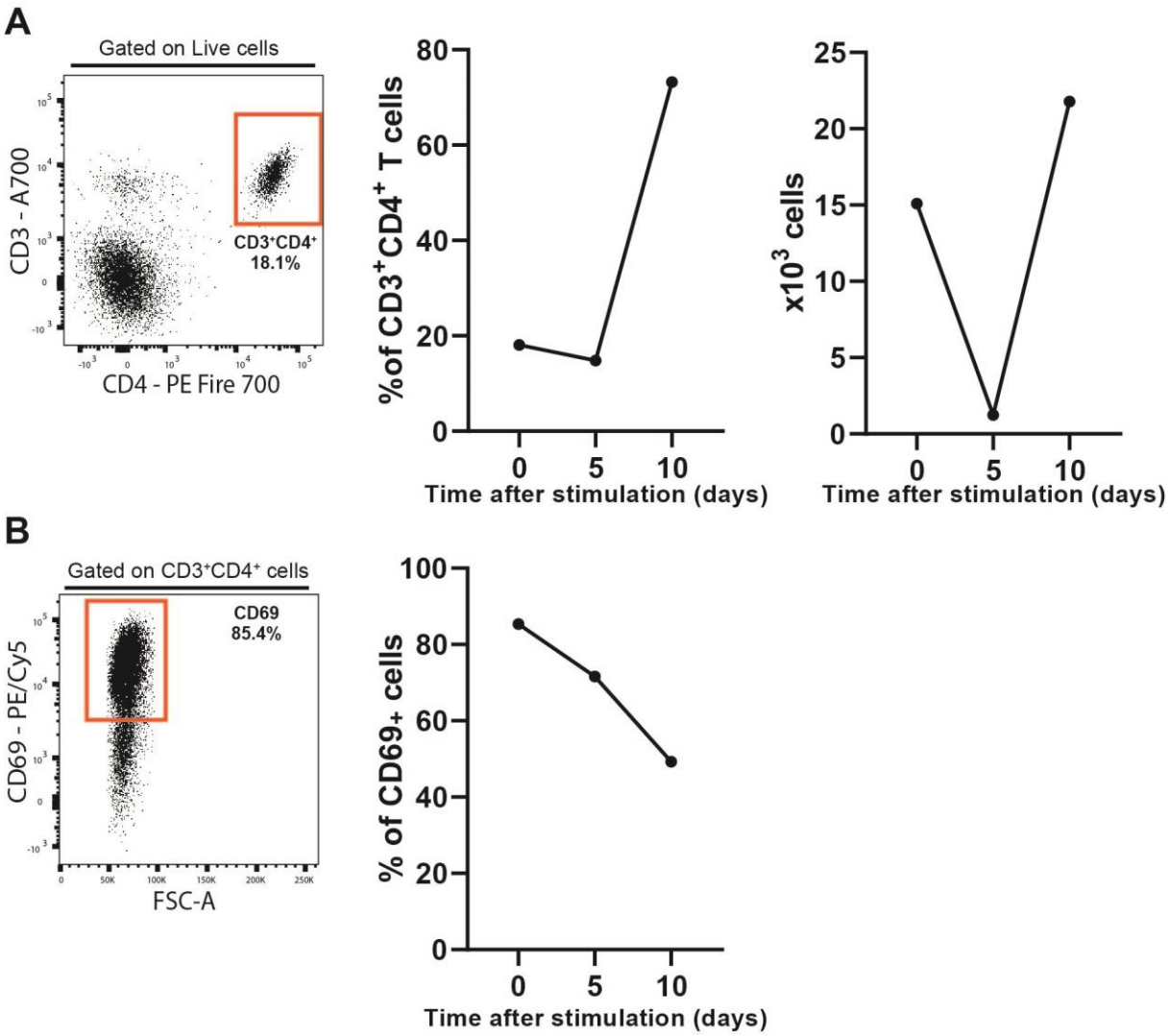

Figure 3.32 -Evolution of T_H lymphocyte frequency and activation state cell on Organoid II. A – Representative plot and evolution of T_H cell frequencies and cell numbers. **B** – representative plot and evolution of CD69 expression by T_H cells during the experiment.

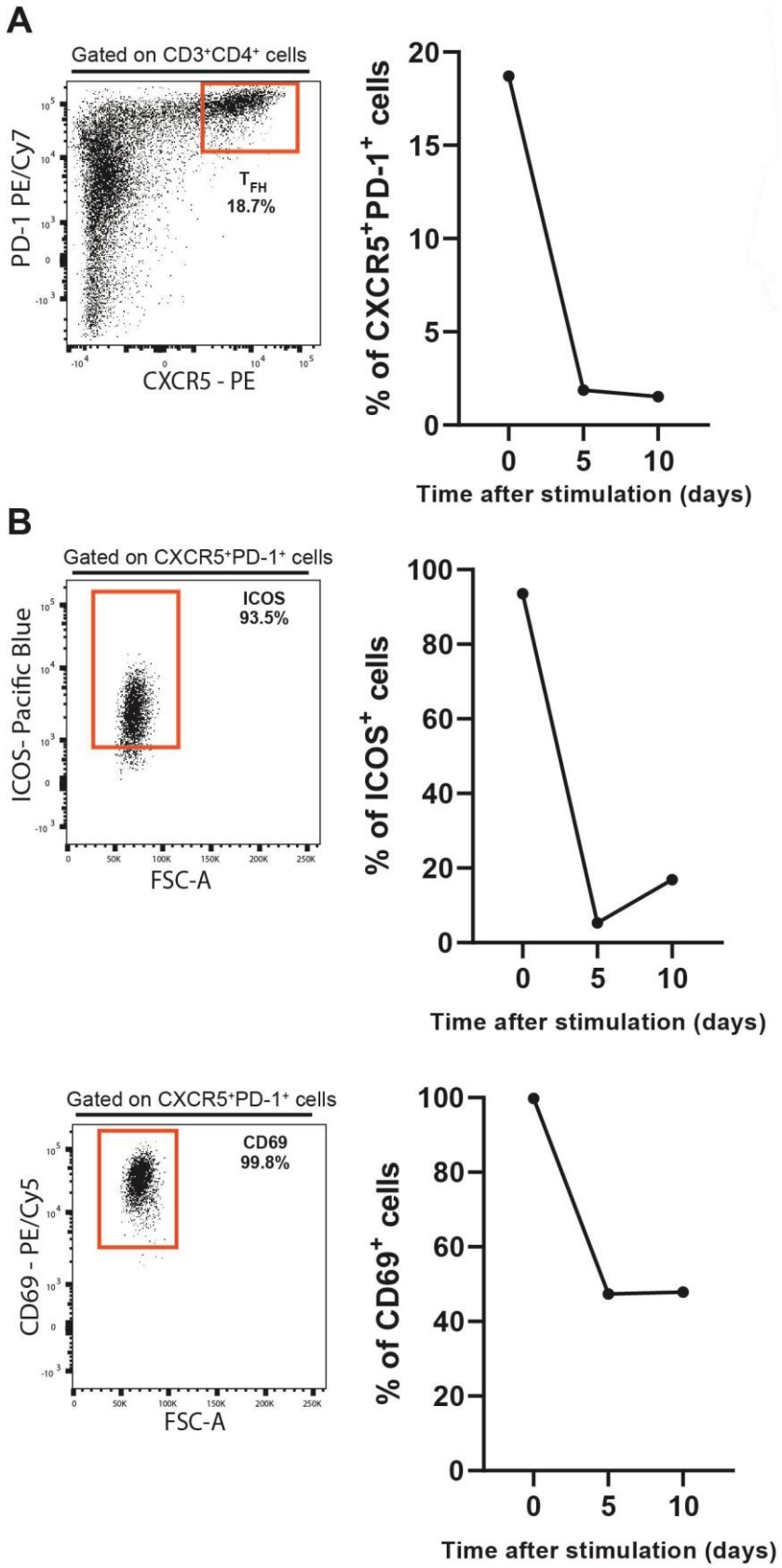

Figure 3.33 – Evolution of T_{FH} cell frequency and activation state on Organoid II. A – Representative plot and evolution of T_{FH} cell for the duration of the experiment. B - representative plot and evolution of CD69 and ICOS expression by T_{FH} cells during the experiment.

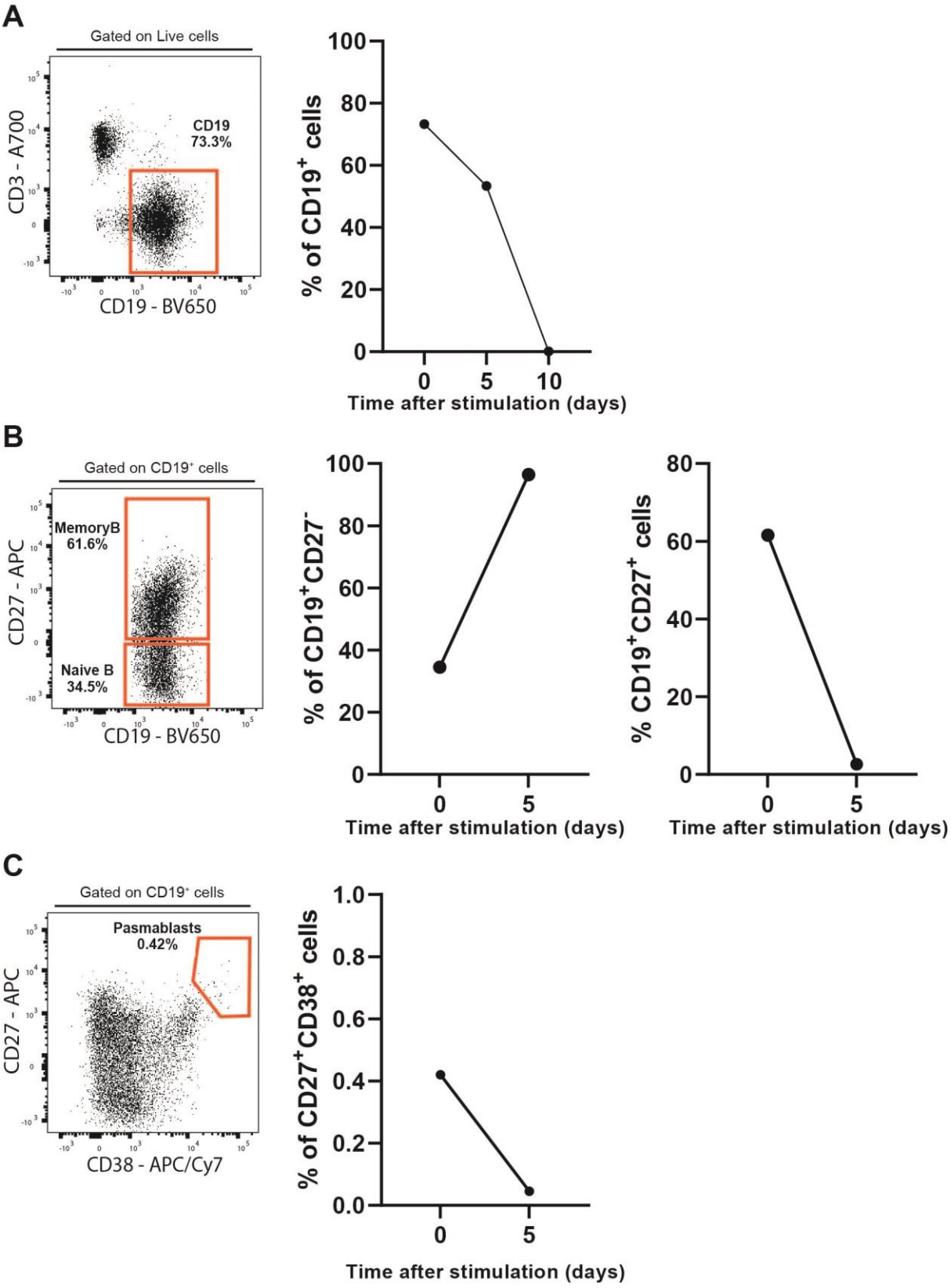

Figure 3.34 -Evolution of B lymphocyte, naïve cells (B_N), memory cells (B_M) and plasmablats (PB) on Organoid II. A – Representative plot and evolution of B cell frequency. **B** – representative plot and evolution of BN and BM frequency. **C** – Representative plot and evolution of plasmablast frequency.

4. Discussion

In the present study, the goal was to assess the immunological landscape of human tonsils, as models for SLOs, and, with the that knowledge, establish a tonsil organoid culture system, for future immunological readouts. Due to limitations in obtaining samples from healthy donors, for the present work we resorted to tonsils obtained from children undergoing tonsillectomy as treatment for OSA. After extraction, tonsils are regarded as a biological waste and are discarded. These characteristics make tonsils great working samples, since they can be used as models for human SLOs and embody no additional procedure for obtaining them.

In this study, the role tonsils play in immune responses, as a place for antigen recognition, lymphocyte activation, and generation of immune memory, is confirmed. We observed that the frequencies of T and B lymphocytes are in accordance with previously demonstrated (Alexopoulos, Papayannis e Gardikas, 1976), with B lymphocytes being the most prevalent population. Tonsils being predominantly B cell organs directly correlates with their function as sites for high-affinity antibody production. A small portion of T_C lymphocytes that retained cytotoxic characteristics, was also detected on tonsils. T_C lymphocytes are not commonly found on lymphoid follicles (Shen *et al.*, 2018), as they are usually recruited to infectious sites, where they participate in the elimination of infected cells. These cells, however, can recirculate between SLOs and the periphery (Piconese, Campello e Natalini, 2020), in search of antigens, which can explain their presence on lymphoid organs. Another possible explanation for the detection of T_C lymphocytes on SLOs is the need to eliminate infected T_{FH} cells (Leong *et al.*, 2016). Additionally, it has been reported that a portion of CD8 T cells can express $CXCR5^+$ and can migrate to B cell follicles and infiltrate GCs. These cells could be involved in maintaining GC structure and function while exerting their classical cytotoxic functions (Quigley *et al.*, 2007; Shen *et al.*, 2018). Another additional role that has been reported for T_C lymphocytes in SLOs is the possibility to control B cell self-tolerance by regulating the production of autoreactive antibodies (Chen *et al.*, 2019). Thus, despite the low frequency, T_C lymphocytes can have important roles in controlling the immune response in SLOs.

An important characteristic to identify cells that are localized to lymphoid follicles is the expression of $CXCR5^+$. One of the most important players in the GC reaction, apart from B lymphocytes, are T_{FH} cells that are identified by being CD4 T cells

expressing not only CXCR5, but also PD-1. The co-expression of these two markers characterizes the follicular helper phenotype. So, the next step in immunophenotyping tonsillar lymphocytes was the identification of these markers on T_H and T_C lymphocytes. As expected, co-expression of these markers was higher on T_H cells, as these are the ones committed to the helper phenotype. Almost no T_C lymphocytes showed co-expression of CXCR5 and PD-1. Taking into account that T_C population had minimal presence on tonsils, the real numbers of $CD8^+CXCR5^+PD\text{-}1^+$ cells are really low and these cells were disregarded for the rest of the study.

Due to their location at the entrance of the respiratory and digestive tracts, tonsil are crucial patrols against pathogens encountered through these routes. To actively respond to pathogens, these organs must develop mechanisms that enable detection of said pathogens. One way of achieving this is by expressing TLRs. TLRs drive innate immunity to initiate an immediate response and, at the same time, act as triggers for the adaptive response, by inducing the secretion of cytokines, chemokines and co-stimulatory factors (Mansson, Adner e Cardell, 2006). From the ten TLRs that have been identified in humans, TLR1, TLR2, TLR3, TLR4, TLR5 TLR7 and TLR9 have been detected on T cells, at least at the mRNA level while TLR6, TLR8 and TLR10 are usually absent or detected in very low levels (Kumar, 2021).

In this study we were able to detect TLR7 and TLR9 but no TLR4 expression on T_H and T_{FH} cells. The presence of these TLRs on tonsillar lymphocytes confers sensitivity to viral pathogens, as both TLR7 and TLR9 are associated with the detection of PAMPs from viral origins. This is in line with previous studies that have reported TLR expression on tonsil cells, in varying degrees (Claeys *et al.*, 2003; Lesmeister, Bothwell e Misfeldt, 2006; Mansson, Adner e Cardell, 2006). It was possible to identify that two donors had a high percentage of $TLR7^+$ cells. This may be due to differences regarding the genetic profile of those donors or can be indicative of a recent infectious episode, that led to the upregulation of this TLR (Dias *et al.*, 2021; Lesmeister, Bothwell e Misfeldt, 2006).

TLRs are commonly expressed on cells from the innate immune system and can respond to signals originating from different microbial origins ensuing an immune response tailored to that specific pathogen. Upon TLRs activation, several cytokines or chemokines, can be produced and can have effects on other immune cells, such as T and B lymphocytes. The expression of TLRs by cells from the adaptive immune system can be a way sensitize them to the invading pathogens in an antigen-

independent manner, initiating the innate response more rapidly. The expression and activation of specific TLRs by T cells can influence the fate of differentiation into the effector subsets of CD4 T cells, as these are controlled by specific cytokines, skewing the response towards tolerance or inflammation (Meager e Wadhwa, 2013). Although the analysis of TLR expression on B lymphocytes has not been performed in this study, it has also been reported that these cells express TLRs. Expression of TLRs is low on naïve B cells but is upregulated on activated B cells upon B cell receptor (BCR) or CD40 stimulation (Browne, 2012). TLR activation synergizes with the BCR stimulation by antigens and CD40 stimulation by T_{FH} cells, supporting the initial activation of B cells and the germinal center reaction (Browne, 2012). Different TLRs can influence the B cell active state, the differentiation into memory cells and antibody class-switching (Kumar, 2021).

TLRs play an important role in coordinating both the innate and adaptive immune responses, ensuring effective defense against pathogens and maintaining immune system homeostasis. Knowing the TLR expression profile on T and B lymphocytes is crucial to better understand how immune responses are initiated and how they can be modulated.

As mentioned previously, cytokines are crucial elements of immune responses. They can definine the type of immune response, by influencing the differentiation of effector T cells, and are also important for the formation of GCs, by recruiting T and B cells to the GC site and by modulating the cellular dynamics and longevity of GC reactions (Hsu *et al.*, 2008). T_{FH} cells are one of the most important cells for GC reactions and they exert their function mainly through the secretion of IL-21. This cytokine is important for GC formation and maintenance but also has an autocrine action on T_{FH} cells, promoting the follicular helper lineage and function in GC B cell development (Gong, Zheng e Zhou, 2019; Spolski e Leonard, 2010). T_{FH} cells have also the ability to secrete cytokines related to non-T_{FH} cells, despite Bcl6 blocking the differentiation into other CD4 T cells subsets (Crotty, 2011; Kurata, Matsumoto e Sumida, 2021). In fact, our results showed that T_{FH} cells were capable of producing IL-4, IL-10, 1L-17 and IFNγ, either constitutively or upon stimulation. By producing other effector cytokines, T_{FH} cells can modulate the antibody responses that are generated.

IL-4 is a crucial cytokine in the GC microenvironment, as it plays a critical role in promoting the differentiation and survival of B cells. It can also enhance the generation of T_{FH} cells, thereby promoting T-B cell interactions. Regarding antibody

production, IL-4 induces class-switching to IgG and IgE antibodies. (Kubo, 2021; Meli *et al.*, 2017).

IL-10 is known to have anti-inflammatory roles and its production is associated to T_{reg} cells, defined by the expression of FoxP3 transcription factor. We were also able to detect FoxP3$^+$ cells among CD4 T cells, including T_{FH} cells, supporting the presence of regulatory cells on human tonsils. The presence of cells with regulatory functions in the context of the GCs allows to control the GC reaction, avoiding the selection of low-affinity or autoreactive B cells by T_{FH} cells and promoting the formation of plasmablasts cells and memory B cells (Linterman *et al.*, 2011). Another role that has been associated to IL-10 is the initiation of DZ polarization of B cells, by upregulating CXCR4 expression (Laidlaw *et al.*, 2017). Regarding antibody production, IL-4 induces class-switching to IgE and IgM antibodies (Cañete *et al.*, 2019; Heine *et al.*, 2014).

IL-17 is a pro-inflammatory cytokine, commonly expressed by T_H17 cells. Its role is associated with the generation of protective responses against bacterial or fungal infections, but when dysregulated, IL-17 can contribute to chronic inflammation related to immune-mediated disorders(Jin e Dong, 2013; Kuwabara *et al.*, 2017). The role of IL-17 in GCs and antibody production has been a subject of ongoing research and it is not totally elucidated. Studies have shown that IL-17 can promote GC formation and maintenance, enhancing the differentiation of antibody-secreting plasma cells (Ferretti *et al.*, 2016; Kim *et al.*, 2022; Mitsdoerffer *et al.*, 2010). Regarding antibody production, IL-17 is reported to induce IgG class-switch (Lee *et al.*, 2017; Patakas *et al.*, 2012).

IFNγ is classically produced by T_H1 cells and have been implicated in the generation of the first wave of antibody response. This already indicates that this cytokine can be involved in the GC reaction. Furthermore, IFNγ is potent regulator of DC function, enhancing their antigen-presenting capacity (Nurieva e Chung, 2010). During GC reaction, DCs are involved in the positive selection of high-affinity B cells. Therefore, by promoting optimal antigen presenting capacity to DCs, IFNγ can influence the quality of B cell responses and antibody production within GCs. The presence of T_{FH} cells with a T_H1 characteristics was supported by the capacity that these cells had in expressing IFNγ as well as the detection of CXCR3$^+$ cells among T_{FH} lymphocytes (Groom e Luster, 2011).

TNFα is a cytokine associated with pro-inflammatory responses. This cytokine is not associate to none of the effector CD4 T cell subsets but, even so, it can greatly influence the immune response. The TNF family of receptors and ligands can control de survival of T cells through a series of stimulatory signals that promote T cell action

when a pro-inflammatory response is needed, or through inhibitory signals the induce cell death (Croft, 2014). In the samples analyzed in this work TNFα expression was not detected which indicates that no inflammatory response was being induced when the samples were obtained.

Regardless of their role, these cytokines play crucial roles in antibody production and maintenance of immune homeostasis. Dysregulation of this delicate and complex balance pro-inflammatory and regulatory signals can lead to inadequate immune responses posing potential harm for the host. Most importantly, our results show that tonsillar T lymphocytes can effectively respond to infection, having the capacity to produce a wide range of cytokines, related to different types of immune responses.

Apart from cytokines, another crucial factor that influences antibody production is the spatial organization of the microenvironment. In fact, when an immune response is initiated, a specialized microstructure forms within B cell follicles – the GC. The number and size of the GCs directly correlates with the degree of the immune response. In this study, we were indeed able confirm that tonsils were developing GCs, which is in accordance with the fact that these SLOs are sites for B cell differentiation and antibody production. The shape and area of the observed GCs were in line to what was observed by Dan *et al* (Dan *et al.*, 2019) with the majority of GCs having an area below 1 mm^2.

Now that T lymphocytes have been characterized, we move on to the B lymphocytes.

During GC reaction, B lymphocytes can differentiate into plasmablasts, antibody-producing cells that can be either short- or long-lived, or into memory B cells, thar will ensure protection in case of future exposures. We observed that B lymphocytes differentiated into memory cells, but most B cells remained as naïve cells. Keeping in mind that the samples were obtain from donors that were not experiencing active infection, this observation is expected. Additionally, once memory B cells are formed, they usually leave the follicle to the circulate the periphery, where they can detect re-exposures (Palm e Henry, 2019). Plasmablast numbers are also in accordance with the fact that no immune response was being initiated. Nevertheless, when examining Ki-67 expression within these three B cell populations, plasmablasts exhibited the most substantial expression, suggesting a higher degree of proliferation compared to the other populations. Proliferation and clonal expansion of B cells, and T cells, is critical for producing high-affinity antibodies and immunological memory and is indicative of a well-established and efficient GC reaction.

It has been established that T:B cell interactions are crucial for an efficient GC reaction and for B cell activation and maturation, resulting in the production of high-affinity antibodies. A stable and successful interaction between T and B cells happens through TCR engagement with antigens presented by B cells, supported by other co-stimulatory signals that increase the adhesiveness of the interaction (Biram, Davidzohn e Shulman, 2019). One of the most crucial co-stimulatory signals that supports the immune synapse between T and B cells is the interaction of CD40, expressed on B cells, with its ligand, CD40L, that is expressed on activated T cells. In combination with IL-4 and IL-21, CD40 signaling pathway provides essential survival signals, promoting B cell activation and proliferation, supporting the GC reaction (Elgueta *et al.*, 2009; Karnell *et al.*, 2019).

Our results show that B cells expressed CD40, and that T cells expressed its ligand, CD40L, confirming the involvement of this signaling pathway in immune interactions of human tonsils.

The initial phase of this study confirms the extraordinary sophistication of the immune system. Immune reactions and antibody production are highly complex and dynamic processes that are intricately regulated by precise timing and spatial organization within the microenvironment, encompassing a diverse array of chemical signals and immune cells. The network of cells, tissues and signaling pathways that constitute the immune system makes it challenging to understand the precise mechanisms underlying immune responses *in vitro*, as the current culture techniques do not fully translate this complexity.

Most of the data that is available to us comes from studies in animal models or 2D cell cultures. These traditional approaches allowed to gather a great amount of knowledge regarding immunity and vaccination, but they do not accurately mimic the complexity and the real dynamics of the human immune system. Most of the data ends up not being translatable to humans, which limits advancements and wastes resources.

In recent years, there has been an increasing need to develop more reliable models,

to study and understand human immunity and to test vaccine response, efficacy and safety in a way that is more transposable to what happens *in vivo.* The trends have been shifting to 3D cell cultures and the more complex OoC technology, that constitute a more realistic representation of the microenvironment of human lymphoid organs.

In this way, our group tried to establish a tonsil organoid, as a starting point to develop a tonsil-on-a-chip, that will model the lymphoid organs and the human immune response. The tonsil organoid protocol was based on the work of Wagar *et al* (Wagar *et al.*, 2021). They were able to develop and maintain organoids in culture, allowing them to characterize the human influenza response. Our goal was to also establish tonsil organoids so that we could have this system available, for future immunological studies.

By comparing the two experiments it was visible that on Organoid I, clusters formation was higher and denser than on Organoid II, with clusters being visible already on day 3 and maintained until day 10. This was in line with what Wagar *et al* observed in their work. On Organoid II, clusters were only visible on day 10. This disparity between the two experiments could indicate that using Ficoll density grandient during MNC isolation is detrimental to organoid formation by delaying cell clustering. As the name implies, Ficoll density gradient isolation separates cells according to their density. By introducing this step, we could be removing some type of cell that is involved in the clustering process, essential to organoid formation. Nonetheless, supported by the results of Organoid I, it was possible to conclude that using a cell concentration of $60X10^6$ cells/mL when plating the cells, allowed the formation of organoids.

Immunoprofiling of the organoid cells was also performed. Again, Organoid I performed better than Organoid II. When establishing organoids, it is expected that cells increase in size and complexity, as they are activated and, in this case, responding to SEB. This was observable on organoid I on both day 5 and 10 of culture, by looking to the cell positioning on the SSC-A vs FSC-A plot, that shifted up and to the right. On organoid II, the shift was only visible on day 10, supporting the fact that cell cluster formation is delayed. Viability was maintained above 90% on Organoid I for the duration of the experiment. On Organoid II, cell viability decreased after day 5 of culture, to the point where, on day 15, it was no longer possible to identify the starting population of total lymphocytes. Again, this difference in cell behavior could be due to the fact that the Ficoll gradient step was introduced, which could be interfering with cell viability.

Overall, organoid cultures were able to maintain T_H and T_{FH} cells, but only to a certain degree, and on day 5 it was already observable a decrease on T_{FH} cell numbers. Since T_{FH} cells are a crucial part of the immune reaction that develops on lymphoid follicles, it is essential that these cells remain available and active on our

cultures, so that they can play their role in providing help to B cells. The decrease of T_{FH} cell numbers that was observed on both organoid experiments, is indicative that the immune reaction could be impaired.

To determine if T_H cells were activated, the expression of CD69 by T_H and T_{FH} cells was assessed. CD69 is a membrane-bound type-II C-lectin receptor that is considered as an early activation marker of lymphocytes, as it is rapidly expressed on the surface of T cells upon TCR engagement (Cibrián e Sánchez-Madrid, 2017). On Organoid I, expression of CD69 remained high for both T_H and T_{FH} cells, indicating that these cells were, in fact, activated. ICOS expression by T_{FH} cells was also high, leading to believe that T_{FH} cell maintained their follicular helper function, despite being reduced in numbers. For Organoid II, CD69 expression, as well as ICOS, were reduced which in accordance with the poorer outcome that was observed on this experiment.

On both experiments, B cell population decreased, this being more drastic on Organoid II. Nonetheless, it was possible to observe memory and plasmablast differentiation, specifically on Organoid I.

The main goal driving us to develop of a tonsil organoid culture system is for it to be available to perform immunological redouts, such as antibody production. This necessarily depends on having highly functional B cells, which was not accomplished with the current culture conditions. We identify this as a major limitation of the current system, that needs to be addressed in future attempts.

5. Conclusions and future perspectives

In this work, the role of human tonsils as SLOs was confirmed by the visualization of B cell follicles and GCs and by the identification of the T and B lymphocytes. Among T lymphocytes, the presence of T_H, T_{FH} and T_C cells was detected and expression of and cytokines related to T_H1, T_H2, T_H17 and T_{regs} cells was identified on T_H and T_{FH} cells. These cells expressed these cytokines either naturally or after stimulation, indicating that T_H and T_{FH} have the capacity to be involved in the mediation of the immune reaction. TLR7 and TLR9 expression was detected but on a low percentage of cells. T_C lymphocytes were detected in lower numbers and their cytotoxic capabilities were maintained, as they expressed GrB, GrK and perforin. Follicular helper functions were not observed on T_C lymphocytes, as these cells did not co-express CXCR5 and PD-1 markers. B cell showed to have the capacity to differentiate into memory B cells and plasmablasts.

Some of these findings were observed on the organoid cultures that were established. T lymphocytes were maintained for the duration of the experiments, but T_{FH} cell numbers decreased. B lymphocytes were more sensible, and it was harder to maintain this population viable. Nonetheless, differentiation into memory B cells and plasmablasts was achieved. The studies that were performed indicate that human tonsils are good models of human SLOs and can be used for the establishment of more complex culture systems However, culture conditions must be optimized to allow for better cells survival, focusing mainly on B cell viability. Regarding the methodologies of the organoid experiments, skipping the Ficoll density gradient could improve the outcome of the experiment. MNCs for Organoid I were isolated without resorting to this method and the overall outcome was a lot better than for Organoid II, where density gradient was applied.

This study had some limitations, the main one being the small size of the cohort. Most of the results could not reach statistical significance, even when a clear trend was visible. Increasing the number of donors will allow to draw more robust conclusions.

6. References

AKHTAR, AYSHA - The Flaws and Human Harms of Animal Experimentation. **Cambridge Quarterly of Healthcare Ethics**. . ISSN 0963-1801. 24:4 (2015) 407–419. doi: 10.1017/S0963180115000079.

ALEXOPOULOS, C.; PAPAYANNIS, A. G.; GARDIKAS, C. - Increased Proportion of B Lymphocytes in Human Tonsils and Appendices. **Acta Haematologica**. . ISSN 0001-5792. 55:2 (1976) 95–98. doi: 10.1159/000208000.

ALLEN, Christopher D. C. *et al.* - Germinal center dark and light zone organization is mediated by CXCR4 and CXCR5. **Nature Immunology**. . ISSN 1529-2908. 5:9 (2004) 943–952. doi: 10.1038/ni1100.

ALLEN, Christopher D. C.; OKADA, Takaharu; CYSTER, Jason G. - Germinal-Center Organization and Cellular Dynamics. **Immunity**. . ISSN 10747613. 27:2 (2007) 190–202. doi: 10.1016/j.immuni.2007.07.009.

AMARANTE-MENDES, Gustavo P. *et al.* - Pattern Recognition Receptors and the Host Cell Death Molecular Machinery. **Frontiers in Immunology**. . ISSN 1664-3224. 9:2018). doi: 10.3389/fimmu.2018.02379.

BALACHANDRAN, Yadu *et al.* - Regulation of TLR10 Expression and Its Role in Chemotaxis of Human Neutrophils. **Journal of Innate Immunity**. . ISSN 1662-811X. 14:6 (2022) 629–642. doi: 10.1159/000524461.

BERGER, A. - Science commentary: Th1 and Th2 responses: what are they? **BMJ**. . ISSN 09598138. 321:7258 (2000) 424–424. doi: 10.1136/bmj.321.7258.424.

BIRAM, Adi; DAVIDZOHN, Natalia; SHULMAN, Ziv - T cell interactions with B cells during germinal center formation, a three-step model. **Immunological Reviews**. . ISSN 0105-2896 (15 mar. 2019). 37–48.

BROWNE, Edward P. - Regulation of B-cell responses by Toll-like receptors. **Immunology**. . ISSN 00192805. 136:4 (2012) 370–379. doi: 10.1111/j.1365-2567.2012.03587.x.

CAÑETE, Pablo F. *et al.* - Regulatory roles of IL-10–producing human follicular T cells. **Journal of Experimental Medicine**. . ISSN 0022-1007. 216:8 (2019) 1843–1856. doi: 10.1084/jem.20190493.

CHEN, Yuhong *et al.* - CXCR5+PD-1+ follicular helper CD8 T cells control B cell tolerance. **Nature Communications**. . ISSN 2041-1723. 10:1 (2019) 4415. doi: 10.1038/s41467-019-12446-5.

CIBRIÁN, Danay; SÁNCHEZ-MADRID, Francisco - CD69: from activation marker to metabolic gatekeeper. **European Journal of Immunology**. . ISSN 00142980. 47:6 (2017) 946–953. doi: 10.1002/eji.201646837.

CLAEYS, S. *et al.* - Human beta-defensins and toll-like receptors in the upper airway. **Allergy**. . ISSN 0105-4538. 58:8 (2003) 748–753. doi: 10.1034/j.1398-9995.2003.00180.x.

COICO, Richard; SUNSHINE, Geoffrey - **Immunology: A Short Course**. 7th edition ed. [S.l.] : John Wiley and Sons, 2015

CROFT, Michael - The TNF family in T cell differentiation and function – Unanswered questions and future directions. **Seminars in Immunology**. . ISSN 10445323. 26:3 (2014) 183–190. doi: 10.1016/j.smim.2014.02.005.

CROTTY, Shane - Follicular Helper CD4 T Cells (TFH). **Annual Review of Immunology**. . ISSN 0732-0582. 29:1 (2011) 621–663. doi: 10.1146/annurev-immunol-031210-101400.

CROTTY, Shane - T Follicular Helper Cell Biology: A Decade of Discovery and Diseases. **Immunity**. . ISSN 10747613. 50:5 (2019) 1132–1148. doi: 10.1016/j.immuni.2019.04.011.

DAN, Jennifer M. *et al.* - Recurrent group A Streptococcus tonsillitis is an immunosusceptibility disease involving antibody deficiency and aberrant T FH cells. **Sci. Transl. Med**. 11:2019) 3776.

DAN, Jennifer M. *et al.* - Recurrent group A *Streptococcus* tonsillitis is an immunosusceptibility disease involving antibody deficiency and aberrant T $_{FH}$ cells. **Science Translational Medicine**. . ISSN 1946-6234. 11:478 (2019). doi: 10.1126/scitranslmed.aau3776.

DIAS, Maria L. *et al.* - Targeting the Toll-like receptor pathway as a therapeutic strategy for neonatal infection. **American Journal of Physiology-Regulatory, Integrative and Comparative Physiology**. . ISSN 0363-6119. 321:6 (2021) R879–R902. doi: 10.1152/ajpregu.00307.2020.

ELGUETA, Raul *et al.* - Molecular mechanism and function of CD40/CD40L engagement in the immune system. **Immunological Reviews**. . ISSN 01052896. 229:1 (2009) 152–172. doi: 10.1111/j.1600-065X.2009.00782.x.

FERRETTI, Elisa *et al.* - IL-17 superfamily cytokines modulate normal germinal center B cell migration. **Journal of Leukocyte Biology**. . ISSN 0741-5400. 100:5 (2016) 913–918. doi: 10.1189/jlb.1VMR0216-096RR.

FORE, Faith *et al.* - TLR10 and Its Unique Anti-Inflammatory Properties and Potential Use as a Target in Therapeutics. **Immune Network**. . ISSN 1598-2629. 20:3 (2020). doi: 10.4110/in.2020.20.e21.

GATTO, Dominique; BRINK, Robert - The germinal center reaction. **Journal of Allergy and Clinical Immunology**. . ISSN 00916749. 126:5 (2010) 898–907. doi: 10.1016/j.jaci.2010.09.007.

GAUDINO, Stephen J.; KUMAR, Pawan - Cross-Talk Between Antigen Presenting Cells and T Cells Impacts Intestinal Homeostasis, Bacterial Infections, and Tumorigenesis. **Frontiers in Immunology**. . ISSN 1664-3224. 10:2019). doi: 10.3389/fimmu.2019.00360.

GONG, Fang; ZHENG, Ting; ZHOU, Pengcheng - T Follicular Helper Cell Subsets and the Associated Cytokine IL-21 in the Pathogenesis and Therapy of Asthma. **Frontiers in Immunology**. . ISSN 1664-3224. 10:2019). doi: 10.3389/fimmu.2019.02918.

GOYAL, Girija *et al.* - Ectopic Lymphoid Follicle Formation and Human Seasonal Influenza Vaccination Responses Recapitulated in an Organ-on-a-Chip. **Advanced Science**. . ISSN 2198-3844. 9:14 (2022) 2103241. doi: 10.1002/advs.202103241.

GROOM, Joanna R.; LUSTER, Andrew D. - CXCR3 in T cell function. **Experimental Cell Research**. . ISSN 00144827. 317:5 (2011) 620–631. doi: 10.1016/j.yexcr.2010.12.017.

HAYNES, Nicole M. *et al.* - Role of CXCR5 and CCR7 in Follicular Th Cell Positioning and Appearance of a Programmed Cell Death Gene-1High Germinal Center-Associated Subpopulation. **The Journal of Immunology**. . ISSN 0022-1767. 179:8 (2007) 5099–5108. doi: 10.4049/jimmunol.179.8.5099.

HEINE, Guido *et al.* - Autocrine IL-10 promotes human B-cell differentiation into IgM- or IgG-secreting plasmablasts. **European Journal of Immunology**. . ISSN 00142980. 44:6 (2014) 1615–1621. doi: 10.1002/eji.201343822.

HOWIE, A. J. - Scanning and transmission electron microscopy on the epithelium of human palatine tonsils. **The Journal of Pathology**. . ISSN 0022-3417. 130:2 (1980) 91–98. doi: 10.1002/path.1711300205.

HSU, Hui-Chen *et al.* - Interleukin 17–producing T helper cells and interleukin 17 orchestrate autoreactive germinal center development in autoimmune BXD2 mice. **Nature Immunology**. . ISSN 1529-2908. 9:2 (2008) 166–175. doi: 10.1038/ni1552.

HUH, Dongeun; HAMILTON, Geraldine A.; INGBER, Donald E. - From 3D cell culture to organs-on-chips. **Trends in Cell Biology**. . ISSN 09628924. 21:12 (2011) 745–754. doi: 10.1016/j.tcb.2011.09.005.

HUSEBYE, Harald *et al.* - Endocytic pathways regulate Toll-like receptor 4 signaling and link innate and adaptive immunity. **The EMBO Journal**. . ISSN 0261-4189. 25:4 (2006) 683–692. doi: 10.1038/sj.emboj.7600991.

IMLER, Jean-Luc; HOFFMANN, Jules A. - Toll receptors in innate immunity. **Trends in Cell Biology**. . ISSN 09628924. 11:7 (2001) 304–311. doi: 10.1016/S0962-8924(01)02004-9.

INGBER, Donald E. - Human organs-on-chips for disease modelling, drug development and personalized medicine. **Nature Reviews Genetics**. . ISSN 1471-0056. 23:8 (2022) 467–491. doi: 10.1038/s41576-022-00466-9.

IOANNIDOU, Kalliopi *et al.* - In Situ Characterization of Follicular Helper CD4 T Cells Using Multiplexed Imaging. **Frontiers in Immunology**. . ISSN 1664-3224. 11:2021). doi: 10.3389/fimmu.2020.607626.

JIN, Wei; DONG, Chen - IL-17 cytokines in immunity and inflammation. **Emerging Microbes & Infections**. . ISSN 2222-1751. 2:1 (2013) 1–5. doi: 10.1038/emi.2013.58.

KABELITZ, Dieter - Gamma Delta T Cells (γδ T Cells) in Health and Disease: In Memory of Professor Wendy Havran. **Cells**. . ISSN 2073-4409. 9:12 (2020) 2564. doi: 10.3390/cells9122564.

KAPAŁCZYŃSKA, Marta *et al.* - 2D and 3D cell cultures – a comparison of different types of cancer cell cultures. **Archives of Medical Science**. . ISSN 1734-1922. 2016). doi: 10.5114/aoms.2016.63743.

KARNELL, Jodi L. *et al.* - Targeting the CD40-CD40L pathway in autoimmune diseases: Humoral immunity and beyond. **Advanced Drug Delivery Reviews**. . ISSN 0169409X. 141:2019) 92–103. doi: 10.1016/j.addr.2018.12.005.

KENNEDY, Melissa A. - A Brief Review of the Basics of Immunology: The Innate and Adaptive Response. **Veterinary Clinics of North America: Small Animal Practice**. . ISSN 01955616. 40:3 (2010) 369–379. doi: 10.1016/j.cvsm.2010.01.003.

KIM, Vera *et al.* - IL-17–producing follicular Th cells enhance plasma cell differentiation in lupus-prone mice. **JCI Insight**. . ISSN 2379-3708. 7:11 (2022). doi: 10.1172/jci.insight.157332.

KUBO, Masato - The role of IL-4 derived from follicular helper T (TFH) cells and type 2 helper T (TH2) cells. **International Immunology**. . ISSN 1460-2377. 33:12 (2021) 717–722. doi: 10.1093/intimm/dxab080.

KUMAR, Vijay - Toll-Like Receptors in Adaptive Immunity. Em . p. 95–131.

KURATA, Izumi; MATSUMOTO, Isao; SUMIDA, Takayuki - T follicular helper cell subsets: a potential key player in autoimmunity. **Immunological Medicine**. . ISSN 2578-5826. 44:1 (2021) 1–9. doi: 10.1080/25785826.2020.1776079.

KUWABARA, Taku *et al.* - The Role of IL-17 and Related Cytokines in Inflammatory Autoimmune Diseases. **Mediators of Inflammation**. . ISSN 0962-9351. 2017:2017) 1–11. doi: 10.1155/2017/3908061.

LAIDLAW, Brian J. *et al.* - Interleukin-10 from CD4 $^{+}$ follicular regulatory T cells promotes the germinal center response. **Science Immunology**. . ISSN 2470-9468. 2:16 (2017). doi: 10.1126/sciimmunol.aan4767.

LEE, Jennifer *et al.* - Interleukin-17 Enhances Germinal Center Formation and Immunoglobulin G1 Production in Mice. **Journal of Rheumatic Diseases**. . ISSN 2093-940X. 24:5 (2017) 271. doi: 10.4078/jrd.2017.24.5.271.

LEONG, Yew Ann *et al.* - CXCR5+ follicular cytotoxic T cells control viral infection in B cell follicles. **Nature Immunology**. . ISSN 1529-2908. 17:10 (2016) 1187–1196. doi: 10.1038/ni.3543.

LESMEISTER, Margaret J.; BOTHWELL, Marcella R.; MISFELDT, Michael L. - Toll-like receptor expression in the human nasopharyngeal tonsil (adenoid) and palantine tonsils: A preliminary report. **International Journal of Pediatric Otorhinolaryngology**. . ISSN 01655876. 70:6 (2006) 987–992. doi: 10.1016/j.ijporl.2005.10.009.

LEUNG, Chak Ming *et al.* - A guide to the organ-on-a-chip. **Nature Reviews Methods Primers**. . ISSN 2662-8449. 2:1 (2022) 33. doi: 10.1038/s43586-022-00118-6.

LINTERMAN, Michelle A. *et al.* - Foxp3+ follicular regulatory T cells control the germinal center response. **Nature Medicine**. . ISSN 1078-8956. 17:8 (2011) 975–982. doi: 10.1038/nm.2425.

LIU, Jing *et al.* - Design and Fabrication of a Liver-on-a-chip Reconstructing Tissue-tissue Interfaces. **Frontiers in Oncology**. . ISSN 2234-943X. 12:2022). doi: 10.3389/fonc.2022.959299.

LUCKHEERAM, Rishi Vishal *et al.* - CD4+ T Cells: Differentiation and Functions. **Clinical and Developmental Immunology**. . ISSN 1740-2522. 2012:2012) 1–12. doi: 10.1155/2012/925135.

MANSSON, Anne; ADNER, Mikael; CARDELL, Lars Olaf - Toll-like receptors in cellular subsets of human tonsil T cells: altered expression during recurrent tonsillitis. **Respiratory Research**. . ISSN 1465-993X. 7:1 (2006) 36. doi: 10.1186/1465-9921-7-36.

MARSHALL, Jean S. *et al.* - An introduction to immunology and immunopathology. **Allergy, Asthma & Clinical Immunology**. . ISSN 1710-1492. 14:S2 (2018) 49. doi: 10.1186/s13223-018-0278-1.

MEAGER, Anthony; WADHWA, Meenu - An Overview of Cytokine Regulation of Inflammation and Immunity. Em **eLS**. [S.l.] : Wiley, 2013

MEHTA, Amit K.; GRACIAS, Donald T.; CROFT, Michael - TNF activity and T cells. **Cytokine**. . ISSN 10434666. 101:2018) 14–18. doi: 10.1016/j.cyto.2016.08.003.

MELI, Alexandre P. *et al.* - T Follicular Helper Cell–Derived IL-4 Is Required for IgE Production during Intestinal Helminth Infection. **The Journal of Immunology**. . ISSN 0022-1767. 199:1 (2017) 244–252. doi: 10.4049/jimmunol.1700141.

MITSDOERFFER, Meike *et al.* - Proinflammatory T helper type 17 cells are effective B-cell helpers. **Proceedings of the National Academy of Sciences**. . ISSN 0027-8424. 107:32 (2010) 14292–14297. doi: 10.1073/pnas.1009234107.

MURPHY, Kenneth; WEAVER, Casey - **Janeway's Immunology** . 9th edition ed. [S.l.] : Garland Science, Taylor & Francis Group, LLC, 2017

NAVE, H.; GEBERT, A.; PABST, R. - Morphology and immunology of the human palatine tonsil. **Anatomy and Embryology**. . ISSN 03402061. 204:5 (2001) 367–373. doi: 10.1007/s004290100210.

NORMAN, Gail A. VAN - Limitations of Animal Studies for Predicting Toxicity in Clinical Trials. **JACC: Basic to Translational Science**. . ISSN 2452302X. 4:7 (2019) 845–854. doi: 10.1016/j.jacbts.2019.10.008.

NURIEVA, Roza I.; CHUNG, Yeonseok - Understanding the development and function of T follicular helper cells. **Cellular & Molecular Immunology**. . ISSN 1672-7681. 7:3 (2010) 190–197. doi: 10.1038/cmi.2010.24.

PALM, Anna-Karin E.; HENRY, Carole - Remembrance of Things Past: Long-Term B Cell Memory After Infection and Vaccination. **Frontiers in Immunology**. . ISSN 1664-3224. 10:2019). doi: 10.3389/fimmu.2019.01787.

PAPA, Ilenia; VINUESA, Carola G. - Synaptic Interactions in Germinal Centers. **Frontiers in Immunology**. . ISSN 1664-3224. 9:2018). doi: 10.3389/fimmu.2018.01858.

PARKIN, Jacqueline; COHEN, Bryony - An overview of the immune system. **Lancet (London, England)**. . ISSN 0140-6736. 357:9270 (2001) 1777–1789. doi: 10.1016/S0140-6736(00)04904-7.

PATAKAS, Agapitos *et al.* - Th17 Effector Cells Support B Cell Responses Outside of Germinal Centres. **PLoS ONE**. . ISSN 1932-6203. 7:11 (2012) e49715. doi: 10.1371/journal.pone.0049715.

PICOLLET-D'HAHAN, Nathalie *et al.* - Multiorgan-on-a-Chip: A Systemic Approach To Model and Decipher Inter-Organ Communication. **Trends in Biotechnology**. . ISSN 01677799. 39:8 (2021) 788–810. doi: 10.1016/j.tibtech.2020.11.014.

PICONESE, Silvia; CAMPELLO, Silvia; NATALINI, Ambra - Recirculation and Residency of T Cells and Tregs: Lessons Learnt in Anacapri. **Frontiers in Immunology**. . ISSN 1664-3224. 11:2020). doi: 10.3389/fimmu.2020.00682.

PRINZ, Immo; SILVA-SANTOS, Bruno; PENNINGTON, Daniel J. - Functional development of γδ T cells. **European Journal of Immunology**. . ISSN 00142980. 43:8 (2013) 1988–1994. doi: 10.1002/eji.201343759.

QUIGLEY, Máire F. *et al.* - CXCR5+ CCR7– CD8 T cells are early effector memory cells that infiltrate tonsil B cell follicles. **European Journal of Immunology**. . ISSN 00142980. 37:12 (2007) 3352–3362. doi: 10.1002/eji.200636746.

RAPHAEL, Itay *et al.* - T cell subsets and their signature cytokines in autoimmune and inflammatory diseases. **Cytokine**. . ISSN 10434666. 74:1 (2015) 5–17. doi: 10.1016/j.cyto.2014.09.011.

REFAT EL-ZAYAT, Salwa; SIBAII, Hiba; MANNAA, Fathia A. - Toll-like receptors activation, signaling, and targeting: an overview. **Bulletin of the National Research Centre**. 2019). doi: 10.1186/s42269-019-0227-2.

RIBOT, Julie C.; LOPES, Noëlla; SILVA-SANTOS, Bruno - γδ T cells in tissue physiology and surveillance. **Nature Reviews Immunology**. . ISSN 1474-1733. 21:4 (2021) 221–232. doi: 10.1038/s41577-020-00452-4.

ROGAL, Julia *et al.* - Autologous Human Immunocompetent White Adipose Tissue-on-Chip. **Advanced Science**. . ISSN 2198-3844. 9:18 (2022) 2104451. doi: 10.1002/advs.202104451.

SAKALEM, Marna Eliana *et al.* - Historical evolution of spheroids and organoids, and possibilities of use in life sciences and medicine. **Biotechnology Journal**. . ISSN 1860-6768. 16:5 (2021) 2000463. doi: 10.1002/biot.202000463.

SAMEER, Aga Syed; NISSAR, Saniya - Toll-Like Receptors (TLRs): Structure, Functions, Signaling, and Role of Their Polymorphisms in Colorectal Cancer Susceptibility. **BioMed Research International**. . ISSN 2314-6141. 2021:2021) 1–14. doi: 10.1155/2021/1157023.

SCHAERLI, Patrick *et al.* - Cxc Chemokine Receptor 5 Expression Defines Follicular Homing T Cells with B Cell Helper Function. **Journal of Experimental Medicine**. . ISSN 0022-1007. 192:11 (2000) 1553–1562. doi: 10.1084/jem.192.11.1553.

SHANTI, Aya *et al.* - Lymph Nodes-On-Chip: Promising Immune Platforms for Pharmacological and Toxicological Applications. **Frontiers in Pharmacology**. . ISSN 1663-9812. 12:2021). doi: 10.3389/fphar.2021.711307.

SHEN, Juan *et al.* - A Subset of CXCR5+CD8+ T Cells in the Germinal Centers From Human Tonsils and Lymph Nodes Help B Cells Produce Immunoglobulins. **Frontiers in Immunology**. . ISSN 1664-3224. 9:2018). doi: 10.3389/fimmu.2018.02287.

SPOLSKI, R.; LEONARD, W. J. - IL-21 and T follicular helper cells. **International Immunology**. . ISSN 0953-8178. 22:1 (2010) 7–12. doi: 10.1093/intimm/dxp112.

STEBEGG, Marisa *et al.* - Regulation of the Germinal Center Response. **Frontiers in Immunology**. . ISSN 1664-3224. 9:2018). doi: 10.3389/fimmu.2018.02469.

STEPHEN, Bettzy; HAJJAR, Joud - Overview of Basic Immunology for Clinical Investigators. **Advances in experimental medicine and biology**. . ISSN 0065-2598. 995:2017) 1–31. doi: 10.1007/978-3-319-53156-4_1.

TAKEDA, Kiyoshi; KAISHO, Tsuneyasu; AKIRA, Shizuo - Toll-Like Receptors. **Annual Review of Immunology**. . ISSN 0732-0582. 21:1 (2003) 335–376. doi: 10.1146/annurev.immunol.21.120601.141126.

THERMOFISHER SCIENTIFIC - 3D cell culture handbook. **3D cell culture handbook**. 2020).

WAGAR, Lisa E. *et al.* - Modeling human adaptive immune responses with tonsil organoids. **Nature Medicine**. . ISSN 1078-8956. 27:1 (2021) 125–135. doi: 10.1038/s41591-020-01145-0.

WATKINS, David I. *et al.* - Nonhuman primate models and the failure of the Merck HIV-1 vaccine in humans. **Nature Medicine**. . ISSN 1078-8956. 14:6 (2008) 617–621. doi: 10.1038/nm.f.1759.

ZHU, Xiaoliang; ZHU, Jinfang - CD4 T Helper Cell Subsets and Related Human Immunological Disorders. **International Journal of Molecular Sciences**. . ISSN 1422-0067. 21:21 (2020) 8011. doi: 10.3390/ijms21218011.

ZOIO, Patrícia; LOPES-VENTURA, Sara; OLIVA, Abel - Biomimetic Full-Thickness Skin-on-a-Chip Based on a Fibroblast-Derived Matrix. **Micro**. . ISSN 2673-8023. 2:1 (2022) 191–211. doi: 10.3390/micro2010013.

ZOIO, Patrícia; OLIVA, Abel - Skin-on-a-Chip Technology: Microengineering Physiologically Relevant In Vitro Skin Models. **Pharmaceutics**. . ISSN 1999-4923. 14:3 (2022) 682. doi: 10.3390/pharmaceutics14030682.

Appendix

1. The scientific content of the present thesis originated:

Chantre T, Gonçalves J, Cerqueira SA, Nascimento J, Soares H, Moreira IA and Sousa H. Immunophenotyping of palatine tonsils in children with OSAS versus Recurrent Tonsillitis. Portuguese Journal of Otorhinolaryngology head and neck surgery. 2023. In press.

2. Additional paper

Daniela Amaral-Silva, Rafael Gonzalez, Laura Gago, Rita Torres, Juliana Gonçalves, Agna Neto[2], Maria José Martins, João Nascimento, Diogo Moreira, Tomás Machado, Jaime C. Branco, Sara Querido, Manuela Costa, Helena Soares T cell intrinsic engagement of TLR4 and TLR9 primes distinct pathogenic profiles in systemic lupus erythematosus patients. 2023. Under revision.

3. Optimization of surface staining protocol for flow cytometry

Introduction

Flow cytometry has become a fundamental technique for the immunology field, by providing powerful insights into the intricate dynamics of the immune system. It is a laser-based technology that, by combining fluorescent tags with specific cellular components or molecules, allows to analyze and characterize cells with increased precision (Cossariz).

When designing panel for flow cytometry, the biological characteristic of the antigen, such localization and level of expression, must be considered, as well as the characteristic of each fluorophore, to limit spectral spread into other channels. Another factor that can greatly influence the resolution of antibody biding is the time of antibody:antigen. According to the work developed by Whyte *et al* (Whyte), biding similar to standard staining protocols can be achieved with fewer antibodies incubated for longer periods of time. This would result in reduced inter experimental variability, reduced costs and increased panel design flexibility (Whyte).

Taking this into account, the staining protocol that was in use in the laboratory was optimized, by combining less antibody concentration with longer periods of incubation.

Methods

In order to optimize the staining protocol, cells were thawed and resuspended in RPMI. Next cells were stained for viability for 20 min at 4 °C in the dark with Fixable Viability Dye eFluor 506. After cells were washed once with FACS buffer (2% FBS in PBS 1x). Surface staining was performed with anti-CD3-APC/Cy7 and anti-CD4-FITC for 30min and 60min at 4 °C in the dark. After surface staining, cells were washed twice with FACS buffer, fixed with 1% PFA for 20 min at RT in the dark. To prepare for flow cytometry analysis, cells were resuspended in FACS buffer and transferred to FACS tubes. Acquisition was performed in a BD FACSCanto II instrument (BD Biosciences) and analyzed with FlowJo v.10.8.1.

Results and discussion

It was possible to observe that lengthening the incubation time from 20min to 60min lead to an increased MFI on both CD3 and CD4 stainings, regardless of the antibody dilution (Fig. A-1). This result by itself, already indicates that incubating the antibodies for 60min instead of 20min, allows for a higher staining resolution, with a more defined separation between the positive and negative populations. In the context of flow cytometry, good peak separation is essential to accurately characterize the samples that are being analyzed, therefore it is possible to infer that higher incaution time positively impact the outcome of flow cytometry.

Perhaps the most interesting result is the fact using a higher antibody dilution resulted in very similar stain index values, when the antibodies were incubated for 60min, for both CD3 and CD4. The logical line of thought would be that fewer antibodies would result in fewer antibody:antigen complexes and therefore a weaker signal would be detected. This is true when the antibodies were incubated for only 20min, however, by increasing the incubation time this limitation is surpassed. Longer periods of incubation mean that the antibody is available for longer, therefor it has more time to interact with the target antigen, resulting in a strong signal detection.

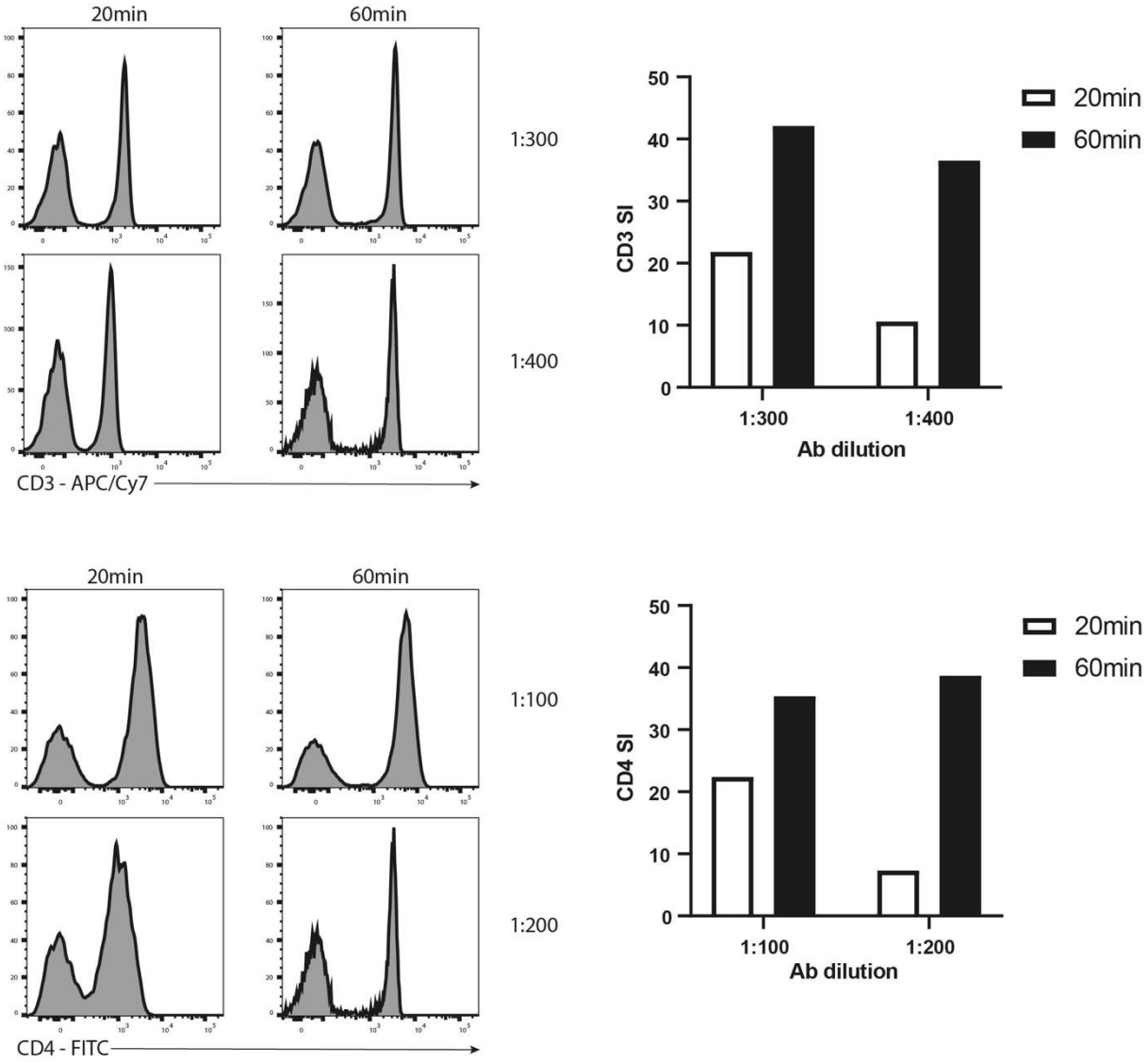

Figure A.1 – Influence of incubation time and antibody concentration on CD3 and CD4 staining. Representative histograms of CD3 and CD4 staining are shown as well as the stain index (SI) (*n*=1).

Conclusions

Flow cytometry has become an essential technique for immunology research. It is a rather simple process but can became expensive, especially when using high-parameter panels.

With this work the staining protocols that were in use in our lab were optimized. The incubation time for surface antibodies was increased to 60min, as it was shown that longer periods of incubation lead to better staining resolutions. Additionally, CD3 and CD4 antibodies were titrated. It was observed that, with a period of incubation of 60min, the dilutions of CD3 and CD4 could be increased to 1:400 and 1:300, respectively.